DEVELOPMENT AND TESTING OF A NEW BIOENERGETIC/BIOACCUMULATION MODEL FOR PERSISTENT ORGANIC POLLUTANTS IN AQUATIC AND TERRESTRIAL FOOD WEBS

by

Yongshu Fan
Bachelor of Science, Simon Fraser University 2005

PROJECT SUBMITTED IN PARTIAL FULFILLMENT OF THE REQUIREMENTS FOR THE DEGREE OF

MASTER OF ENVIRONMENTAL TOXICOLOGY

In the
Department
of
Biological Sciences

SIMON FRASER UNIVERSITY

Fall 2008

APPROVAL

Name: Yongshu Fan

Degree: Master of Environmental Toxicology

Title of Project:

Development and testing of a new bioenergetic/bioaccumulation model for persistent organic pollutants in aquatic and terrestrial food webs

Examining Committee:

Chair: Dr. Z. Punja, Professor

Dr. F. Gobas, Professor, Senior Supervisor
School of Resource and Environmental Management, S.F.U.

Dr. C. Kennedy, Professor
Department of Biological Sciences, S.F.U.

Dr. R. Nicholson, Associate Professor
Department of Biological Sciences, S.F.U.
Public Examiner

---

5 September 2008
Date Approved

Abstract

This project developed and tested a bioenergetic/bioaccumulation model to predict concentrations, bioconcentration factors, bioaccumulation factors (BAF) and trophic magnification factors of persistent organic pollutants (POPs) in organisms in terrestrial and aquatic food webs. This is the first bioaccumulation model that conserves both mass of chemical and energy. This model was tested against concentrations of various POPs in wildlife of Canadian Arctic terrestrial and Lake Ontario aquatic food webs. The model is shown to predict BAFs of POPs in organisms that are in good agreement with observed BAFs as indicated by the model bias, which ranged from 0.62 to 5.31. A comparison of the behaviour of the new model to that of a previous aquatic BAF model by Arnot and Gobas (2004) shows that the models are comparable in their ability to predict BAFs. The model can be used for bioaccumulation screening of chemicals in both aquatic and terrestrial animals.

Key words:

Persistent organic pollutants; bioenergetic model; bioaccumulation; fugacity.

Dedication

To my mother

Acknowledgements

I would like to thank the people who have supported and encouraged me for the completion of this work. I wish to genuinely thank my senior supervisor Dr. Frank Gobas for his interest and guidance in my project and for the time he has taken in relaying some of his knowledge in environmental toxicology and modelling. I would also like to thank Dr. Chris Kennedy for his time, efforts and insights as the second member of my supervisory committee. I would like to extend my thanks to my fellow students and scientists with special appreciation to Yung-Shan Lee, Victoria Otton and Adrain deBruyn. I would also like to acknowledge my friends and family for their support and kindness over the years.

Table of Contents

List of Figures

List of Tables

Glossary

Symbol	Parameter	Unit
BAF	Bioaccumulation factor	Unitless
BMF	Biomagnification factor	Unitless
BCF	Bioconcentration factor	Unitless
TMF	Trophic magnification factor	Unitless
Qox	Oxycalorific coefficient	KJ g^{-1} O_2
Eox	Oxygen uptake efficiency through respiratory system	Unitless
Cox	Volumetric oxygen concentration in the respiratory medium	g O_2 cm^{-3}
E_R	Respiratory chemical uptake efficiency	Unitless
E_D	Dietary chemical uptake efficiency	Unitless
Z_B, Z_D, Z_F	Fugacity capacity, of consumer's body, diet, faeces.	Mol Pa^{-1} m^{-3}
Z_i, Z_{Lip},	Fugacity capacity of biochemical components: lipid, water, protein and carbohydrate.	Mol Pa^{-1} m^{-3}
Z_{Water}, Z_{Air}	Fugacity capacity of respiratory media: water and air	Mol Pa^{-1} m^{-3}
R	The ideal gas constant	m^3 Pa K^{-1} ·mol^{-1}
C_B, C_R, C_W	POP concentrations in consumer's body, respiring medium and water	Mol m^{-3}
f_B, f_R, f_D, f_F	Fugacity of chemicals in consumer's body, respiratory medium, diet and faeces	Pa
e	Net growth efficiency	Unitless

g	The consumer's growth rate	$m^3 d^{-1}$
α_i α_D, α_E,	The dry-matter digestibility of each of the major biochemical constituents (lipid, protein and carbohydrate); digestive efficiency on a dry-matter basis and an energy basis	Unitless
D_{GB}, D_{BG}	The rates of gut-to-body and body-to-gut chemical transport	mol d^{-1} Pa^{-1}
D_R,, D_M, D_D, D_F, D_G	The fugacity-based rate parameter for respiratory uptake or elimination, metabolic transformation, dietary uptake, fecal egestion, growth dilution	mol d^{-1} Pa^{-1}
k_M	First order reaction rate of a chemical	d^{-1}
M_B, M_G	Mass of chemical in the consumer's body and gut	mol
G_R, G_D, G_F	Ventilation rate, consumption rate, and egestion rate	m^3 d^{-1}
ϕ_i, $\phi_{i,D}$,, $\phi_{i,B}$	The approximate composition (lipid, protein, carbohydrate or water) in the diet and the body	Unitless
δ_i, δ_D, δ_B	The energy density of lipid, protein and carbohydrate; the energy density of consumer's diet and body.	kJ cm^{-3}
I	Total energy ingested	kJ d^{-1}
L	Energy loss as fecal and urinary eliminations	kJ d^{-1}
R	Energy used for respiration	kJ d^{-1}
P	Energy used for production	kJ d^{-1}
K_{OW}, K_{OA}	Octanol-water and octanol-air partitioning coefficient	Unitless

Introduction

Bioaccumulation of persistent organic pollutants (POPs) has been of broad concern since Rachel Carson's "Silent Spring". Persistent hydrophobic organic chemicals such as polychlorinated biphenyls (PCBs) and dichlorodiphenyltrichloroethane (DDT) have been demonstrated to bioaccumulate in food webs (Oliver and Niimi 1988).

Bioaccumulation in the food web is the process by which the chemical fugacities (or lipid normalized concentration) in consumer organisms increase with increasing trophic level. Food-web biomagnification is the result of both bioconcentration and biomagnification (Gobas and Morrison 2000; Mackay and Fraser 2000). Bioaccumulation factor (BAF) measures the degree of chemical bioaccumulation relative to the consumer's respiratory medium (e.g. water for fish) (Gobas, Zhang et al. 1993). It can be expressed in terms of a ratio of chemical concentration in the organism and the respiratory medium, i.e. BAF=C_B/C_R or as the ratio of chemical fugacities in the organism and the respiring medium, i.e. BAF*=f_B/f_R. The values for concentration-based BAF and fugacity-based BAF are different, because the fugacity of a chemical in an organism is not only determined by the concentration, but also determined by the fugacity capacity of the chemical in the consumer. Mackay stated that "fugacity is to mass diffusion as temperature is to heat exchange" (Mackay and Paterson 1982). Thus fugacity is equivalent to chemical activity or chemical potential, and a difference in fugacity provides a driving force for net passive transport of chemicals from high to low fugacity (Mackay and Paterson 1982). BAF expresses the degree of chemical accumulation in an organism, which is significant in assessing the impact of the discharge of potentially toxic

chemicals into the ecosystem (Thomann 1989). Thermodynamic studies of certain organochlorines in aquatic food chains have shown that fugacity of these substances in organisms can increase with each step along the food chain; also the fugacity in organisms of higher trophic levels exceed that in the surrounding water of the organism (Connolly and Pedersen 1988). The movement of chemicals from prey (low fugacity) to predator (high fugacity), which appears to occur against the fugacity gradient, is caused by intestinal absorption and biomagnification of organic contaminants (Kelly, Gobas et al. 2004). Because digestive processes in the gastrointestinal tract (GIT) of consumers concentrate the chemical in the gut lumen and reduce the fugacity capacity of digest in the lumen, the fugacity of the chemical in the digestive tract is elevated over that of the ingested diet (Kelly, Gobas et al. 2004).

In addition to the BAF, there are other quantities that describe the accumulation of chemicals in organisms. They include bioconcentration factors (BCF), biomagnification (BMF) and the trophic magnification factors (TMF). Table 1 includes the definitions for BAF, BCF, BMF and TMF. Bioconcentration refers to a condition that is usually achieved under laboratory conditions, where the chemical is absorbed only from the water via the respiratory surface (e.g., gills) and /or the skin (Gobas and Morrison 2000). TMF, also called the food-web magnification factor (FWMF), is the description of the degree of biomagnification in the food web (Mackintosh, Maldonado et al. 2004; Hu, Zhen et al. 2006).

Table 1: Definitions for the concentration- and fugacity-based BAF, BCF, BMF and TMF.

Quantity	Definition
BAF	The ratio of chemical concentration in the organisms and the respiratory medium, i.e. BAF=C_B/C_R.
BAF*	The ratio of chemical fugacities in the organism and the respiring medium, i.e. BAF*=f_B/f_R.
BCF	The ratio of chemical concentration in the organism and water, i.e. BCF=C_B/C_W.
BCF*	The ratio of chemical fugacities in the organism and water, i.e. BCF*= f_B/f_W.
BMF	The ratio of chemical concentration in the organism and the diet, i.e. BMF= C_B/C_D.
BMF*	The ratio of chemical fugacities in the organism and the diet, i.e. BMF*= f_B/f_D.
TMF	The average increase in normalized concentrations of the chemical (ng/g) for a 1.0 unit increase in trophic level (TL).
TMF*	The average increase in fugacity of the chemical (Pa) for a 1.0 unit increase in trophic level (TL).

Because it often is impossible, unethical, costly and time consuming to conduct bioaccumulation experiments in many organisms (i.e. fish, birds and humans), bioaccumulation models play an important role in assessing the bioaccumulative behaviour of chemical substances. Bioaccumulation models are applied in environmental management to identify bioaccumulative substances and in conducting risk assessment. In addition to their application in exposure and risk assessment, BAF models are important tools in identifying bioaccumulative substances. Regulatory authorities evaluate substances based on three criteria, i.e., persistence, bioaccumulation and toxicity. The substances (including metals) with all three characteristics are called PBTs. (CEPA 1999; Webster, Cowan-Ellsberry et al. 2004). In terms of bioaccumulation, CEPA states that when the bioaccumulation factor (BAF) or the bioconcentration factor (BCF) is greater than or equal to 5000, or the Log octanol-water portioning coefficient (K_{OW}) is greater than or equal to 5, the substance is considered bioaccumulative (CEPA 1999).

Bioaccumulation models are also useful in conducting environmental and human health risk assessment, environmental quality criteria development (bioaccumulative criteria), determining the total maximum daily load of substances (TMDL) and risk assessment (e.g. chemical exposure assessment). A TMDL is a calculation of the maximum amount of a pollutant that a water body can receive and still meet water quality standards (USEPA 2008).

The 2004 United Nations Environment Programme (UNEP) persistent organic pollutants (POPs) protocol is currently used to identify bioaccumulative substance used in commerce, in which regulatory authorities rely on octanol-water portioning coefficients (K_{OW}) of substances or, when available, on organism/water chemical

concentration ratios measured in laboratory tests (bioconcentration factors) or in the field (bioaccumulation factors) to identify bioaccumulative substances (Arnot and Gobas 2006). But the protocol is mostly based on bioaccumulation observed in fish (Norstrom 2002). However, the toxic effects of many POPs are observed in a much wider variety of organisms, such as raptors, pinnipeds and even humans (deBruyn and Gobas 2006). For instance, certain substances such as perfluorinated sulphonic acids and endosulfan can bioaccumulate in species like wolves, seals and whales to a much greater extent than in fish. Thus bioaccumulation model that consider food web-specific bioaccumulation of POPs are important tool for regulatory assessment to prevent possible ecosystem and human-health consequences (Kelly, Ikonomou et al. 2007). Consequently, considering the enormous diversity of organisms on earth, there is a need to develop a model that can assess the bioaccumulative nature of chemical substances in a variety of species.

There are several studies that have focused on the development of bioaccumulation models. In 1984, Thomann and Connolly first developed an age-dependent model that considers species bioenergetics and toxicant exposure through water and food, assessing the uptake and accumulation of PCBs in the Lake Michigan lake trout food chain (Thomann and Connolly 1984). Connelly and Pedersen then developed a bioaccumulation model for aquatic organisms which was based on fugacity and kinetic bioenergetic approaches (Connolly and Pedersen 1988). Thomann later used a bioenergetic bioaccumulation model to assess organic chemical distribution in aquatic food chains (Thomann 1989). In 1988, a fugacity-based model describing the uptake and clearance mechanisms of fish was developed by Gobas and his colleagues (Gobas, Muir et al. 1988). The advantage of this model was that it considers contaminant uptake

through diet and water, and loss of contaminants to water or faeces, through metabolic transformation and by growth dilution (Clark, Gobas et al. 1990).

At the same time, Erickson and McKim (Erickson and McKim 1990) developed a simple flow-limited model for exchange of organic-chemicals at fish gills. In 1991, Barber and colleagues developed a bioaccumulation model called the Food and Gill Exchange of Toxic Substances (FGETS) model to quantify the processes for uptake of non-metabolizable organic chemicals from water and food (Barber, Suarez et al. 1991). The FGETS model included detailed physiological attributes of the fish, especially gill structure.

In 1993, Gobas developed a steady-state model in rate constant format to describe bioaccumulation in single organisms and simple aquatic food webs (Gobas 1993). This model has the advantage of considering feeding interactions in the bioaccumulation process. In 2004, Arnot and Gobas building on Gobas' previous works developed a model for food web bioaccumulation of POPs in aquatic ecosystems (Arnot and Gobas 2004). This model is able to provide site-specific estimates of BAF, bioconcentration factors (BCFs) and biota-sediment accumulation factors (BSAFs). This model also included organic carbon in addition to lipids as an important medium in which bioaccumulation occurs (Arnot and Gobas 2004). In 2003, Kelly and Gobas developed a steady-state arctic terrestrial food-chain bioaccumulation model for POPs, and used octanol-air partition coefficient (K_{OA}) for the organism-to-air exchange process (Kelly and Gobas 2003). They considered the chemical uptake through diet and respiration; and chemical elimination via respiration to the air, urinary excretion, fecal egestion, growth dilution, and milk excretion (Kelly and Gobas 2003).

Other than the models specifically designed for either terrestrial or aquatic organisms, efforts have been made to include both aquatic and terrestrial organisms in a BAF model, as in many cases a food web has both water-breathing and air-breathing organisms. For instance, Lake Ontario food web includes herring gulls (Gobas, Zgraggen et al. 1995), and San Francisco Bay food webs involves harbour seals as the top predator. Sharpe and Mackay developed a mass-balance bioaccumulation model for a six-organism food web including aquatic, terrestrial, and avian species (Sharpe and Mackay 2000). But these models require intensive parameterization and calculations and thus are complicated for their application to a large number of chemicals and animals. There is a need to develop a bioaccumulation model that is able to assess bioaccumulative properties of various POPs for many species in the animal kingdom, and does not require intensive parameterization.

There are some of commonalities of these models. They are all mass-balance models, and none of the above models were energy-balanced. Because these models either assigned the values of kinetic rates individually or calculated them from the weight of consumer organisms, the lack of an energy balance in the model can result in some biologically implausible situations. For instance, without energy balance, the model can produce scenarios in which an animal grows faster than it eats. Thus there is a need to develop and test a new energy- and mass-balanced bioaccumulation model that is able to assess bioaccumulative properties of various POPs for the animal kingdom, and which does not require intensive parameterization.

The energy-balanced bioenergetic model developed by deBruyn and Gobas enabled determination of the maximum biomagnification factors for a broad range of

animals (deBruyn and Gobas 2006). However, it did not consider the role of respiration, nor does it take the metabolic transformation rates into account. The difference between BMF and BAF is that BMF is the ratio of chemical concentration in a consumer's body and in its diet, whereas BAF is the ratio of chemical concentration in a consumer's body and in its environment (e.g. air, water or sediment). It is essential that analysis or prediction of bioaccumulation in real systems must include the ecological and physiological variables that have an important influence on the bioaccumulation process (Norstrom 2002). Therefore, a new bioenergetic mass-balance model, which incorporates both uptake and elimination via the digestive tract and respiratory systems, is needed to predict of bioaccumulation of a broad range of POPs in the animal kingdom.

Objectives

The objective of this project is to develop and test a new bioenergetic / bioaccumulation model for POPs in food webs. The aim of the model is to derive and test a relatively simple method to calculate several bioaccumulation measures (including the BCF, BAF, BMF and TMF) used in international regulations, for organic chemicals in a wide variety of food webs. The testing of the model includes comparing the model predicted BAF with the observed ones in the Canadian Arctic food web and Lake Ontario food web. There are several reasons for selecting these two food webs. First, the empirical data for both food webs are available for model testing. Second, the two food webs represent the terrestrial and aquatic food webs, which allows us to test whether model is applicable to both aquatic and terrestrial food webs. Third, testing the model in these two food webs enables the comparisons to be made between the performances of the current model with those of previous models.

Theory

Fugacity and Fugacity Capacity

In the development of the model we apply fugacity, a property of chemical substances used in the description of thermodynamics. Fugacity is basically the chemical's partial pressure and has units of pressure, i.e., Pascal (Pa). It expresses the tendency of a chemical to leave the environmental phase within which it resides. It is related to the concentration of chemical through the use of the fugacity capacity as following (Mackay 1979):

$$C = Z \times f \qquad \textbf{(1)}$$

where C is the concentration of chemical in the medium in which the chemical resides (mol/m^3), Z is the fugacity capacity of the medium (mol Pa^{-1} m^{-3}), and f is the fugacity of the chemical (Pa).

The fugacity capacity, Z, expresses the ability of a phase to retain a chemical. The fugacity capacity of a phase depends on the nature of the chemical and the properties and temperature of the medium or compartment (Fraser, Burkow et al. 2002). Phases with a high Z value for the chemicals can absorb a large amount (unit: mol m^{-3}) of the chemical.

Bioenergetic Model: the Energy Balance

In the bioenergetic model, the energy budget illustrates that the total energy content of the food eaten minus the energy loss through excretion and egestion equals the sum of energy used for respiration or metabolism and production. (Welch 1968):

$$I - L = R + P \qquad (2)$$

The unit of this energy budget is energy expenditure (kJ d^{-1}). I is the total ingested energy, L is the loss of energy, R is the energy used for respiration and P is the energy used for production and growth. The use of the energy budget enables us to calculate bioenergetic parameters from the energy balance model, so that the model is energy balanced. Moreover, through utilizing of energy balance, model parameterization is simplified. This can be further demonstrated in the model parameterization section of this work.

The bioenergetic model illustrated in Equation 2 has been widely accepted and applied to animal and ecological bioenergetic studies (Brody 1945; Welch 1968; Humphreys 1978; Thomann 1989). This model is based on several assumptions.

Energy used for respiration (R) is expressed by the field metabolic rate (FMR). FMR is the total energy an active animal allocates to respiration in the field under natural conditions.

Loss (L) involves fecal and urinary eliminations, and in some cases through ecdysis in arthropods, as energy is lost with molted cuticles. The energy used to perform urination and fecal elimination is included in the energy used for respiration. However,

the chemical energy in urine is of little significance in the energy balance of the animal. Chemical energy loss due to urination was not specifically considered.

Production (P) is considered as net growth, which is the energy allocated to growth (replacement of tissue) and the secretion of sperm, milk and other media (e.g. silk, musk etc). Production (P) is represented by the net production efficiency (e), which is the ratio of energy used in production and energy assimilated:

$$e = \frac{P}{I - L} = \frac{P}{P + R} \quad \textbf{(3)}$$

If the net growth efficiency (P^*) is used instead of the net production efficiency in an animal:

$$e^* = \frac{P^*}{I - L} = \frac{P^*}{P + R} \quad \textbf{(4)}$$

then secretion of sperm, milk and other media are ignored and the model only applies to male and non-reproductive female mammals, which do not have important secretion as a dilution source of internal POP concentrations. In other words, the important secretion as a means of dilution can be taken into account by adjusting growth efficiency. For instance, a female wolf can be assigned to larger net growth efficiency than a male wolf in order to account for the female milk secretion as a means of dilution.

Total energy ingested (I), is the total energy of a consumer's food. The energy of the food can be calculated from the energy density of the food (δ_D, unit: kJ cm^{-3}) and the volume of the diet, V_D (unit: cm^{-3})

$$I = V_D \times \delta_D \quad (5)$$

Mass balance model

Figure 1 illustrates a conceptual diagram showing the mass transfer routes considered in the bioaccumulation model for consumer organisms. The uptake of POPs was assumed to be mainly through respiration and diet. Dermal exchange, which is particularly significant for amphibians, is viewed as part of respiratory uptake.

The model assumes a steady state. Thus POP concentrations in the different environment compartment and animal compartments have reached steady state, and the POP concentrations in the environment do not change over time. In addition, animal net growth efficiency, digestive efficiency and dietary preference do not change over time. In case of the biological parameters changes with an animals life stages, assigning different parameter values for different life stages can be employed. For instance, an adult wolf can be given lower net growth efficiency than a juvenile wolf. Physiological state of mammals such as age, sex and female reproductive state should all influence the uptake and elimination of chemicals as dilution factors.

Figure 1: **The conceptual mass balance model in an animal, showing the key processes considered in the models, i.e. respiration (D_R), metabolism (D_M), growth (D_G), dietary intake (D_D), fecal excretion (D_F), gut to body and body to gut absorption (D_{BG} and D_{GB}), and lung to body and body to lung absorption (D_{BL} and D_{LB}).**

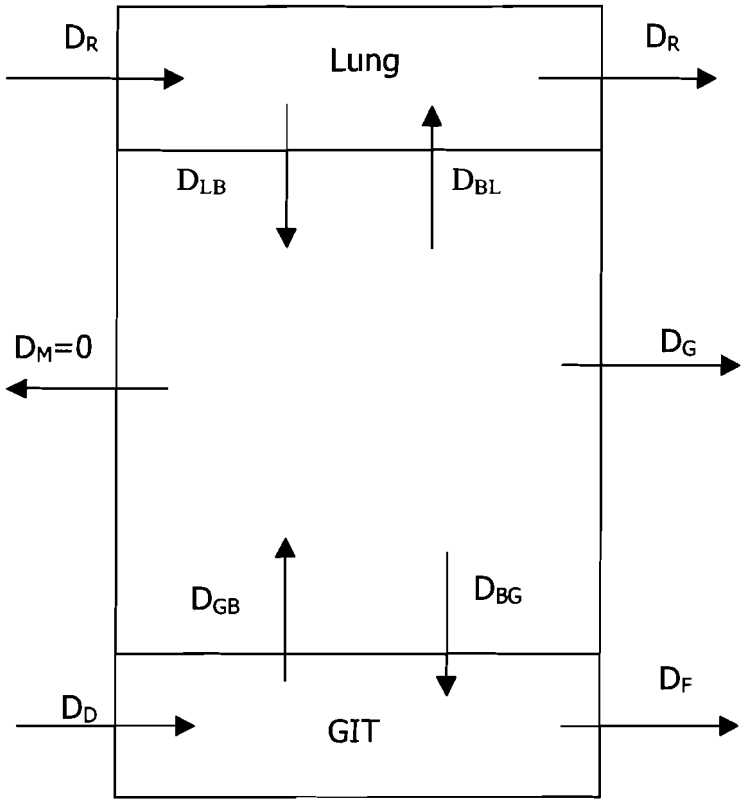

Following previous work of Gobas and colleagues on BAF models (Gobas 1993; deBruyn and Gobas 2006), we express the important processes controlling bioaccumulation by mass balance equations for the organism (B) and the gastro-intestinal tract (G):

$$\frac{dM_B}{dt} = D_R f_R + D_{GB} f_G - (D_G + D_{BG} + D_M + D_R) f_B \quad \textbf{(6)}$$

for the mass of chemical in the consumer's body (M_B, mol), and

$$\frac{dM_G}{dt} = D_D f_D + D_{BG} f_B - (D_{GB} + D_F) f_G \quad \textbf{(7)}$$

for the mass of chemical in the consumer's gut (M_G). D is the fugacity-based transport parameter (mol d^{-1} Pa^{-1}) for respiratory uptake or elimination (D_R), metabolic transformation (D_M), dietary uptake (D_D), fecal egestion (D_F), growth dilution (D_G) and the rates of gut-to-body (D_{GB}) and body-to-gut (D_{BG}) chemical transport. f is the fugacity of chemical in the respiratory medium (f_R), diet (f_D), digested gut contents (f_G) and the consumer's body (f_B).

At steady state, $dM_B/dt = dM_G/dt = 0$. Rearranging Equation 6 and 7 then gives:

$$f_B = \frac{D_R f_R + D_{GB} f_G}{D_G + D_{BG} + D_M + D_R} \quad \textbf{(8)}$$

$$f_G = \frac{D_D f_D + D_{BG} f_B}{D_{GB} + D_F} \quad \textbf{(9)}$$

Substituting Equations 9 in 8 gives:

$$f_B = \frac{D_R f_R (D_{GB} + D_F) + D_{GB} D_D f_D}{(D_F + D_{BG})(D_G + D_M + D_R) + D_{GB} D_F} \quad \textbf{(10)}$$

Diving the right side through by D_{GB} and dividing both sides by f_R gives:

$$BAF^* = \frac{f_B}{f_R} = \frac{D_R\left(\frac{D_{GB} + D_F}{D_{GB}}\right) + D_D\left(\frac{f_D}{f_R}\right)}{\left(\frac{D_{GB} + D_F}{D_{GB}}\right)(D_G + D_M + D_R) + \left(\frac{D_{BG}}{D_{GB}}\right)D_F} \quad \textbf{(4)}$$

The term $[(D_{BG} + D_F)/ D_{BG}]$ is the inverse of gross chemical absorption efficiency (E_D). The rate of absorption of chemical from the gut relative to the total rate of elimination of chemical from the gut multiplying by E_D gives the consumer's bioaccumulation factor:

$$BAF^* = \frac{f_B}{f_R} = \frac{D_R + D_D \cdot E_D\left(\frac{f_D}{f_R}\right)}{(D_G + D_M + D_R) + \left(\frac{D_{BG}}{D_{GB}}\right)D_F \cdot E_D} \quad \textbf{(5)}$$

Where the ratio f_D / f_R is the BAF of the diet. The ratio (D_{BG} / D_{GB}) reflects possible asymmetry in the resistance to chemical movement between a consumer's gut and body. All other terms can be measured or estimated for a particular species and chemical.

If f_D equals zero in Equation 12, it gives the bioconcentration factor (BCF*):

$$BCF^* = \frac{f_B}{f_R} = \frac{D_R}{(D_G + D_M + D_R) + \left(\frac{D_{BG}}{D_{GB}}\right) D_F \cdot E_D} \quad (6)$$

When assuming that uptake of POPs from the respiratory medium is negligible, it is possible to simplify this model further to give the consumer's biomagnification factor (BMF):

$$BMF^* = \frac{f_B}{f_D} = \frac{D_D \cdot E_D}{(D_G + D_M + D_R) + \left(\frac{D_{BG}}{D_{GB}}\right) D_F \cdot E_D} \quad (7)$$

The trophic magnification factor, TMF, represents the average increase in chemical concentrations (normalized) (ng/g) for a 1.0 unit increase in trophic position or trophic level (TL). TMFs are determined as the anti-Log of the slope (m) of the Log-linear regression between Log POP concentrations (normalized) (ng/g) and trophic level, this is illustrated as (Mackintosh, Maldonado et al. 2004):

$$TMF = 10^m \quad (8)$$

$$LogC_B = a + m \cdot TL \quad (9)$$

where $LogC_B$ is the Log transformed POP concentrations in an organism, and TL is the trophic position of the organism.

TMF*, representing the average increase in chemical fugacity for a 1.0 unit increase in trophic level is illustrated as following:

$$TMF^* = 10^{m^*} \quad \textbf{(10)}$$

$$Log f_B = a + m^* \cdot TL \quad \textbf{(11)}$$

The TL of an organism can be determined as:

$$TL = \sum_{i=1}^{n} (TL_{\Pr ey,i} \times P_{\Pr ey,i}) + 1 \quad \textbf{(12)}$$

Where $TL_{Prey,i}$ is the trophic level of the i^{th} prey and $P_{prey,i}$ is the proportion of the prey in the consumer organism's diet (Vander Zanden and Rasmussen 1999).

Bioenergetic Mass-balanced Model

Linking mass-balance bioaccumulation models to the energetic processes underlying bioaccumulation is a useful way to model BAF, BCF, BMF and TMF of chemicals in a variety of food webs. A bioenergetic mass-balance model is able to predict the variation of bioaccumulation of chemicals in a variety of species with different physiological aspects and energy allocations.

Dietary chemical uptake efficiency

E_D represents the chemical absorption efficiency, which is equivalent to $D_{GB}/(D_{GB}+D_F)$, the ratio of the rate of chemical absorption from the gut to the sum of chemical absorption and fecal elimination. Kelly and colleagues have examined data from several studies that investigated the relationship between dietary absorption efficiency and chemical K_{OW} in fish (Gobas, Muir et al. 1988; Gobas, McCorquodale et al. 1993; Fisk, Norstrom et al. 1998), birds (Drouillard and Norstrom 2000), dairy cows and humans (Schlummer, Moser et al. 1998; Moser and McLachlan 2001). The trend

lines of nonlinear regressions of absorption efficiencies of various POPs reported in the literature for several organisms against Log K_{OW} are determined as follows (Kelly, Gobas et al. 2004):

$$\frac{1}{E_D} = 5.3 \times 10^{-8} K_{OW} + 2.3 \quad \textbf{(13)}$$

for fish data,

$$\frac{1}{E_D} = 2.9 \times 10^{-8} K_{OW} + 2.3 \quad \textbf{(14)}$$

for dairy cows;

$$\frac{1}{E_D} = 2.4 \times 10^{-9} K_{OW} + 1.04 \quad \textbf{(15)}$$

for ring doves; and

$$\frac{1}{E_D} = 1.55 \times 10^{-9} K_{OW} + 1.01 \quad \textbf{(16)}$$

for human data.

Chemical respiratory uptake efficiency

Respiratory uptake efficiency, E_R, expresses the actual amount of chemical absorbed via the respiratory surface per unit of time, relative to the amount of chemical brought into contact with the respiratory surface, through ventilation per unit of time. It reflects the rates of chemical permeation through the membranes of the respiratory surface (i.e. gill for fish; lung for mammal) and ventilation.

It was observed that gill uptake efficiencies which vary from 0 to 90%, show a relationship with the K_{OW} (Arnot and Gobas 2004). The gill uptake efficiency increases with increasing K_{OW} for chemical substances with a Log K_{OW} between 0.5 and 3. It was demonstrated that for chemicals with a Log K_{OW} between 3 and approximately 6.5, the gill uptake efficiency is constant at approximately 55% (McKim, Schmieder et al. 1985).

Transport Parameters

This section shows how D_D, D_G, D_R and D_F can be calculated from basic bioenergetic parameters.

D_R, the transport parameter for respiratory exchange, is the product of ventilation rate (G_R), which is the efficiency of chemical exchange across the respiratory surfaces, respiratory chemical uptake efficiency (E_R), and the fugacity capacity of the respiratory medium (Z_R). FMR determines the rate of oxygen consumption, and thus the ventilation rate:

$$G_R = \frac{FMR}{Q_{OX} \cdot C_{OX} \cdot E_{OX}} \qquad \textbf{(17)}$$

where Q_{ox} (kJ g^{-1} O_2) is the oxycalorific coefficient.

D_G, the transport parameter for growth dilution, is the product of growth rate (g) and the fugacity capacity of the consumer's body (Z_B). FMR is related to growth efficiency, e. the total energy assimilated by a consumer allocated between respiration (Metabolic expenditure, FMR) and growth. Net growth efficiency, e, is the fraction of assimilation energy that is allocated to growth. Because energy allocated to growth (P) can be expressed as $P=g\ \delta_B$, energy allocated to respiration (R) can be expressed as

$R=FMR$, then substitute P and R in the formula $of\ e=P/(P+R)$ for growth efficiency and rearrange,

$$e = \frac{P}{I-R} = \frac{P}{P+R} = \frac{g \cdot \delta_B}{g \cdot \delta_B + FMR} \tag{18}$$

$$e \cdot g \cdot \delta_B + e \cdot FMR = g \cdot \delta_B \tag{19}$$

the consumer's growth rate (g) is therefore:

$$g = \frac{FMR \cdot e}{(1-e) \cdot \delta_B} \tag{20}$$

D_D, the transport parameter for dietary intake, is the product of consumption rate (G_D), dietary chemical uptake efficiency (E_D) and the fugacity capacity of the diet (Z_D). G_D is simply the total energy intake (FMR + Growth energy) divided by the consumer's digestive efficiency on a dry-matter basis (α_E) and the energy density of the diet (δ_D):

$$G_D = \frac{FMR}{(1-e) \cdot \alpha_E \cdot \delta_D} \tag{21}$$

D_F, the transport parameter for fecal egestion, is the product of egestion rate G_F and the fugacity capacity of the faeces (Z_F). G_F can be calculated in a manner similar to consumption rate:

$$G_F = \frac{FMR(1-\alpha_E)}{(1-e)\cdot\alpha_E\cdot\delta_D} \quad (22)$$

D_M, the transport parameter for metabolic transformation, is the product of the first-order reaction rate constant (K_M, unit: d^{-1}), the consumer's volume (V_B, unit: m^3), and the consumer's fugacity capacity (Z_B, unit: $mol/m^3/Pa$):

$$D_M = K_M \cdot V_B \cdot Z_B \quad (23)$$

Digestive efficiency on a dry-matter basis (α_D) and an energy basis (α_E) are

$$\alpha_D = \sum_i \alpha_i \cdot \phi_{i,D} \quad (24)$$

$$\alpha_E = \frac{\sum_i \alpha_i \cdot \phi_{i,D} \cdot \delta_i}{\sum_i \phi_{i,D} \cdot \delta_i} \quad (25)$$

α_i represents the dry-matter digestibility of each of the major biochemical constituents (lipid, protein and carbohydrate) of the diet by the consumer; ϕ_i represents the approximate composition of lipid, protein, carbohydrate or water in the diet ($\phi_{i,D}$) or the body ($\phi_{i,B}$) of consumers. The digestive efficiency scaled to the fugacity capacity of the diet for a chemical substance is measured by α_Z, calculated as

$$\alpha_E = \frac{\sum_i \alpha_i \cdot \phi_{i,D} \cdot Z_i}{\sum_i \phi_{i,D} \cdot Z_i} \quad (26)$$

α_i is the digestibility of lipid, protein and carbohydrate for consumers were mainly obtained from the previous bionergetic biomagnification model developed by deBruyn and Gobas (Arnot and Gobas 2004).

Z_i represents the fugacity capacity of the major biochemical constituents. Z_i can be derived from Z_{Lipid}. Because fugacity capacity for carbohydrate and protein can be expressed as a fraction of the fugacity capacity of lipids, i.e., Z_i/Z_{Lipid} is approximately 0.05, 0.1, and 1.0 for simple hydrophobic organic chemicals in proteins, carbohydrates, and lipids, respectively (Gobas, Wilcockson et al. 1999; deBruyn and Gobas 2006).

δ_B and δ_D, the energy density of the consumer's body and diet, are calculated from the sum of energy density of lipid, protein and carbohydrate in the body and the diet of the consumer organisms:

$$\delta_D = \sum_i \delta_i \cdot \phi_{i,D} \quad \textbf{(27)}$$

$$\delta_B = \sum_i \delta_i \cdot \phi_{i,B} \quad \textbf{(28)}$$

where δ_i represents the energy density (kJ cm^{-3}) of the major biochemical constituents of the diet or consumer.

The fugacity capacities of the diet (Z_D) and the consumer (Z_B) can be derived as:

$$Z_D = \sum_i Z_i \cdot \phi_{i,D} \quad \textbf{(29)}$$

$$Z_B = \sum_i Z_i \cdot \phi_{i,B} \quad \textbf{(30)}$$

Z_{Lipid} is calculated from Z_{water} as:

$$Z_{Lipid} = K_{OW} \times Z_{Water} \quad (31)$$

and Z_{Water} is calculated from Z_{Air} as:

$$Z_{Water} = \frac{K_{OA}}{K_{OW}} \times Z_{Air} \quad (32)$$

Where Z_{Air} can be calculated as:

$$Z_{Air} = \frac{1}{RT} \quad (33)$$

POP concentrations in phytoplankton can be calculated as a biphasic relationship for k_1 and k_2 based on a water–organic carbon two-phase resistance model (Arnot and Gobas 2004), because phytoplankton are not consumer organisms and the model did not include an energy balance. The concentrations of POPs in phytoplankton are calculated as following:

$$C_{Phyto} = \frac{k_1 \times C_{WT,O}}{(k_2 + k_G)} \quad (34)$$

Where k_1 is the clearance rate constant (L kg^{-1} d^{-1}) for chemical uptake via respiratory area, k_2 is the rate constant (d^{-1}) for chemical elimination via respiratory area, and K_G (d^{-1}) is the growth rate constant. C_{Phyto} is the concentration of POPs in phytoplankton and $C_{WT,O}$ is the concentration of POPs in the water.

k_1 was calculated as the following:

$$k_1 = (A + (\frac{B}{K_{OW}}))^{-1} \quad \textbf{(35)}$$

A (equals 0.00006) and B (equals 5.5) are constants with unit of time describing the resistance to chemical uptake through the aqueous and organic phases, respectively, of phytoplankton (Arnot and Gobas 2004). k_2 was calculated from k_2/K_{PW}. K_{PW} is the phytoplankton-water partition coefficiency on a wet weight basis, calculated as:

$$k_{PW} = v_{LP} \times K_{OW} + v_{NP} \times 0.35 \times K_{OW} + v_{WP} \quad \textbf{(36)}$$

where v_{LP}, v_{NP} and v_{WP} are the lipid, non-lipid and water proportion, respectively, in phytoplankton (Kg/Kg organism wet weight).

Methods

To test this new bioenergetic / bioaccumulation model, the model was applied to an aquatic food web in Lake Ontario and a terrestrial food web (e.g. lichen-caribou-wolves) in the Canadian Arctic. The goal was to compare the model predicted BAF to the previously measured and documented observed BAF in a various type of organisms in the animal kingdom. There are a variety of organisms in these food webs including benthic invertebrates, herbivorous and predatory fish, a bird species, a terrestrial herbivorous mammal and a carnivorous. The concentration of POPs in the consumers for selected species in the aquatic food web and the terrestrial food web can be determined using the predicted BAF values, since $C_B = BAF \times C_R$.

Model Parameterization

Model parameterization is one of the most important processes in modelling, since the preference of suitable parameters will directly influence the predictions of the model.

The standard value of oxycalorific coefficiency, Q_{ox}, for an animal is usually given as 3.38 cal for each mg of oxygen consumed (McKenzie, Pedersen et al. 2007). The present study used the Q_{ox} value of 13.5 KJ g^{-1} O_2 (McKenzie, Pedersen et al. 2007). C_{ox} (g O_2 cm^{-3}), the volumetric oxygen concentration in the respiratory medium, was set at 0.0000085 g O_2 cm^{-3} for water (Thomann and Connolly 1984) and 0.0003 g O_2 cm^{-3} for air (calculated from the volumetric proportion of oxygen in the air: 20.95% (Jason

Pelish 2003)) and E_{OX} (Unitless), the efficiency of exchange of oxygen across the respiratory surfaces, was set at 0.8 for fish (Piiper, Dejours et al. 1971), 0.15 for mammals (Piiper, Dejours et al. 1971) and 0.3 for birds (Scheid and Piiper 1970).

Respiratory chemical uptake efficiencies (E_R) for barren-ground caribou and Arctic wolf were set to be the same as their efficiencies of exchange of oxygen across the respiratory surfaces (E_{OX}). For fish and invertebrates, E_R was calculated as (Arnot and Gobas 2004):

$$E_R = \frac{1}{1.85 + \frac{155}{K_{OW}}} \quad \textbf{(37)}$$

The values of biological parameters of organisms included in the model are shown in Table 2. Net growth efficiencies (e) for caribou and wolf were set at 0.015 and 0.005 respectively (Golley 1968; Vucetich and Peterson 2004). Net growth efficiencies for zooplankton and mysids were set at 0.33 (Welch 1968; Gorokhova 1998), and for diporeia this was set at 0.15 (Humphreys 1978), and for oligochaetes, 0.62 (Welch 1968). Fish net growth efficiencies are highly variable, largely due to variation in the energetics of food acquisition (Kovecses, Sherwood et al. 2005). Fish growth efficiencies vary between 10 to 20% in wild fish (Welch 1968), but may approach zero in lakes without appropriate prey (Sherwood, Kovecses et al. 2002). Net growth efficiency for herring gull was set at 0.0035 (Boyd 2002). Digestibility of lipid, protein and carbohydrate in the organisms included in the model are shown in Table 2. The approximate composition of lipid, protein, carbohydrate or water in the diet ($\phi_{i,D}$) or the body ($\phi_{i,B}$) of consumers used in the model are listed in Table 2. As energy densities of lipid, protein, and carbohydrate

vary little among organisms, we used standard values for δ_i of 35.6 kJ cm^{-3} for lipid, 26.8 kJ cm^{-3} for protein, 26.2 kJ cm^{-3} for carbohydrate, and 0 kJ cm^{-3} for water (Board 2005; deBruyn and Gobas 2006).

Dietary chemical uptake efficiency (E_D) for caribou and wolf was assumed to be comparable to the observations in dairy cows and humans respectively, and they were calculated as (Kelly, Gobas et al. 2004):

$$E_D = \frac{1}{2.9 \times 10^{-8} \times K_{OW} + 1.2} \quad \textbf{(38)}$$

$$E_D = \frac{1}{1.55 \times 10^{-9} \times K_{OW} + 1.01} \quad \textbf{(39)}$$

for aquatic organisms were calculated as (Arnot and Gobas 2004):

$$E_D = \frac{1}{3.0 \times 10^{-7} \times K_{OW} + 2.0} \quad \textbf{(40)}$$

Metabolic transformation for chemicals was not included in the prediction, as it was considered to be negligible in previous bioaccumulation models (Kelly and Gobas 2003; Arnot and Gobas 2004; deBruyn and Gobas 2006). R is the ideal gas law constant, equals 8.314 $m^3 \cdot Pa \cdot K^{-1} \cdot mol^{-1}$ and T is the temperature in the unit of K.

Octanol-water (K_{OW}) and octanol air partition coefficient (K_{OA}) vary with temperature (Li, Wania et al. 2003). The values of K_{OW} and K_{OA} implemented in the current model are listed in Table 2 for Arctic food web and in Table 4 for Lake Ontario food web. The present study used the same K_{OW} and K_{OA} values for Canadian arctic food chain as the previous model for the same food chain (Kelly and Gobas 2003). For Lake

Ontario food web, the values of K_{OW} and K_{OA} for the chemicals were obtained from the Excel datasheet of Harner (Harner 2008) and from a previous study (Shen and Wania 2005).

Table 2: Biological parameters for the organisms included in the Arctic and Lake Ontario food webs.

	Body composition, ϕ_i, Unitless			**Digestive efficiency, α_i, Unitless**			**Growth Efficiency, e Unitless**
Organism	Lipid	Protein	Carbo-hydrate	Lipid	Protein	Carbo-hydrate	
Caribou [a]	0.08	0.23	0	0.65	0.50	0.50	0.025
Wolf [a]	0.09	0.20	0	0.95	0.70	0.00	0.01
Zooplankton [b]	0.02	0.20	0	0.95	0.75	0.90	0.33 [c]
Diporeia [b]	0.03	0.20	0	0.75	0.75	0.75	0.20 [d]
Mysid [b]	0.03	0.20	0	0.75	0.75	0.75	0.33 [c]
Oligochaete [b]	0.01	0.20	0	0.75	0.75	0.10	0.62 [c]
Slimy sculpin [b]	0.08	0.20	0	0.95	0.50	0.50	0.20 [c]
Alewife [b]	0.07	0.20	0	0.95	0.50	0.50	0.01 [c]
Rainbow smelt [b]	0.04	0.20	0	0.95	0.50	0.50	0.20 [a]
Lake trout [b]	0.20	0.20	0	0.95	0.50	0.50	0.50 [a]
Herring Gulls [a]	0.09	0.87	0	0.93	0.86	0.00	0.0035 [e]
	Lipid	**Non-lipid organic carbon**					**Growth rate**
Phytoplankton [b]	0.005	0.195					0.08

Source: [a] (deBruyn and Gobas 2006), [b] (Arnot and Gobas 2004), [c] (Welch 1968)., [d] (Humphreys 1978), [e] (Boyd 2002).

Table 3: Chemical properties for the chemicals included in the arctic food web.

Chemicals	Molecular Weight (g/mol)	Log K_{OA} at 37°C	Log K_{OW} at 37°C
beta-HCH	290.83	8.05	4.00
HCB	285.00	6.83	5.50
Mirex	391.00	8.75	6.00
Dieldrin	391.00	7.95	6.20
PCB28	257.54	7.46	5.60
PCB52	292.00	7.88	5.84
PCB66/95	292.00	8.57	6.20
PCB99	292.00	8.57	6.39
PCB118	326.00	9.22	6.74
PCB153	360.88	8.65	6.92
PCB105	326.00	9.41	6.65
PCB138	360.90	9.22	6.83
PCB182/187	395.00	9.64	7.20
PCB180	395.00	9.93	7.50
PCB170/190	395.00	9.93	7.46
PCB194	430.00	9.93	7.80
PCB206	430.00	9.93	8.09

Source: (Kelly and Gobas 2003)

Table 4: Chemical properties for the chemicals included in the Lake-Ontario food web.

	Molecular Weight (g/mol)	Log K_{OA} 14.9°C [a]	Log K_{OW} 8°C [b]	Log K_{OA} at 42 °C [a]	Log K_{OW} at 42 °C [c]
PCB28	257.43	8.78	5.80	7.38	5.70
PCB18	257.43	8.32	5.60	6.98	5.27
PCB22	257.43	8.95	5.60	7.52	5.61
PCB17	257.43	8.34	5.60	7.00	5.28
PCB32	257.43	8.46	5.80	7.11	5.47
PCB66	292.00	9.72	5.80	8.18	6.23
PCB70	292.00	9.69	5.90	8.15	6.23
PCB56	292.00	9.88	6.00	8.31	6.14
PCB52	292.00	9.12	6.10	7.67	5.87
PCB47	292.00	9.19	5.90	7.72	5.88
PCB44	292.00	9.31	6.00	7.83	5.78
PCB74	292.00	9.65	6.10	8.12	6.23
PCB49	292.00	9.16	6.10	7.70	5.88
PCB64	292.00	9.43	6.10	7.93	5.98
PCB42	292.00	9.35	5.60	7.86	5.69
PCB53	292.00	0.00	6.10		5.65
PCB40	292.00	9.51	5.60	8.00	5.69
PCB101	326.43	9.94	6.40	8.37	6.41
PCB84	326.43	9.92	6.10	8.35	6.07
PCB118	326.43	10.75	6.40	8.85	6.77
PCB110	326.43	10.27	6.40	8.65	6.51
PCB87	326.43	10.18	6.50	8.57	6.32
PCB105	326.43	11.01	6.40	9.05	6.68
PCB95	326.43	9.73	6.40	8.18	6.16
PCB85	326.43	10.22	6.20	8.60	6.33
PCB92	326.43	0.00	6.50		6.38
PCB82	326.43	10.37	6.20	8.73	6.23
PCB91	326.43	9.79	6.30	8.23	6.16
PCB99	326.43	9.99	6.60	8.41	6.42
PCB153	360.88	10.71	6.90	9.02	6.95
PCB138	360.88	10.95	7.00	9.23	6.86
PCB149	360.88	10.49	6.80	8.84	6.70
PCB146	360.88	10.66	6.90	8.98	6.92
PCB141	360.90	10.82	6.90	9.12	6.85

Table 4 continued....

	Molecular Weight (g/mol)	Log K_{OA} 14.9°C [a]	Log K_{OW} 8°C [b]	Log K_{OA} at 42 °C [a]	Log K_{OW} at 42 °C [c]
PCB128	360.90	11.19	7.00	9.43	6.77
PCB151	360.90	10.39	6.90	8.75	6.67
PCB132	360.88	10.74	7.30	9.04	6.61
PCB156	360.88	11.74	6.90	9.61	7.21
PCB136	360.88	10.25	6.70	8.63	6.25
PCB180	395.32	11.54	7.00	9.73	7.39
PCB187	395.32	11.10	7.00	9.36	7.20
PCB170	395.32	0.00	6.90	9.95	7.30
PCB183	395.32	11.15	7.00	9.39	7.23
PCB177	395.32	11.35	7.00	9.57	7.11
PCB174	395.32	11.30	7.00	9.53	7.14
PCB203	429.77	11.92	7.10	10.05	7.68
PCB201	429.77	11.45	7.50	9.65	7.65
PCB194	429.77	12.33	7.10	10.40	7.83
PCB31	257.54	8.77	5.70	7.37	5.70
PCB76	292.00	9.69	6.00	8.15	6.16
PCB60	292.00	9.88	5.90	8.31	6.14
PCB81			6.10		6.39
PCB48	292.00	9.20	6.10	7.73	5.81
PCB97	326.50	10.13	6.60	8.53	6.32
PCB182	395.32	0.00	7.00		7.23
PCB190	395.32	11.81	7.00	9.96	7.49
PCB196	429.77	11.92	7.50	10.05	7.68
ppDDE	391.00	10.74	5.70	8.75	5.70
ppDDD	391.00	10.95		9.35	
ppDDT	391.00	10.75	5.80	8.98	5.80
mirex	545.54	10.15	6.89	8.53	6.89
photomirex	545.54				
gamma-chlordane	409.80	8.54	6.00	7.23	6.00
alpha-HCH	290.83	0.00	3.81	0.00	3.81
gamma-HCH	290.83	0.00	3.80	0.00	3.80

Source: [a] (Harner 2008), [b] (Gobas 1993), [c] (Shen and Wania 2005).

Table 5: Environmental conditions in the Canadian Arctic and Lake Ontario Food webs used in the model.

	Canadian Arctic	Source	Lake Ontario	Source
Ambient Temperature °C	18.0	(Kelly and Gobas 2001)	Water: 8.0 Air: 14.9	(Arnot and Gobas 2004)
Species internal temperature °C	37.0	(Kelly and Gobas 2001)	Herring gull: 42.0 The others: 8	(Arnot and Gobas 2004)
Oxygen Concentration g/cm^3	0.0003	(Jason Pelish 2003)	Air: 0.0003 Water: 0.0000085	(Thomann and Connolly 1984)

For the Canadian Arctic food web, the dietary preferences of the organisms are displayed in Table 6. The POP concentrations and BAF for caribou and wolf were predicted from the model; for the Lake Ontario food web, the organisms included in the model and there trophic interactions were illustrated in Table 7. The biochemical compositions of consumer organisms' diet were determined from their dietary preference. Trophic levels of the predator organisms were calculated from the basic dietary items, i.e., phytoplankton and sediment for the organisms in the Lake Ontario food web; lichen for the animals in the Arctic food web. The trophic levels for these organisms are shown in Table 6 and 7.

Model Implementation

The bioenergetic bioaccumulation model was constructed in Microsoft ® Office Excel 2003.

There are variables that are animal specific, chemical specific and both chemical and animal specific. Growth efficiency, digestive efficiency for biochemical in diet (i.e., protein, carbohydrate, lipid and water) varies with animal species. Assimilation efficiency, octanol water partitioning coefficient (K_{OW}) and octanol air partitioning coefficient (K_{OA}) vary with POPs. The major calculation involves solving fugacity capacities of POPs in consumers' body, diet and faeces. The parameters required as model input were the environmental POP concentrations, i.e., air and water as respiratory medium, sediment and lichen as diet. Proportions of sediment pore water ventilations were taken into account in the respiratory uptake of POPs in diporeia (5%) and mysids (1.5%) in the Lake Ontario food web. The fugacities of POPs in sediment pore water were the same as they were in the sediment because of chemical partition in sediment and

sediment pore water reached equilibrium. The starting concentrations or fugacities for model calculations are shown in Table 8 for Lake Ontario food web and in Table 9 for Arctic food web.

Input parameters also include K_{OW}, K_{OA}, biochemical composition of consumer organisms' body and diet (i.e., protein, lipid, carbohydrate and water proportions), and digestive efficiency of the animal to each biochemical in diet. The model output included fugacity capacity of POPs in air, water and sediments; and in consumers' body, diet and faeces, these parameters were further used to calculate BAF in terms of a fugacity ratio, and a concentration ratio. The model prediction of BAF is the fugacity ratio of POPs in consumers' body and their respiratory medium (i.e. air for caribou, wolf and herring gulls; water for amphipod and shiner surfperch). The model prediction of BCF is the fugacity ratio of POPs in aquatic consumers' body and the water. The model prediction of BMF is the fugacity ratio of POPs in consumers' body and the diet. The model prediction of TMF is an average factor by which the normalized concentrations or fugacities of POPs increase with a 1.0 increase in trophic level for the Arctic and Lake Ontario food webs.

Table 6: Dietary preferences in the Arctic food-web model.

Prey / Predator	Trophic Level	Lichen	Caribou
Lichen	1	0	0
Caribou	2	100%	0
Wolf	3	0	100%

Table 7: Dietary preferences for the Lake Ontario food-web model.

Prey / Predator	Trophic Level	Sediment	Phytoplankton	Zooplankton	Diporeia	Mysids	Oligochaete	Slimy sculpin	Alewife	Rainbow smelt
Sediment	2.50	0	0	0	0	0	0	0	0	0
Phyto-plankton	1.00	0	0	0	0	0	0	0	0	0
Zooplankton	2.00	0	100%	0	0	0	0	0	0	0
Diporeia	2.63	35%	55%	10%	0	0	0	0	0	0
Mysids	2.83	20%	40%	20%	20%	0	0	0	0	0
Oligochaete	3.28	85%	15%	0	0	0	0	0	0	0
Slimy sculpin	3.49	0	0	25%	65%	10%	0	0	0	0
Alewife	3.18	0	0	75%	15%	10%	0	0	0	0
Rainbow smelt	3.68	0	0	15%	25%	55%	0	5%	0	0
Lake trout	4.32	0	0	0	0	0	0	5%	70%	25%
Herring Gull	4.46	0	0	0	0	0	0	0	45%	55%

Table 8: Input concentrations of the test chemicals for the calculation of BAF in the environment of the Lake Ontario food web.

	Concentration in Water [a] ng/g	Concentration in Air [b] ng/g	Concentration in Sediment [a] ng/g
PCB28	4.25E-05	1.27E-05	17.00
PCB18	6.85E-05	5.25E-06	4.00
PCB22	6.37E-06	5.41E-06	2.00
PCB17	8.08E-06	6.28E-06	0.50
PCB32	4.62E-07	7.00E-06	0.40
PCB66	2.86E-05	1.11E-06	46.00
PCB70	4.08E-05	5.17E-06	23.00
PCB56	8.58E-06	0.00E+00	33.00
PCB52	5.41E-05	6.68E-06	25.00
PCB47	3.72E-05	0.00E+00	12.00
PCB44	4.42E-05	1.27E-06	23.00
PCB74	8.59E-06	3.66E-06	2.70
PCB49	2.06E-05	6.60E-06	11.00
PCB64	7.99E-06	1.67E-06	9.40
PCB42	3.14E-06	1.83E-06	4.70
PCB53	3.95E-06	0.00E+00	0.20
PCB40	3.42E-06	0.00E+00	3.10
PCB101	9.80E-05	2.70E-06	27.00
PCB84	1.29E-05	5.09E-06	21.00
PCB118	2.56E-05	9.54E-07	15.00
PCB110	4.15E-05	1.83E-06	37.00
PCB87	1.49E-05	4.69E-07	20.00
PCB105	1.06E-05	2.39E-07	10.00
PCB95	3.92E-05	0.00E+00	14.00
PCB85	7.79E-06	3.18E-06	9.80
PCB92	3.83E-06	0.00E+00	9.10
PCB82	2.16E-06	0.00E+00	2.90
PCB91	3.18E-05	6.36E-07	5.70
PCB99	7.25E-06	5.80E-07	7.20
PCB153	2.46E-05	2.54E-06	25.00
PCB138	1.22E-05	2.23E-06	15.00
PCB149	1.87E-05	2.23E-06	20.00
PCB146	1.87E-06	4.13E-07	6.70
PCB141	4.08E-06	5.25E-07	7.40

Table 8 continued...

	Concentration in Water [a] ng/g	Concentration in Air [b] ng/g	Concentration in Sediment [a] ng/g
PCB128	0.00E+00	2.39E-07	4.90
PCB151	1.33E-06	1.27E-05	3.70
PCB132	4.73E-06	0.00E+00	11.00
PCB156	0.00E+00	5.57E-08	2.10
PCB136	9.69E-06	1.03E-06	0.70
PCB180	1.17E-05	8.75E-07	13.00
PCB187	7.83E-06	1.35E-06	8.40
PCB170	1.33E-06	3.82E-07	10.00
PCB183	1.09E-06	5.88E-07	3.10
PCB177	4.78E-07	3.34E-07	2.50
PCB174	8.26E-07	7.32E-07	5.10
PCB203	9.86E-07	0.00E+00	8.20
PCB201	0.00E+00	7.32E-07	7.20
PCB194	2.96E-06	8.75E-08	3.70
PCB31	4.32E-05	9.54E-06	17.00
PCB76	3.98E-05	5.17E-06	23.00
PCB60	8.79E-06	8.75E-07	33.00
PCB81	8.34E-06	0.00E+00	33.00
PCB48	3.52E-05	5.49E-06	12.00
PCB97	1.38E-05	1.59E-06	20.00
PCB182	7.83E-06	0.00E+00	8.40
PCB190	1.17E-06	0.00E+00	10.00
PCB196	5.09E-07	4.77E-07	8.20
ppDDE	7.14E-05	4.21E-05	51.00
ppDDD	9.30E-05	7.08E-07	72.00
ppDDT	1.76E-05	1.59E-05	18.00
mirex	1.54E-05	2.78E-07	31.00
Photo-mirex	8.36E-06	0.00E+00	3.90
gamma-chlordane	3.40E-05	4.77E-05	2.10
alphaBHC	2.80E-03	0.00E+00	1.50
lindane	3.00E-04	0.00E+00	1.00

Source: [a] (Oliver and Niimi 1988), [b] (Hoff, Muir et al. 1992).

Table 9: Input fugacities of the test chemicals for the calculation of BAF in the air and lichen of the Arctic food web.

Chemicals	Fugacity in Air Pa	Fugacity in Lichen Pa
beta-HCH	1.65E-12	1.89E-11
HCB	5.70E-10	2.40E-08
Mirex	1.42E-13	3.92E-12
Dieldrin	7.44E-12	3.49E-11
PCB28	5.70E-12	1.15E-10
PCB52	9.44E-12	8.08E-11
P66/95	5.30E-13	3.75E-11
PCB99	2.92E-12	1.51E-11
PCB118	4.18E-12	2.41E-12
PCB153	1.29E-12	1.97E-11
PCB105	4.74E-13	1.02E-12
PCB138	1.64E-12	4.52E-12
182/187	2.61E-12	7.64E-13
PCB180	3.26E-13	4.21E-13
170/190	1.04E-12	2.56E-13
PCB194	4.20E-13	2.35E-13
PCB206	2.78E-13	2.35E-13

Source: (Kelly and Gobas 2001)

Model Performance Analysis

The model performance analysis involved the comparison of the model predicted bioaccumulation factor for each POP, *i*, $BAF_{P,i,}$ to the biota concentration, $BAF_{O,i,}$ for all POPs for which relevant observed concentration data were available. To do this, we used measured POP concentrations in air, water and sediment as input parameters for the calculation of the POP concentrations in the various biological organisms considered in the model. We then calculated the $BAF_{P,i}$ by dividing the calculated concentration in the organisms by the concentration in the respiratory medium (water or air). The $BAF_{O,i}$ was derived by dividing measured POP concentration in biota by the measured concentration in the respiratory medium (water or air). Empirical POP concentration data were available for all biota considered in the model except for phytoplankton.

Model performance was analyzed by comparing observed BAFs in biota with those predicted. The observed concentrations in biota and the ambient environment (i.e. sediment, air or water) were obtained from previous studies on the same food web for Canadian Arctic (Kelly and Gobas 2001) and Lake Ontario (Clark, Norstrom et al. 1987; Oliver and Niimi 1988; Braune and Norstrom 1989; Hoff, Muir et al. 1992; Gobas 1993).

To quantitatively express model performance, we used the mean model bias (MB), which is derived on a species-specific basis. MB was calculated for individual POP and for each biota, j, in the model:

$$MB_j = 10^{\left(\sum_{i}^{n} \frac{\left(\log\left(BAF_{P,i} / BAF_{O,i}\right)\right)}{n}\right)} \quad \textbf{(41)}$$

In essence, MB_j is the geometric mean (assuming a Log-normal distribution of the ratio $BAF_{P,i} / BAF_{O,i}$) of the ratio of predicted and observed BAFs for all POPs, i, in a particular species j included in the analysis. MB is a measure of the systematic over-prediction (MB>1) or under-prediction (MB<1) of the model (Arnot 2003). For example, a MB of 2 indicates that the model over-predicts the empirical POP concentrations in the species of interest on average by a factor of 2. Conversely, a model bias of 0.5 indicates that the model under-predicts PCB congener concentrations on average by a factor of 2. It should be stressed that in the calculation of MB, over- and under-estimations of the observed BAF values for individual POP have a tendency to cancel out. Hence, MB tracks the central tendency of the ability of the model to predict POP concentrations.

The variability of over- and under-estimation of measured values is represented by the 95% confidence interval of MB (i.e. 95% CI = antilog (geometric mean ± ($tv_{,0.05}$ × standard deviation)) (Arnot 2003). The 95% confidence interval represents the range of predicted BAFs that includes 95% of the observed BAFs. Due to the Log - normal distribution of the ratio of predicted and observed BAFs, this variability can be expressed as a factor (rather than a term) of the geometric mean (Arnot 2003).

Model predicted BAFs were plotted against those of the observed ones in consumer organisms of Lake Ontario food web; model predicted lipid normalized POP concentrations were plotted against those of the observed ones in caribou and wolf of the Canadian Arctic food web. PCBs were divided into four groups according to their ability to be metabolized in mammals. Group I PCBs are the most persistent and least likely to be enzymatically metabolized and most suitable for model performance testing (Kelly and Gobas 2003). Group IV PCBs are the least persistent PCBs and are most likely to be

metabolized. PCB 153, PCB 182, PCB 180 and PCB 206 belong Group I that are known as the least likely to be metabolized PCBs (Boon, vanderMeer et al. 1997; Fraser, Burkow et al. 2002; Kelly and Gobas 2003). Because metabolic transformation of chemicals was considered as zero during model parameterization, model performance on analysis only included for PCB 153, PCB 180, PCB 206, HCB, beta-HCH and Dieldrin, which are least likely to be metabolized was only included. In addition, relationships between Log MB and Log K_{OW} or Log K_{OA} were examined by plotting Log MB as a function of K_{OW} or K_{OA} for each consumer organisms in the model.

Sensitivity Analysis

The purpose of the sensitivity analysis is to assess the relative importance of the different state variables of the model. Sensitivity analysis is useful in the assessment of the internal mechanics of the model, hence can be used to characterize potential errors in the model and to develop a better understanding of the relationship between the processes that control the behaviour of POPs in the food webs.

The sensitivity analysis examined the response of the BAF to the change of the following model parameters: K_{OW}, K_{OA}, oxygen uptake efficiency, E_{OX}; Chemical uptake efficiency through ventilation, E_R; chemical assimilation efficiency constant, A and B; animal digestive efficiency, α_{Pro}, α_{Lip}; and animal growth efficiency, e; fraction of lipid, $F_{Lip,\ B}$, and protein, $F_{Pro,\ B}$, in consumer's body. The contribution to the variance of model outcomes by each of these parameters was examined by Monte Carlo simulation using Crystal Ball (2007). The state variables for different biota were given different mean, standard deviation and their own proper range to reflect the variations of the input parameters. The mean for each variable was set at the same value as used in model. The

standard deviation of the mean for each state variable in Monte Carlo simulation was set at 1/10 of the mean or at a constant value (e.g. 0.05). The range of each variable was further constrained by minimum and maximum realistic value (e.g. maximum digestibility is 1). Within this range, determined by its standard deviation, a normal distribution was assumed.

In Monte Carlo simulation, the distributions of the state variables are repeatedly sampled and the sampled values are used in the model to produce a distribution of model outcomes (i.e. in our model, the BAF). This distribution of model outcomes represents the variability in the model outcomes due to variability in the model's state variables. Model sensitivity analysis was assessed for caribou, wolf, rainbow smelt and herring gull representing herbivorous mammals, carnivorous mammals, fish and birds, correspondingly. The model state variables that were included in the Monte Carlo simulation, their values and distributions are summarized in Table 10 and 11.

Model Uncertainty Analysis

The model uncertainty analysis involved Monte Carlo simulation to assess the effect of uncertainty or error in the model state variables on the model outcome (i.e. the BAF). This methodology represents model state variables by statistical distributions. The distribution represents the uncertainty in the value of the model variable selected for use in the model. The distribution represents how the state variable may vary spatially, temporally and among individuals of a species or other factors. The distribution of model outcomes represents the variability in the model outcomes due to variability and error in the state variables (e.g., protein content, carbohydrate content, lipid content, etc). The uncertainty in all state variables contributes to the magnitude of the range of model

outcomes, but the uncertainties in these state variables are not necessarily additive (Arnot 2003). The 95% confidence intervals of model predicted BAFs of PCB 153 for Barren-ground caribou and Arctic wolf, and Lake Ontario rainbow smelt and herring gull were analyzed in the uncertainty analysis. The parameters included in the Monte Carlo simulation are oxygen uptake efficiency (E_{OX}), chemical uptake efficiency through ventilation (E_R), chemical assimilation efficiency (E_D), animal digestive efficiency (α_{pro}, α_{lip}, α_{ch}), and animal growth efficiency (e), but not K_{OW} and K_{OA}. Each state variable were assumed to be normal distribution, n=10,000. The values and distributions of the model state variables that were included in the Monte Carlo simulation in the uncertainty analysis of the model are summarized in Table 10 and 11, excluding chemical K_{OW} and K_{OA}.

Monte Carlo simulations were conducted within the Excel spreadsheets using Crystal Ball (2007). There are two assumptions in the uncertainty analysis. First, only model parameters that were found to be sensitive (i.e. contribute to 0.1% of variance in the sensitivity analysis) were included in the uncertainty analysis. Hence, relatively insensitive model parameters were excluded from the analysis. The uncertainties in these model variables were assumed to have an insignificant effect on the uncertainty in the model outcome (i.e. BAF). For example, mean air temperature is not used in the bioaccumulation calculation of many species in the food web model and is not a sensitive variable in the calculation of bioaccumulation in air breathing organisms where the variable is used. Biotic parameters such as the organism's water content and absorption efficiency of water were also considered as insensitive model variables. This is because water does not contribute significantly to the storage capacity of hydrophobic chemicals

like PCBs in biota. In addition, because most of the organisms do not have significant carbohydrate content in the body, the carbohydrate content and uptake efficiency for carbohydrate in these animals were considered as insensitive parameters. Second, uncertainties in the feeding preferences were excluded from the Monte Carlo simulation due to several reasons: there was insufficient information to characterize the uncertainties in these state variables; feeding preferences were highly interdependent and therefore unsuitable for Monte Carlo simulations; feeding preferences were not sensitive variables as long as changes in feeding preferences did not involve large changes in trophic level of the consumer organism's diet items.

Table 10: State variables included in Monte Carlo simulations with their mean, standard deviation and range to analyze model sensitivity and uncertainty for rainbow smelt and herring gull.

Chemical Parameters	Symbol	Distribution	Mean	Stdv.	Min	Max
Log transformed Octanol-water partition coefficient at 8°C	Log K_{OW}	Normal	6.90E+00	5.00E-01	4.5 E+00	9.5 E+00
Log transformed Octanol-air partition coefficient at 8°C	Log K_{OA}	Normal	1.07E+01	5.00E-01	9.00E+00	1.25 E+01
Log transformed Octanol-water partition coefficient at 42oC	Log K_{OW}	Normal	6.95E+00	5.00E-01	5.00E+00	9.00 E+00
Log transformed Octanol-air partition coefficient at 42oC	Log K_{OA}	Normal	9.02E+00	5.00E-01	7.00E+00	1.10E+01

Biological parameters

Rainbow smelt	Symbol	Distribution	Mean	Stdv.	Min	Max
Fraction of protein in consumer's body	$F_{Pro,\ B}$	Normal	2.00E-01	2.00E-02	1.00E-01	3.00E-01
Fraction of lipid in consumer's body	$F_{Lip,\ B}$	Normal	4.00E-02	4.00E-03	1.00E-02	8.00E-02
Net Growth Efficiency	e	Normal	2.00E-01	2.00E-02	1.40E-01	2.60E-01
Chemical assimilation efficiency constant A	A	Normal	3.00E-07	3.00E-08	2.00E-07	4.00E-07
Chemical assimilation efficiency constant B	B	Normal	2.00E+00	5.00E-02	1.80E+00	2.15E+00
Oxygen uptake efficiency	E_{OX}	Normal	8.00E-01	5.00E-02	6.00E-01	9.60E-01
Consumer digestive efficiency of lipid	α_{Lip}	Normal	9.20E-01	5.00E-02	7.31E-01	9.95E-01
Consumer digestive efficiency of protein	α_{Pro}	Normal	6.00E-01	5.00E-02	4.33E-01	7.67E-01

Table 10 continued...

Phytoplankton	Symbol	Distribution	Mean	Stdv.	Min	Max
Fraction of protein in consumer's body	$F_{Non\_lip,B}$	Normal	1.95E-01	1.95E-02	1.00E-01	3.00E-01
Fraction of lipid in consumer's body	$F_{Lip,B}$	Normal	5.00E-03	5.00E-04	3.50E-03	6.50E-03
Net Growth Efficiency	e	Normal	8.00E-02	8.00E-03	6.00E-02	9.9E-02

Zooplankton	Symbol	Distribution	Mean	Stdv.	Min	Max
Fraction of protein in consumer's body	$F_{Pro,B}$	Normal	2.00E-01	2.00E-02	1.00E-01	3.00E-01
Fraction of lipid in consumer's body	$F_{Lip,B}$	Normal	2.00E-02	2.00E-03	1.00E-02	3.00E-02
Net Growth Efficiency	e	Normal	3.30E-01	3.30E-02	2.40E-01	4.2E-01
Chemical assimilation efficiency constant A	A	Normal	3.00E-07	3.00E-08	2.00E-07	4.00E-07
Chemical assimilation efficiency constant B	B	Normal	2.00E+00	5.00E-02	1.80E+00	2.15E+00
Oxygen uptake efficiency	E_{OX}	Normal	8.00E-01	5.00E-02	5.00E-01	9.60E-01
Consumer digestive efficiency of lipid	α_{Lip}	Normal	7.50E-01	5.00E-02	6.00 E-01	9.00E-01
Consumer digestive efficiency of protein	α_{Pro}	Normal	6.00E-01	5.00E-02	4.33E-01	7.67E-01
Consumer digestive efficiency of carbohydrate	α_{Ch}	Normal	9.00E-01	5.00E-02	7.50E-01	9.95E-01

Table 10 continued...

Diporeia	Symbol	Distribution	Mean	Stdv.	Min	Max
Fraction of protein in consumer's body	$F_{Pro,\ B}$	Normal	2.00E-01	2.00E-02	1.00E-01	3.00E-01
Fraction of lipid in consumer's body	$F_{Lip,\ B}$	Normal	3.00E-02	3.00E-03	2.00E-02	4.00E-02
Net Growth Efficiency	e	Normal	2.00E-01	2.00E-02	1.40E-01	2.60E-01
Chemical assimilation efficiency constant A	A	Normal	3.00E-07	3.00E-08	2.00E-07	4.00E-07
Chemical assimilation efficiency constant B	B	Normal	2.00E+00	5.00E-02	1.80E+00	2.15E+00
Oxygen uptake efficiency	E_{OX}	Normal	8.00E-01	5.00E-02	5.00E-01	9.60E-01
Consumer digestive efficiency of lipid	α_{Lip}	Normal	7.50E-01	5.00E-02	6.00 E-01	9.00E-01
Consumer digestive efficiency of protein	α_{Pro}	Normal	7.50E-01	5.00E-02	6.00 E-01	9.00E-01
Consumer digestive efficiency of carbohydrate	α_{Ch}	Normal	7.50E-01	5.00E-02	6.00 E-01	9.00E-01
Proportion of sediment pore water ventilation	m_p	Normal	5.00E-02	5.00E-03	3.50E-02	6.50E-02

Table 10 continued...

Mysids	Symbol	Distribution	Mean	Stdv.	Min	Max
Fraction of protein in consumer's body	$F_{Pro,\ B}$	Normal	2.00E-01	2.00E-02	1.00E-01	3.00E-01
Fraction of lipid in consumer's body	$F_{Lip,\ B}$	Normal	3.00E-02	3.00E-03	2.00E-02	4.00E-02
Net Growth Efficiency	e	Normal	3.30E-01	3.30E-02	2.40E-01	4.2E-01
Chemical assimilation efficiency constant A	A	Normal	3.00E-07	3.00E-08	2.00E-07	4.00E-07
Chemical assimilation efficiency constant B	B	Normal	2.00E+00	5.00E-02	1.80E+00	2.15E+00
Oxygen uptake efficiency	E_{OX}	Normal	8.00E-01	5.00E-02	5.00E-01	9.60E-01
Consumer digestive efficiency of lipid	α_{Lip}	Normal	7.50E-01	5.00E-02	6.00 E-01	9.00E-01
Consumer digestive efficiency of protein	α_{Pro}	Normal	7.50E-01	5.00E-02	6.00 E-01	9.00E-01
Consumer digestive efficiency of carbohydrate	α_{Ch}	Normal	7.50E-01	5.00E-02	6.00 E-01	9.00E-01
Proportion of sediment pore water ventilation	m_p	Normal	1.50E-02	1.50E-03	1.00E-02	3.00E-02

Table 10 continued...

Slimy sculpin	Symbol	Distribution	Mean	Stdv.	Min	Max
Fraction of protein in consumer's body	$F_{Pro,\ B}$	Normal	2.00E-01	2.00E-02	1.00E-01	3.00E-01
Fraction of lipid in consumer's body	$F_{Lip,\ B}$	Normal	8.00E-02	8.00E-03	6.00E-02	1.00E-01
Net Growth Efficiency	e	Normal	2.00E-01	2.00E-02	1.40E-01	2.60E-01
Chemical assimilation efficiency constant A	A	Normal	3.00E-07	3.00E-08	2.00E-07	4.00E-07
Chemical assimilation efficiency constant B	B	Normal	2.00E+00	5.00E-02	1.80E+00	2.15E+00
Oxygen uptake efficiency	E_{OX}	Normal	8.00E-01	5.00E-02	5.00E-01	9.60E-01
Consumer digestive efficiency of lipid	α_{Lip}	Normal	9.50E-01	5.00E-02	7.00 E-01	9.95E-01
Consumer digestive efficiency of protein	α_{Pro}	Normal	5.00E-01	5.00E-02	3.50 E-01	6.50E-01

Table 10 continued...

Alewife	Symbol	Distribution	Mean	Stdv.	Min	Max
Fraction of protein in consumer's body	$F_{Pro,\ B}$	Normal	2.00E-01	2.00E-02	1.00E-01	3.00E-01
Fraction of lipid in consumer's body	$F_{Lip,\ B}$	Normal	7.00E-02	7.00E-03	5.00E-02	9.00E-01
Net Growth Efficiency	e	Normal	1.00E-02	1.00E-03	7.00E-03	1.30E-02
Chemical assimilation efficiency constant A	A	Normal	3.00E-07	3.00E-08	2.00E-07	4.00E-07
Chemical assimilation efficiency constant B	B	Normal	2.00E+00	5.00E-02	1.80E+00	2.15E+00
Oxygen uptake efficiency	E_{OX}	Normal	8.00E-01	5.00E-02	5.00E-01	9.60E-01
Consumer digestive efficiency of lipid	α_{Lip}	Normal	9.50E-01	5.00E-02	7.00 E-01	9.95E-01
Consumer digestive efficiency of protein	α_{Pro}	Normal	5.00E-01	5.00E-02	3.50 E-01	6.50E-01

Table 10 continued...

Herring gull	Symbol	Distribution	Mean	Stdv.	Min	Max
Fraction of protein in consumer's body	$F_{Pro,\ B}$	Normal	8.70E-01	5.00E-02	6.00 E-01	9.90E-01
Fraction of lipid in consumer's body	$F_{Lip,\ B}$	Normal	9.00E-02	9.00E-03	6.50E-02	1.20E-01
Net Growth Efficiency	e	Normal	3.50E-03	3.50E-04	2.00E-03	5.00E-03
Chemical assimilation efficiency constant A	A	Normal	2.40E-09	2.40E-10	1.00E-09	3.20E-09
Chemical assimilation efficiency constant B	B	Normal	1.04E+00	5.00E-02	0.80E+00	1.20E+00
Oxygen uptake efficiency	E_{OX}	Normal	3.00E-01	3.00E-02	2.00E-01	4.00E-01
Consumer digestive efficiency of lipid	α_{Lip}	Normal	9.30E-01	5.00E-02	7.00 E-01	9.95E-01
Consumer digestive efficiency of protein	α_{Pro}	Normal	8.60E-01	5.00E-02	6.00 E-01	9.90E-01

Table 11: State variables included in Monte Carlo simulation with their mean, standard deviation and minimum and maximums values to determine model sensitivity and uncertainty tests for caribou and wolf.

Chemical Parameters	Symbol	Distribution	Mean	Stdv.	Min	Max
Log transformed Octanol-water partition coefficient at 8C	Log K_{OW}	Normal	6.92E+00	5.00E-01	4.50E+00	1.00E+01
Log transformed Octanol-air partition coefficient at 8C	Log K_{OA}	Normal	8.65 E+00	5.00E-01	6.00E+00	1.20E+01

Biological parameters

Caribou	Symbol	Mean	Stdv.	Min	Max
Fraction of protein in consumer's body	$F_{Pro,\ B}$	2.27E-01	2.27E-02	1.60E-01	3.00E-01
Fraction of lipid in consumer's body	$F_{Lip,\ B}$	8.00E-02	8.00E-03	5.50E-02	1.00E-01
Net Growth Efficiency	e	1.50E-02	1.50E-03	1.00E-02	2.00E-02
Chemical assimilation efficiency constant A	A	2.90E-08	2.90E-09	2.00E-08	4.00E-08
Chemical assimilation efficiency constant B	B	1.20E+00	1.2E-01	9.00E-01	1.5E+00
Oxygen uptake efficiency	E_{OX}	1.50E-01	1.50E-02	1.00E-01	2.00E-01
Consumer digestive efficiency of lipid	α_{Lip}	6.50E-01	5.00E-02	4.50E-01	8.50E-01
Consumer digestive efficiency of protein	α_{Pro}	5.00E-01	5.00E-02	3.50E-01	6.50E-01
Consumer digestive efficiency of carbohydrate	α_{Ch}	5.00E-01	5.00E-02	3.50E-01	6.50E-01

Table 11 continued...

Wolf	Symbol	Mean	Stdv.	Min	Max
Fraction of protein in consumer's body	$F_{Pro,\ B}$	2.00E-01	2.00E-02	1.40E+00	2.60E+00
Fraction of lipid in consumer's body	$F_{Lip,\ B}$	9.00E-02	9.00E-03	6.00E-02	1.20E-01
Net Growth Efficiency	e	5.00E-03	1.00E-03	1.00E-03	5.50E-02
Chemical assimilation efficiency constant A	A	1.55E-09	1.55E-10	1.00E-09	2.00E-09
Chemical assimilation efficiency constant B	B	1.01E+00	1.01E-01	7.00E-01	1.35E+00
Oxygen uptake efficiency	E_{OX}	1.50E-01	1.50E-02	1.00E-01	2.00E-01
Consumer digestive efficiency of lipid	α_{Lip}	9.80E-01	5.00E-02	7.55E-01	9.95E-01
Consumer digestive efficiency of protein	α_{Pro}	7.00E-01	5.00E-02	5.43E-01	9.00E-01

Results and Discussion

Chemical Flux

The flux of PCB180 in Lake Ontario rainbow smelt, herring gull, barren-ground caribou and Arctic wolf are displayed in Figures 2 to 5. For both terrestrial and aquatic animals, diet was the major route of PCB 180 uptake. For herring gull, caribou and wolf, uptake and elimination of PCB 180 through respiration were negligible. However, for aquatic animals (e.g. rainbow smelt), respiration was an important route for chemical exchange between biota and water. Elimination of PCB 180 for rainbow smelt through the most to the least important route was growth dilution, respiration and fecal egestion. Elimination of PCB 180 for herring gull, caribou and wolf through the most to the least important route was fecal egestion and growth dilution, accordingly. Chemical total uptake and elimination in the model were all balanced as shown in the figures for rainbow smelt, herring gull, caribou and wolf.

For water breathing animals, respiratory uptake is an important contribution to the bioaccumulation of the investigated chemicals. There are two reasons for this. Firstly, chemical uptake efficiency, E_R through respiration for water breathing animals is high (around 0.8), whereas for air breathing animals, the E_R was between 0.1 and 0.3. Secondly, chemical concentrations in water were relatively higher than the chemical in the air for Lake Ontario and Canadian Arctic air, for example, PCB 180 in Canadian Arctic air was 1.3×10^{-16} mol/m^3 versus 3.0×10^{-11} mol/m^3 in Lake Ontario water.

Figure 2: Flux diagram for PCB 180 in Lake Ontario rainbow smelt.

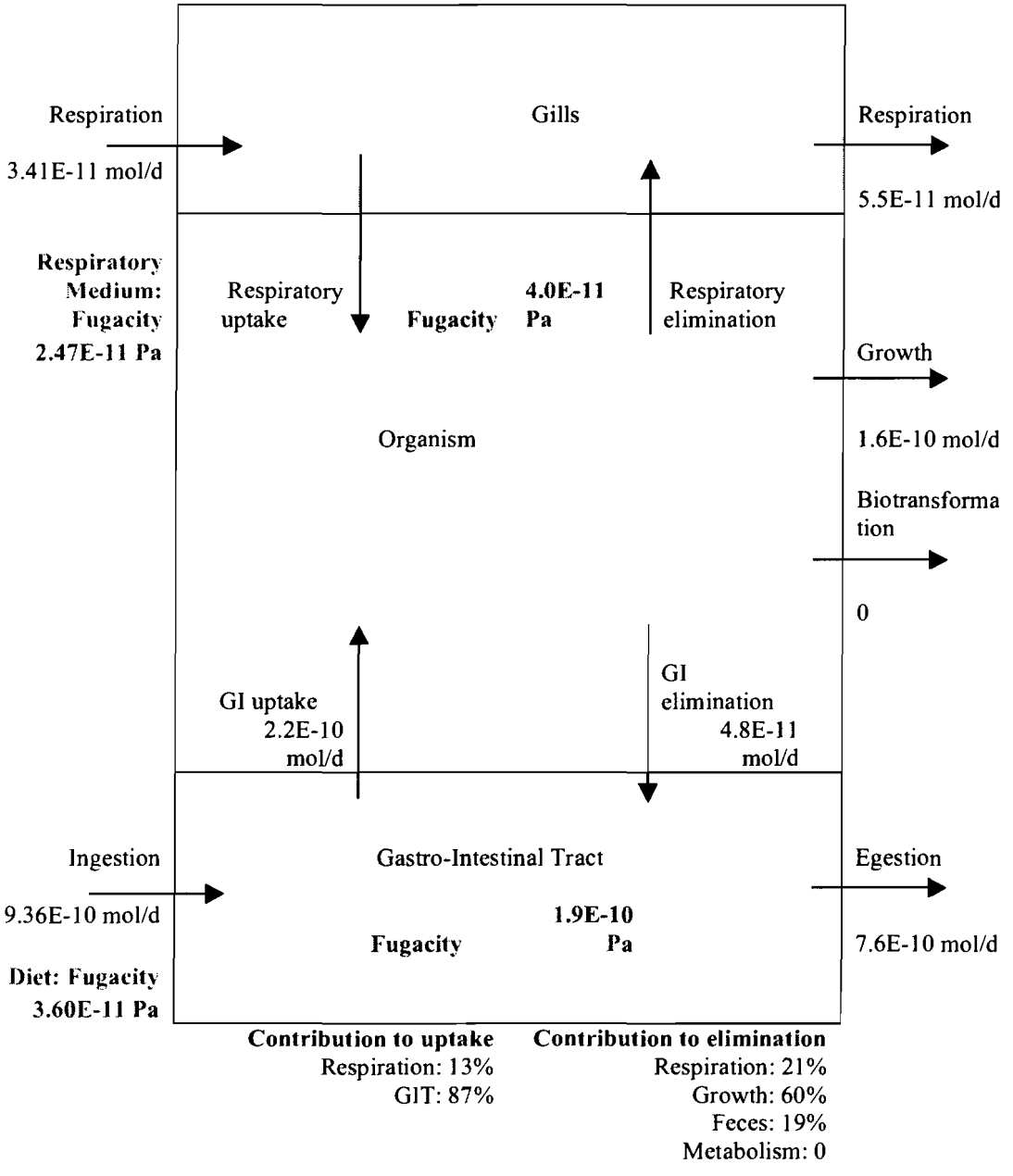

Figure 3: Flux diagram for PCB 180 in Lake Ontario herring gull.

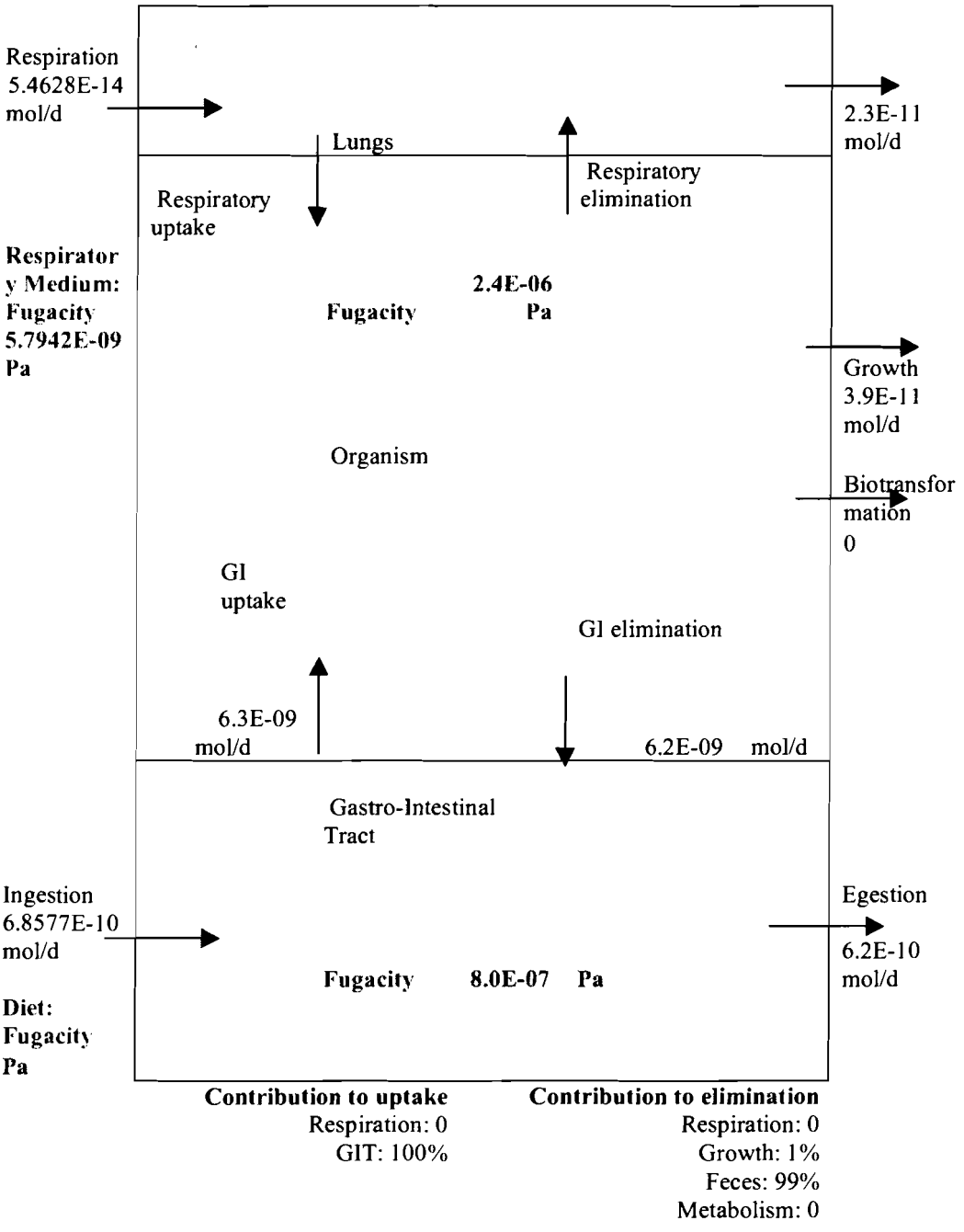

Figure 4: Flux diagram for PCB 180 in the barren-ground caribou.

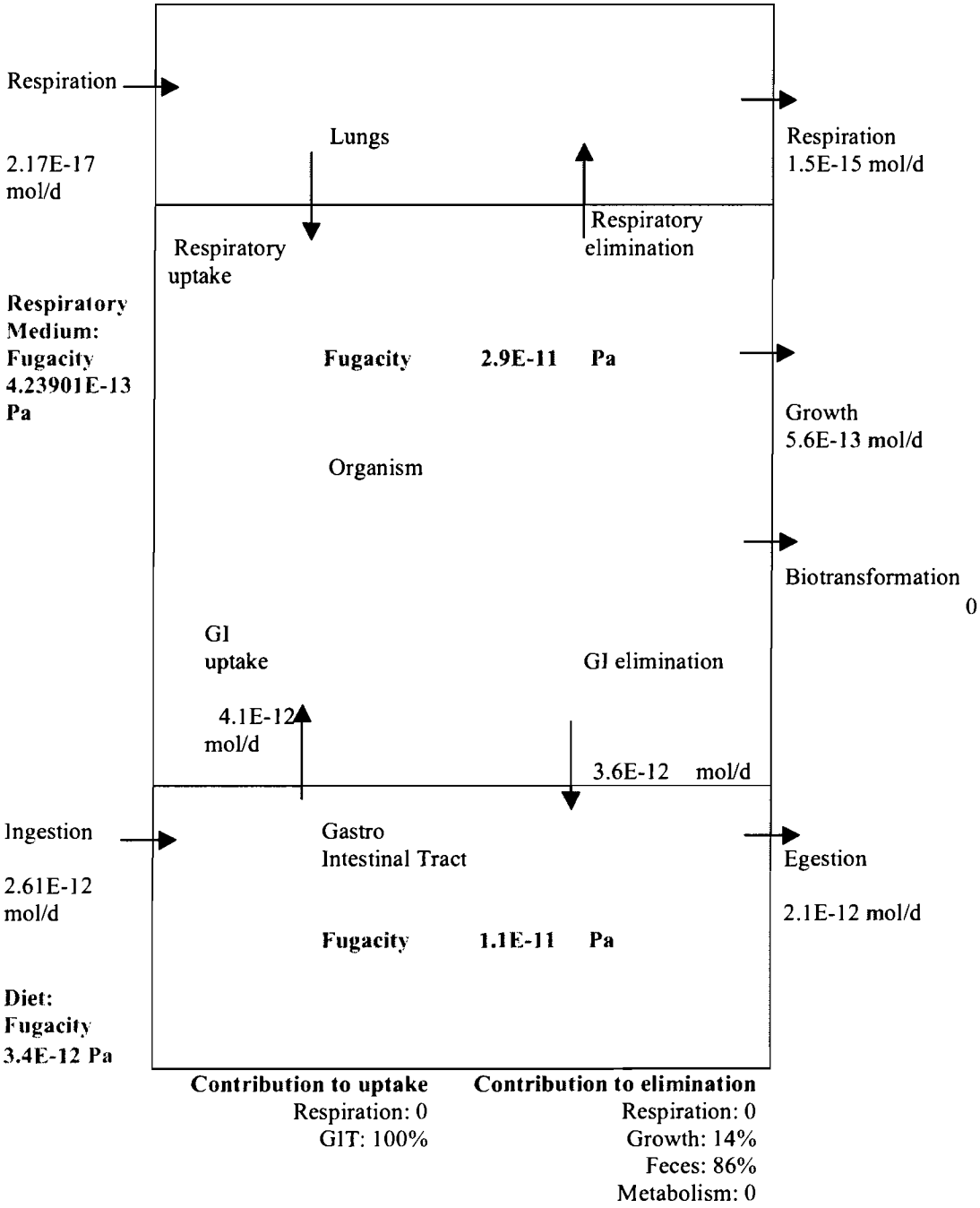

Figure 5: Flux diagram of PCB 180 in the Canadian Arctic wolf.

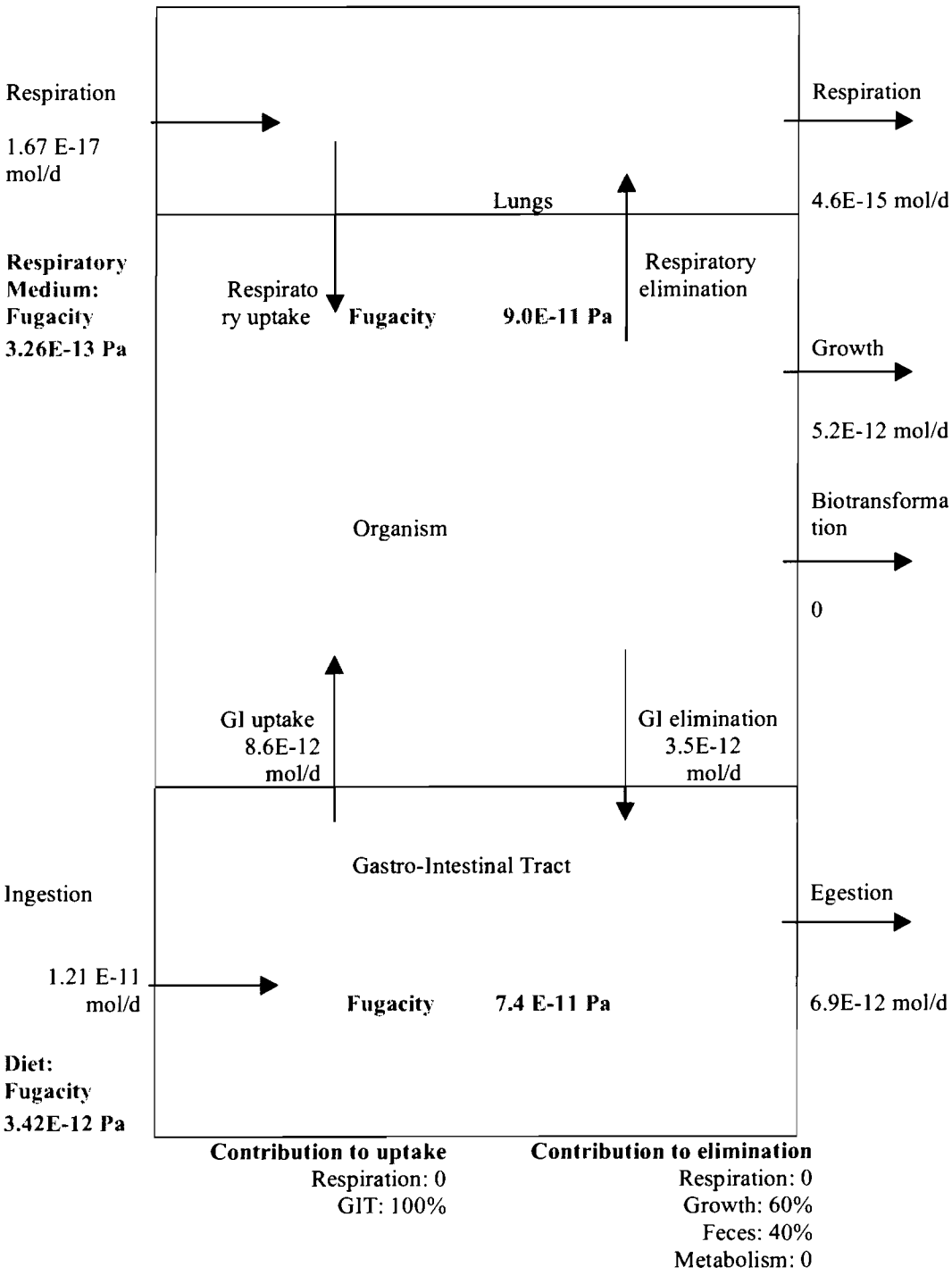

Energy Budget

Figure 6 to Figure 9 illustrate the energy budget of the Lake Ontario rainbow smelt, herring gull, the barren-ground caribou and Arctic wolf, correspondingly. Figure 6 illustrates that rainbow smelt spends 46% of its energy on respiration (i.e. lost as heat via respiration), loses 43% of the energy through fecal egestion, and spends 11% on growth and production of the total energy assimilated. The feeding rate of smelt is much higher than the rate of fecal egestion and growth. This indicates that the rate of POP intake through diet is faster then the rate of elimination through fecal egestion. Figure 7 illustrates that the Lake Ontario herring gull spends 88% of its energy on respiration (i.e. lost as heat via respiration) and the majority of the remainder is lost through fecal egestion. Growth and production energy expenditure is insignificant in herring gull. This implies that the major route of chemical elimination in herring gull is through fecal egestion and respiration, rather than through growth dilution. However, feeding rate of the herring gull was much higher than the rate of fecal egestion and growth, this indicates that the rate of POP intake through diet is faster then the rate of elimination through fecal egestion.

Figure 8 illustrates that the barren-ground caribou spends 50% of its energy on respiration (i.e. lost as heat via respiration). The rest of the energy is lost through fecal egestion (growth and production counted only 1% of the total energy assimilated). This implies that the major route of chemical elimination is through fecal egestion and expiration. The feeding rate of the caribou is much higher than the rate of fecal egestion and growth. This indicates that the rate of POP intake through diet is faster then the rate of elimination through fecal egestion. Figure 9 illustrates that the loss of energy through

respiration in the Arctic wolf (77%), as a carnivore, is much greater than that of barren-ground caribou's (50%), as an herbivore. The Arctic wolf loses 22% of the energy through fecal egestion, whereas growth and production account for only 1% of the total energy assimilated. The feeding rate wolf is much higher than the rate of fecal egestion and growth; this indicates that the rate of POP intake through diet is faster then the rate of elimination through fecal egestion.

Figure 6: Rainbow smelt energy diagrams.

a

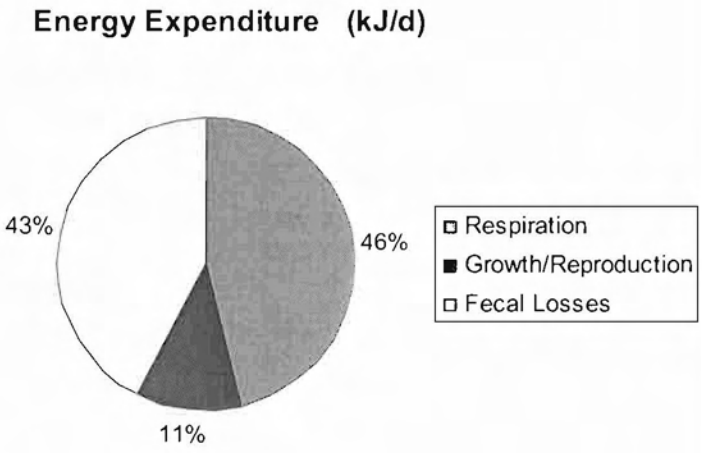

b

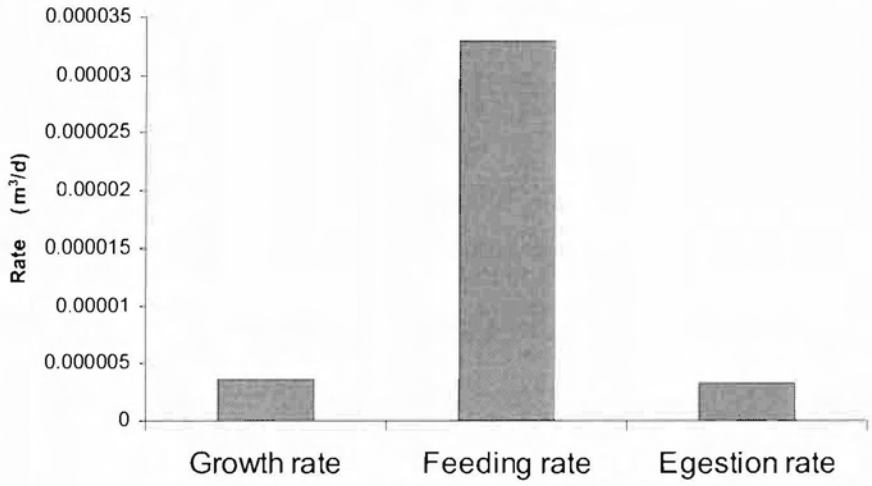

Figure 7: Herring gull energy diagrams.

a

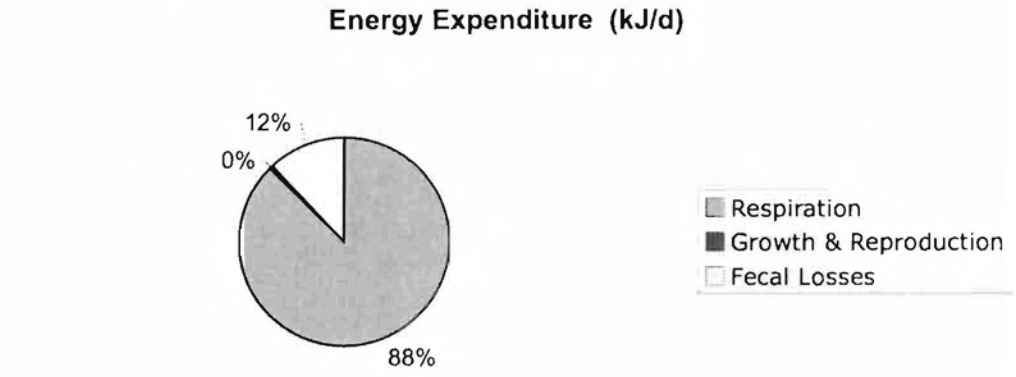

b

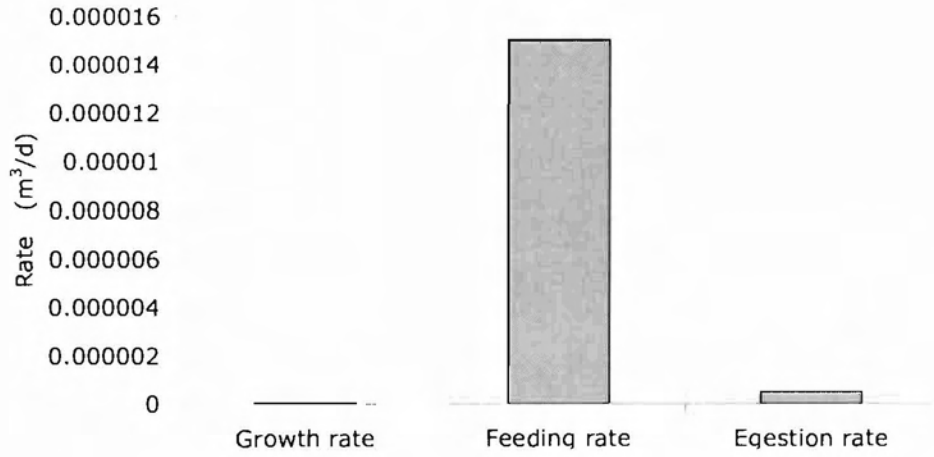

Figure 8: Barren-ground caribou energy diagram.

a

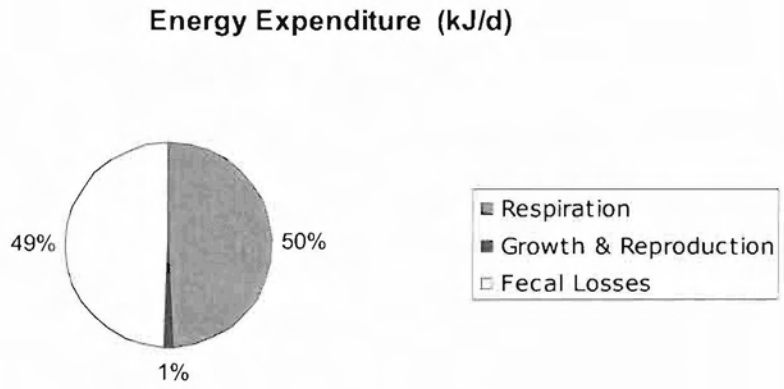

b

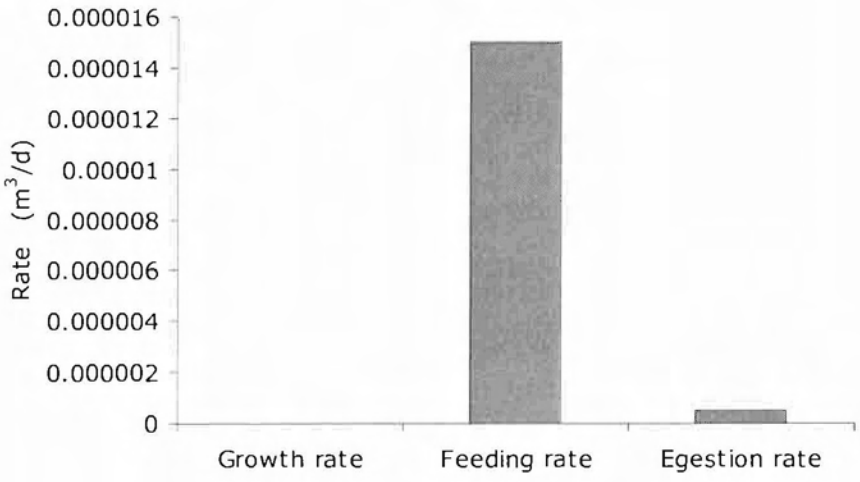

Figure 9: Canadian Arctic wolf energy diagram.

a

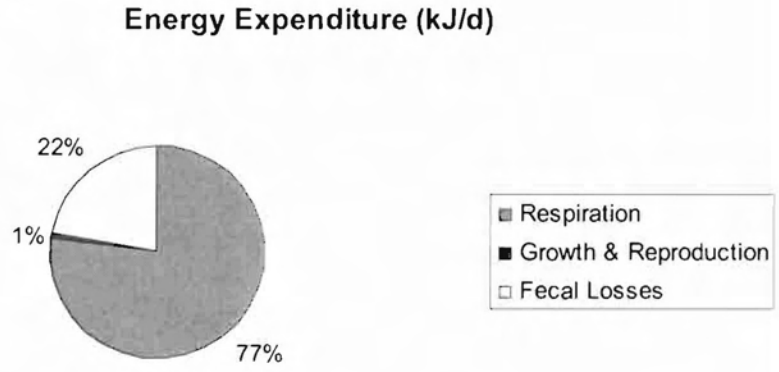

b

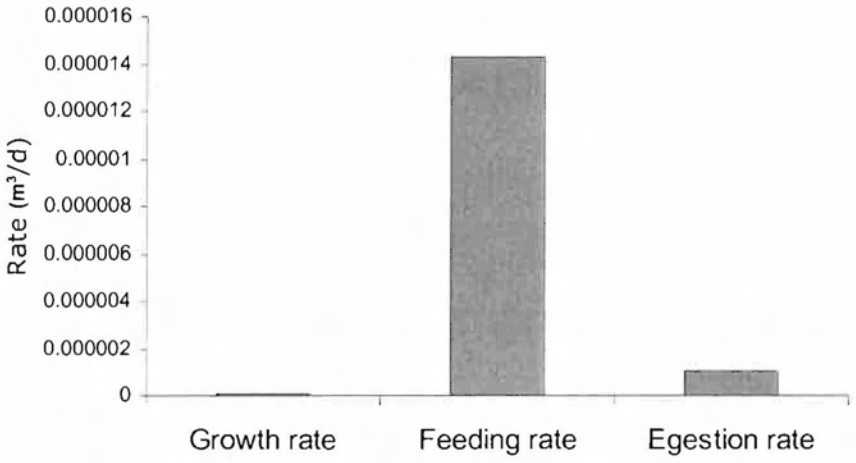

Bioaccumulation In the Aquatic and Terrestrial Food Webs

Model calculated Log BAFs and Log BMFs in caribou and wolf, and Log TMFs (based on lipid normalized concentrations) for the Arctic food web for various POPs are displayed in Table 12. Model calculated Log BAF*and Log BMF* in caribou and wolf, and Log TMF*s (based on fugacity) for the Arctic food web for various POPs are displayed in Table 13. The *p*-values and 95% confidence intervals for the Log TMFs and Log TMF*s are also presented in the table. BAFs of POPs in terms of fugacity ratios for caribou ranged from 4.8 for PCB 170/190 to 380 for PCB 66/95; and for wolf ranged from 33 for PCB 170/190 to 1.05×10^4 for PCB 66/95. BAFs in terms of lipid based concentration ratio for caribou ranged from 1.19×10^9 for PCB 31 to 1.40×10^9 for PCB 66/95, for wolf it ranged from 2.76×10^{10} for hexachlorobenzene (HCB) to 3.89×10^{12} for PCB 66/95. The concentration ratio of BAF in wolf is about 10 times higher than that of caribou's, which demonstrates that these POPs are bioaccumulative in the lichen-caribou-wolf food chain. The Log TMF and Log TMF* of all selected POPs in the Canadian Arctic food web are greater than zero, this indicates that the POPs are biomagnifying in the lichen-caribou-wolf food web. The TMFs for the Arctic food web ranged from 49 for HCB to 63 for mirex. This indicates the lipid-normalized concentration for HCB increased 49 fold and for mirex, 63 fold, for every 1-step increase of trophic level. The *p*-values for the Arctic TMF are higher than the commonly used significant *p*-value (0.05). This is because there are only three organisms (lichen, caribou and wolf) included in the Arctic food web. The highest *p*-values for the Log TMF of the POPs in the arctic food web is 0.08, which indicates that the probability that the distribution the POP concentrations in the organisms result from random distribution is 8%. In other words,

the probability that the distribution of the POP concentrations in the organisms is the result of organism trophic level variation is 92%. This means it is 92% sure that the concentration of POPs increased with increased trophic level, given the small sample size (3).

As shown in Figure 4 and Figure 5, chemical uptake for caribou and wolf is mainly through the diet. The digestive processes in the GIT of consumers concentrate the chemical in the gut lumen and hence elevate the fugacity of the chemical above that of the consumer's diet (Figure 5). The wolf spends 77% (compared to 50% in caribou) of its energy on respiration, and only 22% of the energy (compared to 49% in caribou) is lost through fecal egestion (Figure 8 & 9). Fecal elimination of the POPs in wolf is therefore not as large as that in caribou, hence the BMF*s in wolf is greater than that in caribou. This can be generalized to herbivorous and carnivorous mammals that have the similar energy expenditures and biological processes.

Model predicted Log BAF, Log BMF and Log BCF in rainbow smelt, and Log TMF for the Lake Ontario food web are displayed in Table 14. Table 15 shows the model predicted Log BAF*, Log BMF* and Log BCF* in rainbow smelt, and Log TMF* for the Lake Ontario food web. The Log BCF*s in rainbow smelt were negative, in other words, the BCF*s in terms of fugacity ratio were less than 1. This indicates BCF*s underestimates the accumulation of the POPs when only considering respiratory uptake of the POPs. On the other hand, all of the BMF*s for the smelt were positive, indicating that diet is a much more important route of the POP intake in rainbow smelt.

Table 16 displays the model predicted Log BAFs and Log BMFs of selected organic chemicals in herring gull. Model predicted Log BAF* and Log BMF* for

selected chemicals are shown in Table 17. The predicted BAF in herring gull for POPs are about 100 times higher than they are in rainbow smelt. In the Lake Ontario food web, the predicted BAFs for POPs increase with increasing trophic levels, which is consistent with previous BAF model prediction in the same food web (Arnot and Gobas 2004). Almost all the Log TMF and Log TMF* of selected POPs in the Lake Ontario food web are greater than zero. This indicates that the POPs are biomagnifying in the Lake Ontario food web. The TMF for the Lake Ontario food web ranged from 1.2 for alpha-BHC to 13 for PCB60. This indicates that the concentration of alpha-BHC increased 1.22 fold and for PCB60, 13 fold, for every 1-step increase in trophic level. Most of the *p*-values for POPs in the Lake Ontario food web were less than 0.05, which indicates that the probability that the distribution the POP concentrations in the organisms were due to random distribution was less than 5%. In other words, it means there is more than 95% certainty that the concentration of POPs in Lake Ontario food web increased with increased trophic level.

The bioaccumulation and trophic biomagnification of POPs in the Lake Ontario food web is mainly the result of dietary magnification (Kelly, Gobas et al. 2004), as dietary intake of chemicals was the major exposure route for the smelt and herring gull (Figure 5 & 6). However, the elimination of POPs in smelt occurred through growth dilution, respiration into water and fecal egestion whereas elimination of POPs in herring gulls occurs through respiration into air (which is negligible) and through growth dilution and is less than that in smelt. In addition, the herring gull spent 88% (compared to 46% in smelt) of its energy on respiration (Figure 9 &10). This further demonstrates that the differences of the allocation of energy in herring gull and rainbow smelt affected the POP

uptake and eliminations. Therefore, BAFs and BMF*s for herring gulls were greater than that of rainbow smelt.

Table 12: Model calculated Log BAF, Log BMF and Log TMF of various POPs in caribou and wolf.

Chemical	Log K_{OA} 37 ^{o}C	Log K_{OW} 37 ^{o}C	Log BAF		Log BMF		Log TMF			
			Caribou	Wolf	Caribou	Wolf	Log TMF	*p*	95% CI	
									Lower	Upper
beta-HCH	8.05	4.00	9.87	11.50	1.03	1.48	1.78	0.07	-0.71	4.26
HCB	6.83	5.50	9.16	10.60	0.98	1.35	1.69	0.08	-1.10	4.48
Mirex	8.75	6.00	10.95	12.59	1.03	8.75	1.78	0.07	-0.68	4.24
Dieldrin	7.95	6.20	9.38	11.01	7.95	1.47	1.77	0.07	-0.71	4.25
PCB28	7.46	5.60	9.51	11.10	7.46	1.45	1.76	0.07	-0.79	4.30
PCB52	7.88	5.84	9.57	11.19	1.03	1.47	1.77	0.07	-0.72	4.26
PCB66/95	8.57	6.20	11.18	12.82	1.03	1.48	1.78	0.07	-0.68	4.24
PCB99	8.57	6.39	10.04	11.68	1.03	1.48	1.78	0.07	-0.67	4.23
PCB118	9.22	6.74	9.73	11.38	1.02	1.48	1.78	0.07	-0.67	4.23
PCB153	8.65	6.92	10.58	12.22	1.02	1.48	1.78	0.07	-0.65	4.20
PCB105	9.41	6.65	10.50	12.14	1.02	1.48	1.77	0.07	-0.64	4.19
PCB138	9.22	6.83	10.41	12.05	1.02	1.48	1.78	0.07	-0.66	4.21
PCB182 /187	9.64	7.20	9.84	11.49	1.00	1.48	1.78	0.07	-0.65	4.20
PCB180	9.93	7.50	10.77	12.41	0.98	1.48	1.77	0.07	-0.60	4.13
PCB170 /190	9.93	7.46	10.05	11.69	0.98	1.48	1.75	0.06	-0.53	4.03
PCB194	9.93	7.80	10.37	12.01	9.93	1.48	1.75	0.07	-0.54	4.05
PCB206	9.93	8.09	10.49	12.12	0.85	1.47	1.72	0.06	-0.40	3.85

Table 13: Model calculated Log BAF*, Log BMF* and Log TMF* of selected chemicals in caribou and wolf.

Chemical	Log K_{OA} 37 °C	Log K_{OW} 37 °C	Log BAF*		Log BMF*		Log TMF*			
			Caribou	Wolf	Caribou	Wolf	Log TMF*	*p*	95% CI	
									Lower	Upper
beta-HCH	8.05	4.00	1.79	3.22	0.73	1.44	1.63	0.04	0.20	3.06
HCB	6.83	5.50	2.31	3.61	0.68	1.31	1.61	0.04	0.33	2.89
Mirex	8.75	6.00	2.17	3.61	0.73	0.00	1.81	0.10	-1.85	5.46
Dieldrin	7.95	6.20	1.39	2.83	0.72	1.43	1.81	0.07	-0.85	4.46
PCB28	7.46	5.60	2.02	3.43	0.72	1.41	1.41	0.01	1.26	1.56
PCB52	7.88	5.84	1.66	3.09	0.72	1.43	1.72	0.07	-0.53	3.96
PCB66/95	8.57	6.20	2.58	4.02	0.73	1.44	1.54	0.03	0.73	2.36
PCB99	8.57	6.39	1.44	2.88	0.72	1.44	2.01	0.10	-2.14	6.16
PCB118	9.22	6.74	0.48	1.93	0.72	1.45	1.43	0.00	1.37	1.50
PCB153	8.65	6.92	1.90	3.34	0.71	1.44	1.44	0.00	1.41	1.47
PCB105	9.41	6.65	1.06	2.50	0.72	1.45	0.96	0.18	-2.58	4.50
PCB138	9.22	6.83	1.16	2.60	0.72	0.00	1.67	0.05	0.00	3.34
PCB182 /187	9.64	7.20	0.17	1.61	0.70	1.44	1.25	0.06	-0.18	2.68
PCB180	9.93	7.50	0.79	2.23	0.68	1.44	1.30	0.04	0.24	2.36
PCB170 /190	9.93	7.46	0.07	1.51	0.68	1.44	0.81	0.27	-3.87	5.49
PCB194	9.93	7.80	0.38	1.81	0.63	1.44	1.11	0.11	-1.29	3.52
PCB206	9.93	8.09	0.48	1.90	0.55	1.43	0.76	0.31	-4.28	5.79

Table 14: Model calculated Log BAF, Log BMF and Log BCF of various POPs in rainbow smelt and Log TMF for the Lake Ontario food web.

	Log K_{OW} 8 ^{o}C	Log BAF C_B/C_R	Log BCF C_B/C_R	Log BMF C_B/C_D	Log TMF	*p*	95% CI	
							Lower	Upper
PCB28	5.80	4.97	4.37	-0.15	0.56	0.003	0.26	0.87
PCB18	5.60	4.48	4.21	-0.30	0.34	0.007	0.12	0.55
PCB22	5.60	4.66	4.21	-0.30	0.50	0.007	0.18	0.82
PCB17	5.60	4.49	4.21	-0.30	0.34	0.007	0.12	0.56
PCB32	5.80	5.16	4.37	-0.15	0.69	0.002	0.33	1.05
PCB66	5.80	5.36	4.37	-0.15	0.89	0.002	0.43	1.35
PCB70	5.90	5.17	4.44	-0.09	0.66	0.002	0.31	1.01
PCB56	6.00	5.92	4.51	-0.04	1.00	0.006	0.39	1.61
PCB52	6.10	5.34	4.57	0.01	0.61	0.001	0.32	0.89
PCB47	5.90	5.05	4.44	-0.09	0.41	0.005	0.17	0.65
PCB44	6.00	5.27	4.51	-0.04	0.62	0.001	0.32	0.91
PCB74	6.10	5.27	4.57	0.01	0.58	0.002	0.27	0.89
PCB49	6.10	5.38	4.57	0.01	0.63	0.001	0.34	0.92
PCB64	6.10	5.59	4.57	0.01	0.79	0.001	0.44	1.13
PCB42	5.60	5.07	4.21	-0.30	0.84	0.005	0.34	1.33
PCB53	6.10	5.08	4.57	0.01	0.29	0.023	0.05	0.53
PCB40	5.60	4.91	4.21	-0.30	0.62	0.022	0.12	1.12
PCB101	6.40	5.49	4.74	0.12	0.59	0.003	0.26	0.92
PCB84	6.10	5.70	4.57	0.01	0.86	0.001	0.48	1.25
PCB118	6.40	5.63	4.74	0.12	0.67	0.002	0.34	1.00
PCB110	6.40	5.74	4.74	0.12	0.73	0.001	0.40	1.05
PCB87	6.50	5.90	4.78	0.13	0.78	0.001	0.45	1.10
PCB105	6.40	5.76	4.74	0.12	0.74	0.001	0.41	1.07
PCB95	6.40	5.54	4.74	0.12	0.43	0.001	0.23	0.63
PCB85	6.20	5.70	4.63	0.06	0.81	0.001	0.45	1.16
PCB92	6.50	6.09	4.78	0.13	0.76	0.002	0.40	1.12
PCB82	6.20	5.73	4.63	0.06	0.69	0.003	0.33	1.04
PCB91	6.30	5.37	4.69	0.09	0.55	0.004	0.23	0.87
PCB99	6.60	5.84	4.83	0.14	0.71	0.001	0.39	1.03
PCB153	6.90	5.85	4.93	0.11	0.68	0.002	0.33	1.02
PCB138	7.00	5.86	4.96	0.08	0.67	0.002	0.33	1.02
PCB149	6.80	5.88	4.90	0.13	0.70	0.001	0.36	1.03
PCB146	6.90	6.22	4.93	0.11	0.87	0.001	0.51	1.24
PCB141	6.90	6.00	4.93	0.11	0.75	0.001	0.41	1.09

Table 14 continued...

	Log Kow 8 °C	Log BAF C_B/C_R	Log BCF* C_B/C_R	Log BMF* C_B/C_D	Log TMF			
					Log TMF	*p*	95% CI	
							Lower	Upper
PCB128	7.00		4.96	0.08				
PCB151	6.90	6.14	4.93	0.11	0.82	0.001	0.47	1.17
PCB132	7.30	5.85	5.03	-0.05	0.47	0.005	0.20	0.75
PCB156	6.90		4.93	0.11				
PCB136	6.70	5.52	4.87	0.14	0.55	0.015	0.14	0.97
PCB180	7	5.84	4.96	0.08	0.67	0.003	0.31	1.02
PCB187	7	5.83	4.96	0.08	0.66	0.003	0.31	1.02
PCB170	6.9	6.50	4.93	0.11	1.04	0.000	0.62	1.47
PCB183	7	6.10	4.96	0.08	0.80	0.001	0.44	1.15
PCB177	7	6.32	4.96	0.08	0.92	0.001	0.53	1.30
PCB174	7	6.38	4.96	0.08	0.95	0.001	0.56	1.35
PCB203	7.1	6.43	4.99	0.04	0.55	0.002	0.40	1.25
PCB201	7.5		5.07	-0.18				
PCB194	7.1	5.82	4.99	0.04	0.66	0.003	0.29	1.02
PCB31	5.7	4.84	4.29	-0.22	0.55	0.004	0.23	0.88
PCB76	6	5.29	4.51	-0.04	0.66	0.002	0.33	0.99
PCB60	5.9	5.80	4.44	-0.09	1.10	0.002	0.56	1.64
PCB81	6.1		4.57	0.01				
PCB48	6.1	5.28	4.57	0.01	0.56	0.001	0.29	0.84
PCB97	6.6	5.95	4.83	0.14	0.77	0.001	0.45	1.09
PCB182	7	5.83	4.96	0.08	0.47	0.002	0.24	0.70
PCB190	7	6.50	4.96	0.08	0.57	0.002	0.44	1.34
PCB196	7.5	6.29	5.07	-0.18	0.91	0.002	0.45	1.38
ppDDE	5.7	4.98	4.29	-0.22	0.67	0.004	0.29	1.04
ppDDD		-1.26	-1.30	-3.86	0.68	0.488	-2.86	1.49
ppDDT	5.8	5.22	4.37	-0.15	0.76	0.002	0.36	1.15
mirex	6.89	6.04	4.93	0.11	0.77	0.001	0.42	1.11
gamma-chlordane	2.78	1.48	4.51	-0.04	0.012	0.14	0.79	0.012
alpha-HCH	3.81	2.51	2.51	-1.97	0.259	-0.12	0.37	0.259
gamma-HCH	3.8	2.50	2.50	-1.98	0.366	-0.16	0.37	0.366

Table 15: Model calculated Log BAF*, Log BMF* and Log BCF* of various POPs in rainbow smelt and Log TMF for the Lake Ontario food web.

	Log K_{OW} 8 ^{O}C	Log BAF f_B/f_R	Log BCF f_B/f_R	Log BMF* f_B/f_D	Log TMF			
					Log TMF	p	95% Cl	
							Lower	Upper
PCB28	5.80	0.96	-0.11	0.51	0.84	0.06	-0.04	1.73
PCB18	5.60	0.28	-0.08	0.36	0.62	0.12	-0.21	1.44
PCB22	5.60	0.86	-0.08	0.36	0.82	0.08	-0.12	1.77
PCB17	5.60	0.29	-0.08	0.36	0.62	0.12	-0.21	1.45
PCB32	5.80	1.46	-0.11	0.51	0.96	0.03	0.12	1.80
PCB66	5.80	1.93	-0.11	0.51	1.23	0.02	0.20	2.26
PCB70	5.90	1.12	-0.14	0.59	1.00	0.05	-0.01	2.01
PCB56	6.00	2.49	-0.17	0.68	0.87	0.01	0.24	1.51
PCB52	6.10	0.91	-0.20	0.77	0.91	0.05	-0.01	1.84
PCB47	5.90	0.81	-0.14	0.59	0.28	0.07	-0.03	0.59
PCB44	6.00	1.03	-0.17	0.68	0.96	0.05	-0.01	1.94
PCB74	6.10	0.73	-0.20	0.77	0.91	0.07	-0.08	1.91
PCB49	6.10	0.98	-0.20	0.77	0.94	0.05	0.01	1.87
PCB64	6.10	1.48	-0.20	0.77	1.12	0.03	0.15	2.09
PCB42	5.60	1.97	-0.08	0.36	1.20	0.03	0.16	2.24
PCB53	6.10	0.32	-0.20	0.77	0.16	0.00	0.09	0.23
PCB40	5.60	1.58	-0.08	0.36	0.49	0.08	-0.09	1.07
PCB101	6.40	0.52	-0.32	0.99	0.94	0.07	-0.10	1.97
PCB84	6.10	1.72	-0.20	0.77	1.26	0.03	0.20	2.32
PCB118	6.40	0.80	-0.32	0.99	1.08	0.06	-0.05	2.21
PCB110	6.40	1.02	-0.32	0.99	1.10	0.04	0.04	2.17
PCB87	6.50	1.14	-0.37	1.04	1.17	0.04	0.10	2.24
PCB105	6.40	1.05	-0.32	0.99	1.20	0.05	0.00	2.39
PCB95	6.40	0.60	-0.32	0.99	0.30	0.00	0.13	0.47
PCB85	6.20	1.44	-0.24	0.85	1.21	0.03	0.12	2.29
PCB92	6.50	1.52	-0.37	1.04	0.63	0.01	0.25	1.01
PCB82	6.20	1.49	-0.24	0.85	0.56	0.01	0.17	0.95
PCB91	6.30	0.47	-0.28	0.93	0.91	0.08	-0.14	1.96
PCB99	6.60	0.83	-0.43	1.07	1.06	0.04	0.04	2.09
PCB153	6.90	0.39	-0.61	1.01	1.05	0.06	-0.05	2.15
PCB138	7.00	0.29	-0.68	0.95	1.10	0.06	-0.08	2.28
PCB149	6.80	0.57	-0.55	1.05	1.08	0.05	-0.01	2.17
PCB146	6.90	1.07	-0.61	1.01	1.25	0.03	0.18	2.32
PCB141	6.90	0.66	-0.61	1.01	1.16	0.05	0.03	2.29

Table 15 continued...

	Log K_{OW} 8 °C	Log BAF* f_B/f_R	Log BCF* f_B/f_R	Log BMF* f_B/f_D	Log TMF*			
					Log TMF*	p	95% CI	
							Lower	Upper
PCB128	7.00		-0.68	0.95				
PCB151	6.90	0.91	-0.61	1.01	1.19	0.03	0.13	2.25
PCB132	7.30	-0.04	-0.90	0.71	0.35	0.05	0.01	0.68
PCB156	6.90		-0.61	1.01				
PCB136	6.70	0.11	-0.49	1.07	0.96	0.09	-0.21	2.14
PCB180	7	0.25	-0.68	0.95	1.10	0.07	-0.10	2.30
PCB187	7	0.24	-0.68	0.95	1.06	0.06	-0.08	2.21
PCB170	6.9	1.61	-0.61	1.01	-0.13	0.84	-1.60	1.34
PCB183	7	0.72	-0.68	0.95	1.20	0.04	0.07	2.32
PCB177	7	1.11	-0.68	0.95	1.36	0.03	0.18	2.54
PCB174	7	1.23	-0.68	0.95	1.39	0.03	0.22	2.55
PCB203	7.1	1.20	-0.75	0.88	0.70	0.01	0.24	1.16
PCB201	7.5		-1.07	0.54				
PCB194	7.1	0.11	-0.75	0.88	1.14	0.07	-0.14	2.42
PCB31	5.7	0.97	-0.09	0.43	0.83	0.06	-0.06	1.73
PCB76	6	1.09	-0.17	0.68	1.01	0.05	0.00	2.02
PCB60	5.9	2.55	-0.14	0.59	1.47	0.01	0.40	2.55
PCB81	6.1		-0.20	0.77				
PCB48	6.1	0.76	-0.20	0.77	1.27	0.23	-1.01	3.55
PCB97	6.6	1.04	-0.43	1.07	1.57	0.19	-0.95	4.09
PCB182	7	0.24	-0.68	0.95	0.34	0.01	0.11	0.58
PCB190	7	1.47	-0.68	0.95	1.62	0.32	-1.95	5.18
PCB196	7.5	0.57	-1.07	0.54	1.85	0.18	-1.08	4.77
ppDDE	5.7	1.37	-0.09	0.43	1.67	0.20	-1.09	4.42
ppDDD		5.55	0.00	0.00	1.16	0.45	-2.23	4.55
ppDDT	5.8	1.59	-0.11	0.51	1.75	0.18	-1.01	4.51
mirex	6.89	0.74	-0.61	1.02	1.50	0.20	-0.99	3.98
gamma-chlordane	2.78	0.34	-0.17	0.68	0.89	0.17	-0.49	2.28
alpha-HCH	3.81	0.0035	0.00	0.01	0.00	0.93	-0.07	0.06
gamma-HCH	3.8	0.01		0.01	-0.02	0.85	-0.25	0.21

Table 16: Model calculated Log BAF, Log BMF of various POPs in herring gulls.

	Log K_{OA} 42 ^{O}C	Log BAF C_B/C_R	Log BMF C_B/C_D
PCB28	7.38	7.31	1.40
PCB18	6.98	6.84	1.08
PCB22	7.52	6.50	1.34
PCB17	7.00	5.86	1.09
PCB32	7.11	5.93	1.24
PCB66	8.18	9.38	1.65
PCB70	8.15	8.20	1.65
PCB56	8.31		1.62
PCB52	7.67	8.08	1.50
PCB47	7.72		1.50
PCB44	7.83	8.66	1.45
PCB74	8.12	7.55	1.65
PCB49	7.70	7.74	1.50
PCB64	7.93	8.44	1.55
PCB42	7.86	7.76	1.39
PCB53			1.36
PCB40	8.00		1.39
PCB101	8.37	8.98	1.71
PCB84	8.35	8.44	1.59
PCB118	8.85	9.13	1.78
PCB110	8.65	9.21	1.73
PCB87	8.57	9.53	1.68
PCB105	9.05	9.56	1.76
PCB95	8.18		1.63
PCB85	8.60	8.36	1.69
PCB92			1.70
PCB82	8.73		1.65
PCB91	8.23	8.89	1.63
PCB99	8.41	8.99	1.71
PCB153	9.02	8.95	1.79
PCB138	9.23	8.73	1.79
PCB149	8.84	8.89	1.77
PCB146	8.98	9.22	1.79
PCB141	9.12	7.31	1.78

Table 16 continued....

	Log K_{OA} 42 ^{o}C	Log BAF C_B/C_R	Log BMF C_B/C_D
PCB128	11.19		1.78
PCB151	10.39	7.07	1.76
PCB132	10.74		1.75
PCB156	11.74		1.81
PCB136	10.25	8.40	1.66
PCB180	11.54	9.03	1.82
PCB187	11.10	8.65	1.81
PCB170	0.00	8.97	1.82
PCB183	11.15	8.37	1.81
PCB177	11.35	8.43	1.81
PCB174	11.30	8.39	1.81
PCB203	11.92		1.82
PCB201	11.45		1.82
PCB194	12.33	9.46	1.83
PCB31	8.77	6.95	1.40
PCB76	9.69	7.86	1.63
PCB60	9.88	8.40	1.62
PCB81	0.00		1.70
PCB48	9.20	7.64	1.46
PCB97	10.13	8.67	1.68
PCB182	0.00		1.81
PCB190	11.81		1.82
PCB196	11.92	8.48	1.82
ppDDE	10.74	6.64	1.40
ppDDD	10.95	-0.87	-4.11
ppDDT	10.75	6.74	1.46
mirex	10.15	9.73	1.79
photomirex	0.00		
gamma-chlordane	8.54	1.91	1.56
alpha-HCH	0.00		-0.30
gamma-HCH	0.00		-0.31

Table 17: Model calculated Log BAF*, Log BMF* of various POPs in herring gulls.

	Log K_{OA} 42 ^{o}C	Log BAF* f_B/f_R	Log BMF* f_B/f_D
PCB28	7.38	2.56	1.11
PCB18	6.98	2.48	0.79
PCB22	7.52	1.85	1.05
PCB17	7.00	1.49	0.80
PCB32	7.11	1.43	0.95
PCB66	8.18	4.13	1.37
PCB70	8.15	2.93	1.37
PCB56	8.31		1.34
PCB52	7.67	3.15	1.21
PCB47	7.72		1.21
PCB44	7.83	3.83	1.16
PCB74	8.12	2.26	1.37
PCB49	7.70	2.81	1.21
PCB64	7.93	3.42	1.27
PCB42	7.86	3.06	1.10
PCB53			1.08
PCB40	8.00		1.10
PCB101	8.37	3.48	1.42
PCB84	8.35	3.33	1.31
PCB118	8.85	3.29	1.49
PCB110	8.65	3.63	1.44
PCB87	8.57	4.14	1.40
PCB105	9.05	3.81	1.48
PCB95	8.18		1.34
PCB85	8.60	2.98	1.40
PCB92			1.41
PCB82	8.73		1.37
PCB91	8.23	3.64	1.34
PCB99	8.41	3.49	1.42
PCB153	9.02	2.89	1.51
PCB138	9.23	2.76	1.50
PCB149	8.84	3.09	1.48
PCB146	8.98	3.21	1.51
PCB141	9.12	3.12	1.11

Table 17 continued....

	Log K_{OA} 42 ^{O}C	Log BAF* f_B / f_R	Log BMF* f_B/f_D
PCB128	11.19		1.50
PCB151	10.39	1.64	1.49
PCB132	10.74		1.47
PCB156	11.74		1.46
PCB136	10.25	3.04	1.53
PCB180	11.54	2.62	1.37
PCB187	11.10	2.43	1.53
PCB170	0.00	3.27	1.52
PCB183	11.15	2.32	1.53
PCB177	11.35	2.70	1.53
PCB174	11.30	2.69	1.52
PCB203	11.92		1.52
PCB201	11.45		1.54
PCB194	12.33	2.59	1.54
PCB31	8.77	2.61	1.54
PCB76	9.69	3.03	1.11
PCB60	9.88	4.50	1.34
PCB81			1.34
PCB48	9.20	2.95	1.42
PCB97	10.13	3.60	1.18
PCB182			1.40
PCB190	11.81		1.53
PCB196	11.92	2.17	1.54
ppDDE	10.74	2.56	1.54
ppDDD	10.95	3.11	1.11
ppDDT	10.75	2.65	-4.39
mirex	10.15	4.00	1.17
photomirex			1.50
gamma-chlordane	8.54	1.47	
alpha-HCH			1.28
gamma-HCH			-0.59

Model Sensitivity

Figures 10 to 13 illustrate the model sensitivity of the BAF to K_{OW}, K_{OA}, growth efficiencies, digestive efficiencies, assimilation efficiencies and consumer compositions in the consumer organisms and their preys for rainbow smelt, herring gull, caribou and wolf.

For rainbow smelt, K_{OW} was the variable that contributed the most to the model outcome. This is because the exchange of POPs between the water and the smelt is an important route of uptake and elimination of POPs in rainbow smelt. Chemicals with low K_{OW} tend to be cleared to water via gill ventilation. Other than the important role of the parameter, K_{OW}, in the model, the relatively large variations (standard deviations) of the parameters also affected its contribution to the variance of the model outcome. Among biological properties, the most important parameter that contributed to the model outcome was the net growth efficiency of the smelt. The greater the growth efficiency, the lower the BAF. The greater the proportion of energy used for production results in a higher degree of growth dilution of contaminants in the body, and hence the lower the BAF. The second most important biological parameter contributing to the BAF was the fraction of protein in smelt. This is because the fraction of protein in rainbow smelt was five times greater than lipid. On the other hand, variation of the biological parameters in the preys of smelt did not contribute significantly to the variance of prediction in BAF smelt. Except the fraction of non-lipid organic carbon in phytoplankton negatively contributed 1.1% of the variance. This means that increasing the non-lipid organic carbon content in phytoplankton decreases the BAF (concentration based) in smelt. There are two reasons for this. First, increasing non-lipid organic carbon content effectively lowers

the bioconcentration of POPs in phytoplankton. Second, phytoplankton is the primary food-source of organisms in the food web, thus it affects the predictions of BAF in organisms of all other consumer organisms of the food web.

In herring gulls, the variable that contributed the most to the model output, Log BAF (concentration based), was the digestive efficiency for lipid. This is because the greater proportion the lipid is digested, the less lipid is eliminated into the faeces. A low lipid content of the faeces produced a low fugacity capacity of POPs in the faeces. This lowers the rate of fecal elimination, which leads to a higher degree of POP accumulation in the body of the gull. The second most important parameter contributing 12.2% to the variance of the model outcome was the K_{OW} of POPs at 42°C. Increasing the K_{OW} of the tested chemicals increased the BAF (concentration ratio) in the herring gull. Lipid fraction in alewife contributed 1.4% of the variance of BAF (concentration ratio) in herring gull. This is because alewife made up 45% of the diet of herring gull, and the lipid content of alewife was relatively higher (7%) compared to other prey items (e.g. rainbow smelt) of the herring gull.

In caribou, the variable contributed most to the model outcome was the K_{OA} of the POPs. This is because chemicals with low K_{OA} tend to be eliminated to air via respiration. Moreover, K_{OA} for POPs were used to derive other parameters such as fugacity capacity of the POPs caribou's body; increasing K_{OA} increased the fugacity capacity of the POP in the caribou. Among Biological properties, the most important parameter contributed to the outcome variance was the digestive efficiency of carbohydrate in caribou. This is because most of diet of caribou (35%) was made up of

carbohydrate. Increasing carbohydrate digestibility increased the BAF (concentration ratio) in caribou.

In wolf, the variable contributed the most to the model outcome was the K_{OA} of the POPs. Among the biological properties, the most important parameter contributing to the model outcome was the digestive efficiency of lipid, Reducing the lipid content in the faeces lowers the fugacity capacity of POPs in the faeces, and reduces elimination through faeces. A lower rate of fecal elimination leads to a higher degree of POP accumulation in the body of the wolf. The digestibility of carbohydrate in caribou also contributed to the variance in the model predicted BAF. This was due to the importance of this biological parameter in caribou. Caribou accounted for 100% of the wolf's diet.

Figure 10: Sensitivity test for smelt. Parameters' contribution to the variance of model output, Log BAF.

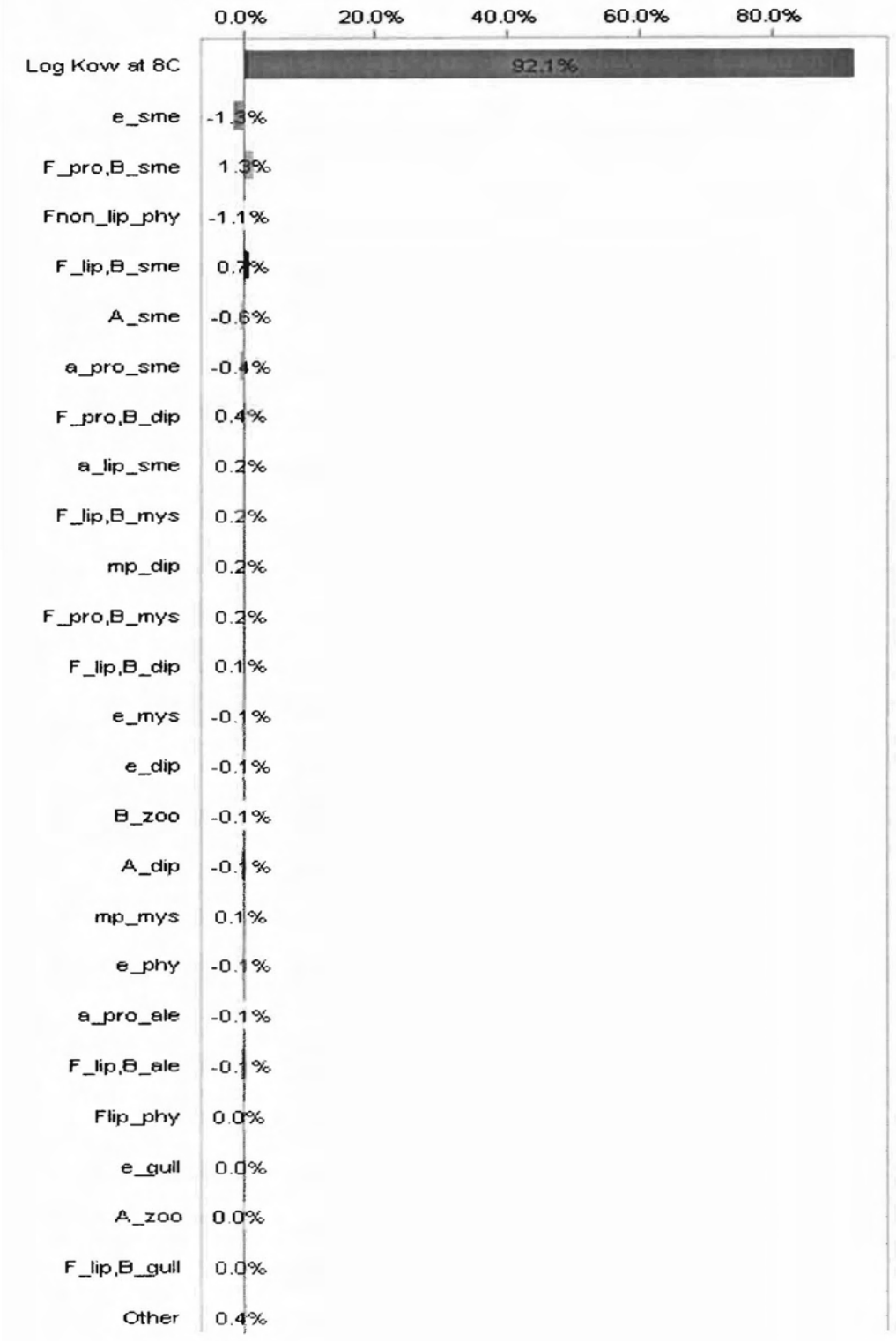

Figure 11: Sensitivity test for herring gull. Parameters' contribution to the variance of model output, Log BAF.

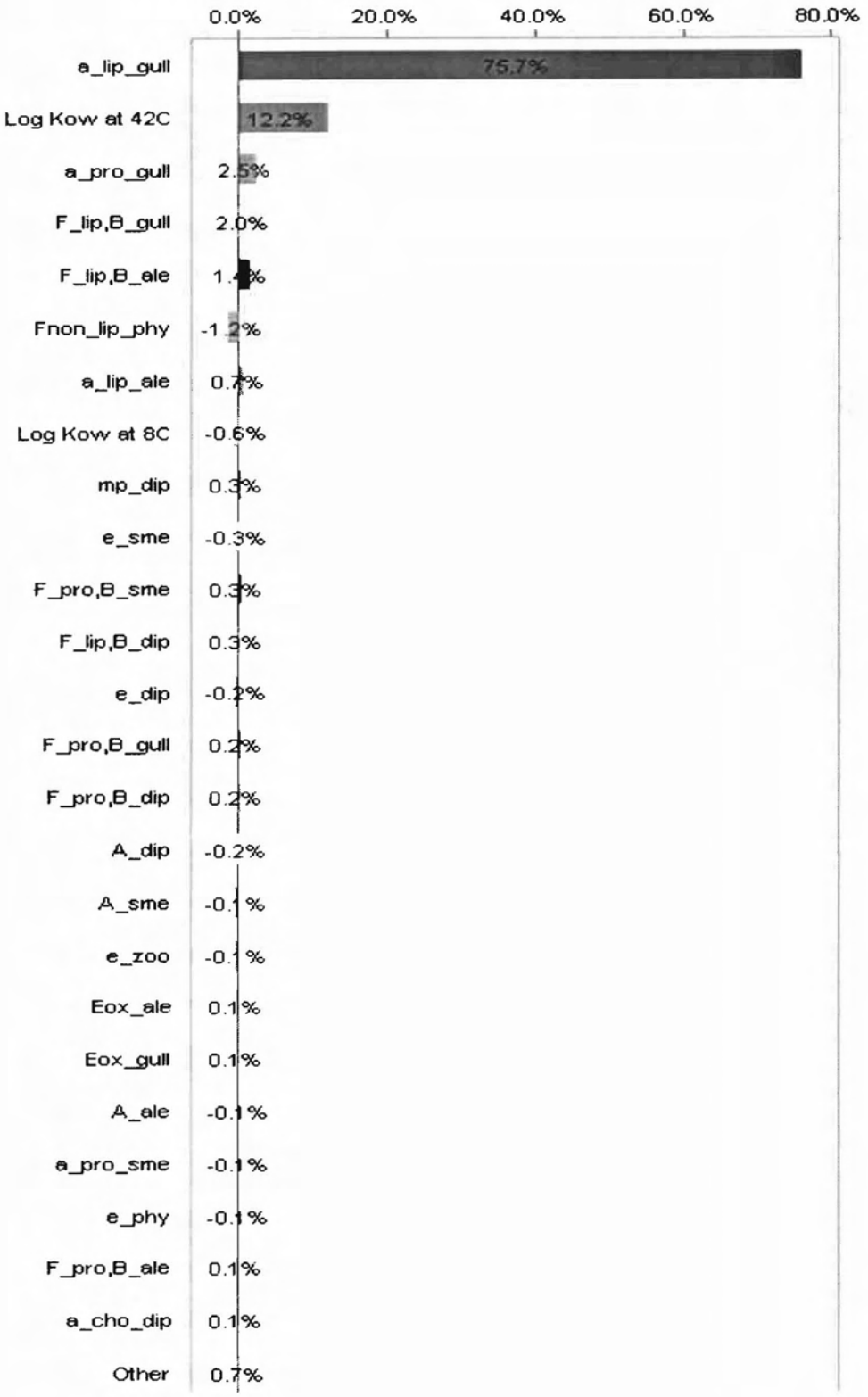

Figure 12: Sensitivity test for caribou. Parameters' contribution to the variance of model output, Log BAF.

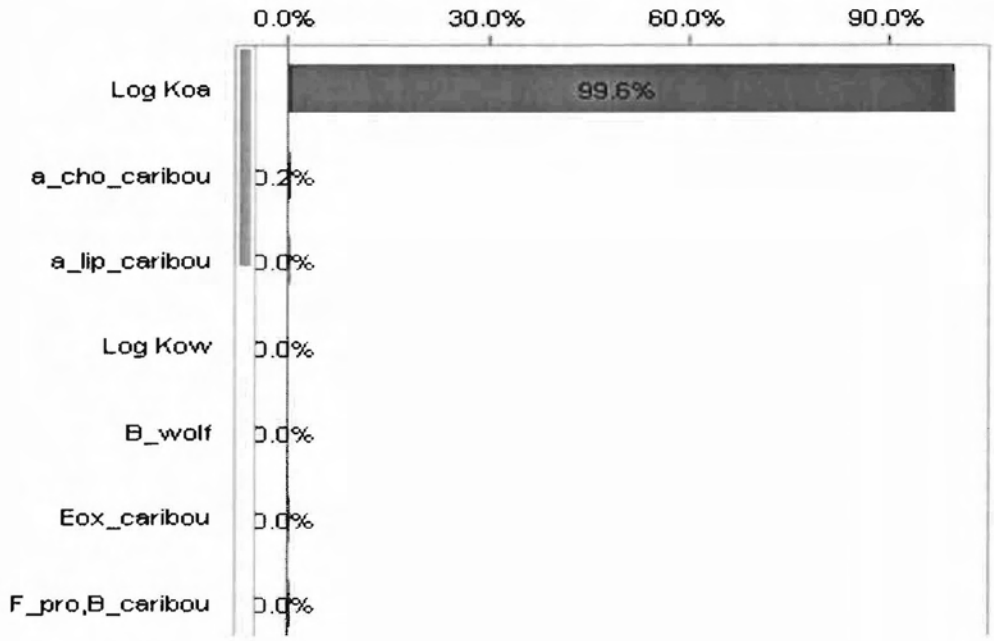

Figure 13: Sensitivity test for wolf. Parameters' contribution to the variance of model output, Log BAF.

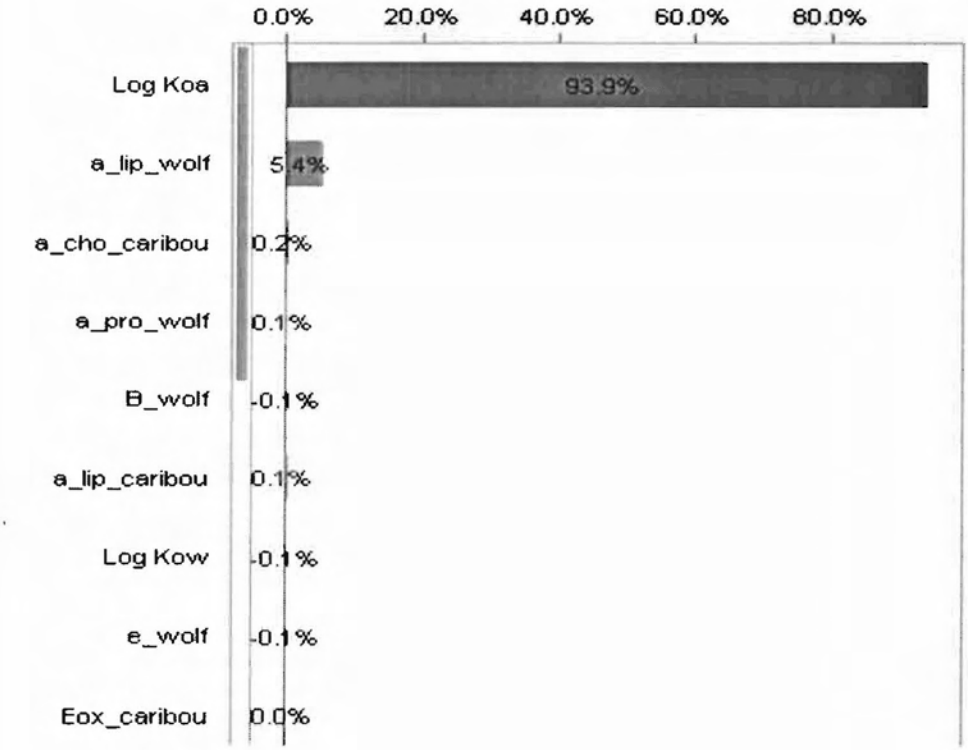

Model Uncertainty Analysis

Figure 14 to 17 illustrate the probability distributions for the BAF concentration and fugacity based) and BMF (fugacity based) interval of model predictions of PCB 153 through Monte Carlo simulation. Monte Carlo simulation calculated 95% confidence interval for rainbow smelt Log BAF (concentration based) was (5.8, 7.4), for fugacity-based Log BAF was (0.23, 0.45) (Figure 14) and for fugacity based BMF was (0.77, 1.2). The 95% for herring gull Log BAF (concentration based) was (8.7, 9.3), for fugacity-based Log BAF was (2.6, 3.2) (Figure 15) and for fugacity based BMF was (17, 71). The 95% confidence interval for caribou Log BAF (concentration based) was (10.5, 10.6), for fugacity-based Log BAF was (1.9, 2.0) (Figure 16) and for fugacity based BMF was (17, 71). Monte Carlo simulation calculated 95% confidence interval for rainbow smelt Log transformed model bias was (5.0, 6.5) (Figure 14). The 95% confidence interval for wolf Log BAF (concentration based) was (11.8, 12.3), for fugacity-based Log BAF was (3.2, 3.7) (Figure 16) and for fugacity based BMF was (18.3, 55.4).

The distributions of both Log BAF concentration based and fugacity based appeared to be normal in rainbow smelt, herring gull, caribou and wolf. However, the distributions for BMF appeared to be Lognormal in herring gull and wolf. This is because the outcome of Monte Carlo Simulation for BAF was Log transformed, whereas for BMF was not.

Figure 14: Monte Carlo simulation of model uncertainty test for rainbow smelt.

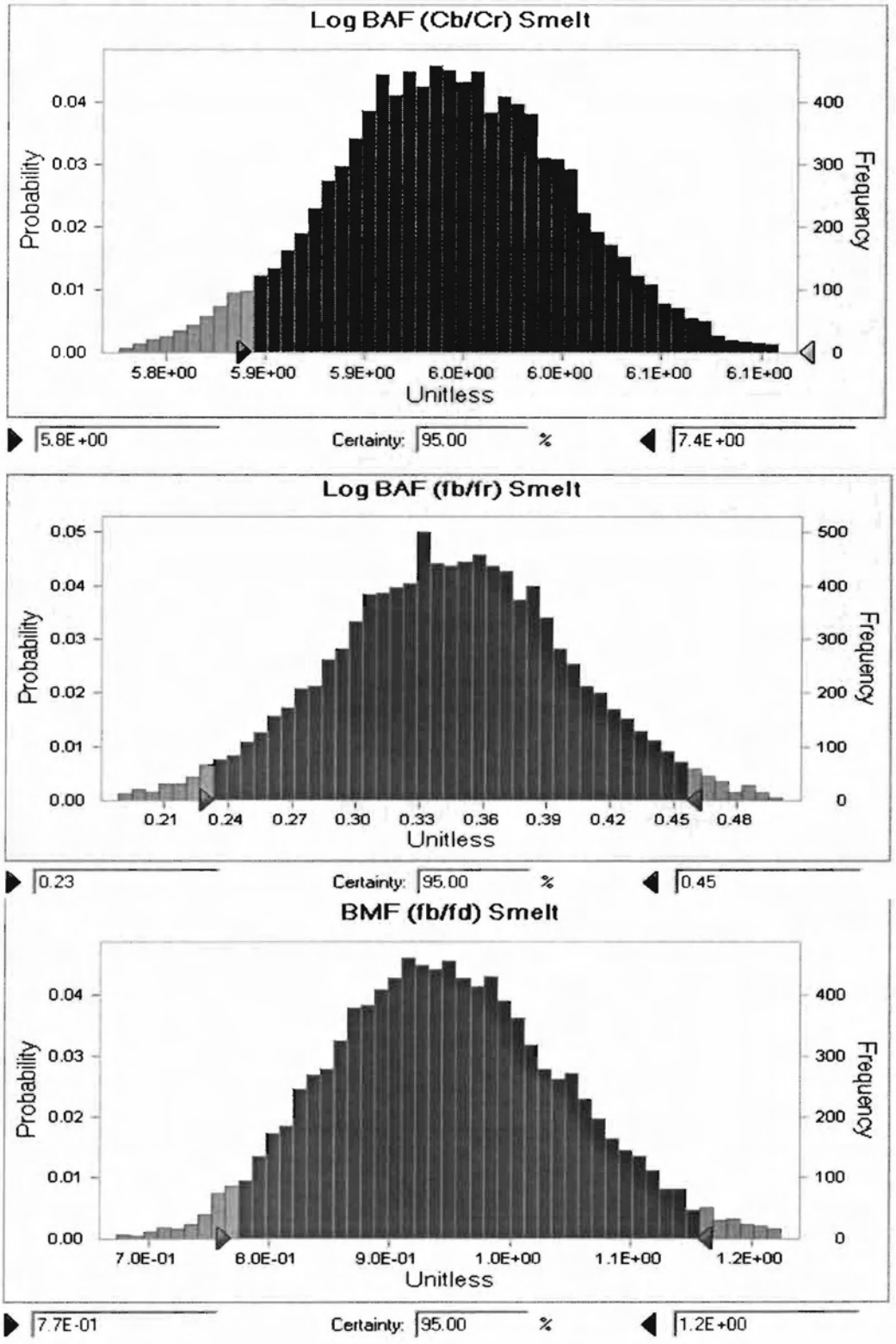

Figure 15: Monte Carlo simulation of model uncertainty test for herring gull.

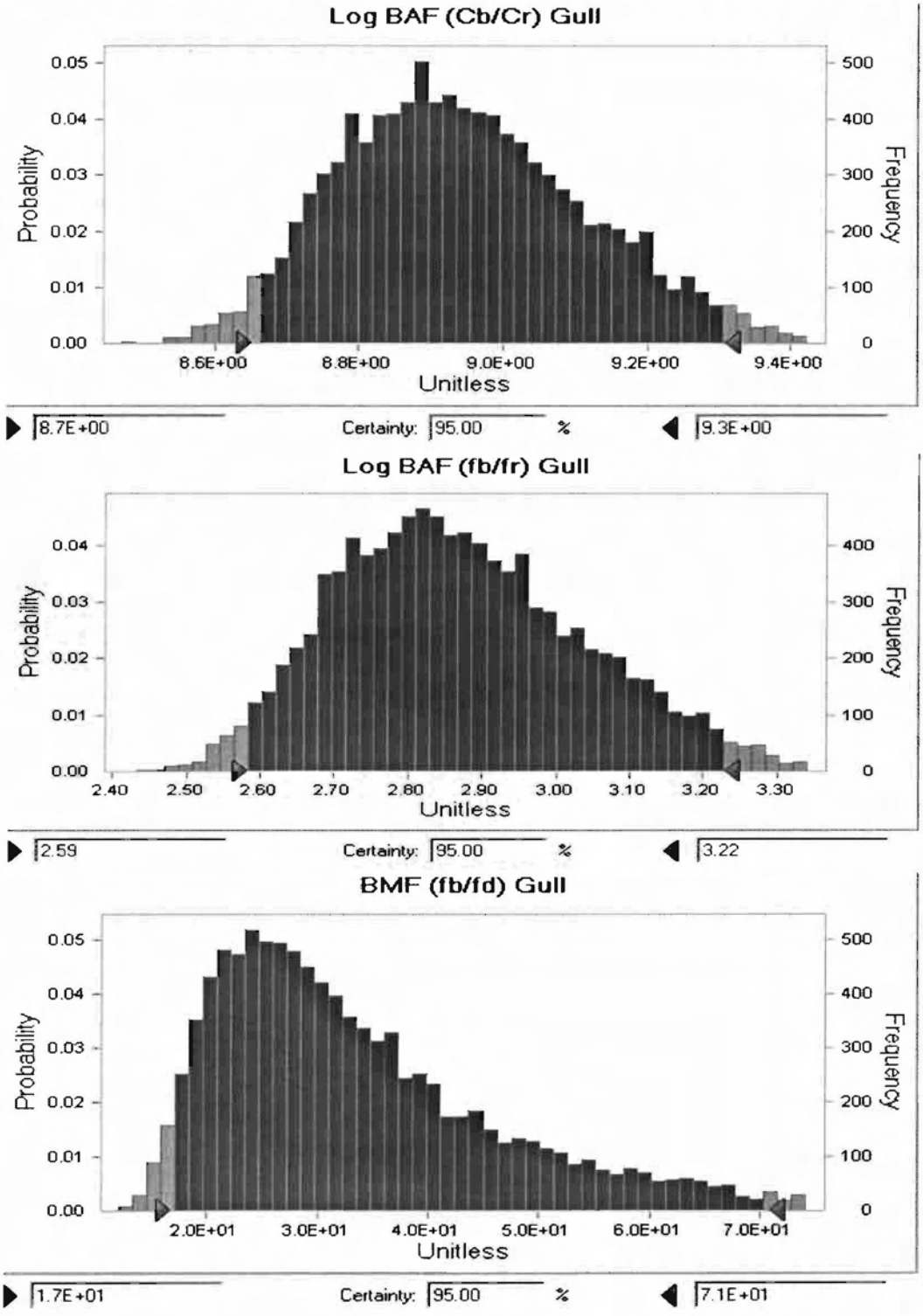

Figure 16: Monte Carlo simulation of model uncertainty test for caribou.

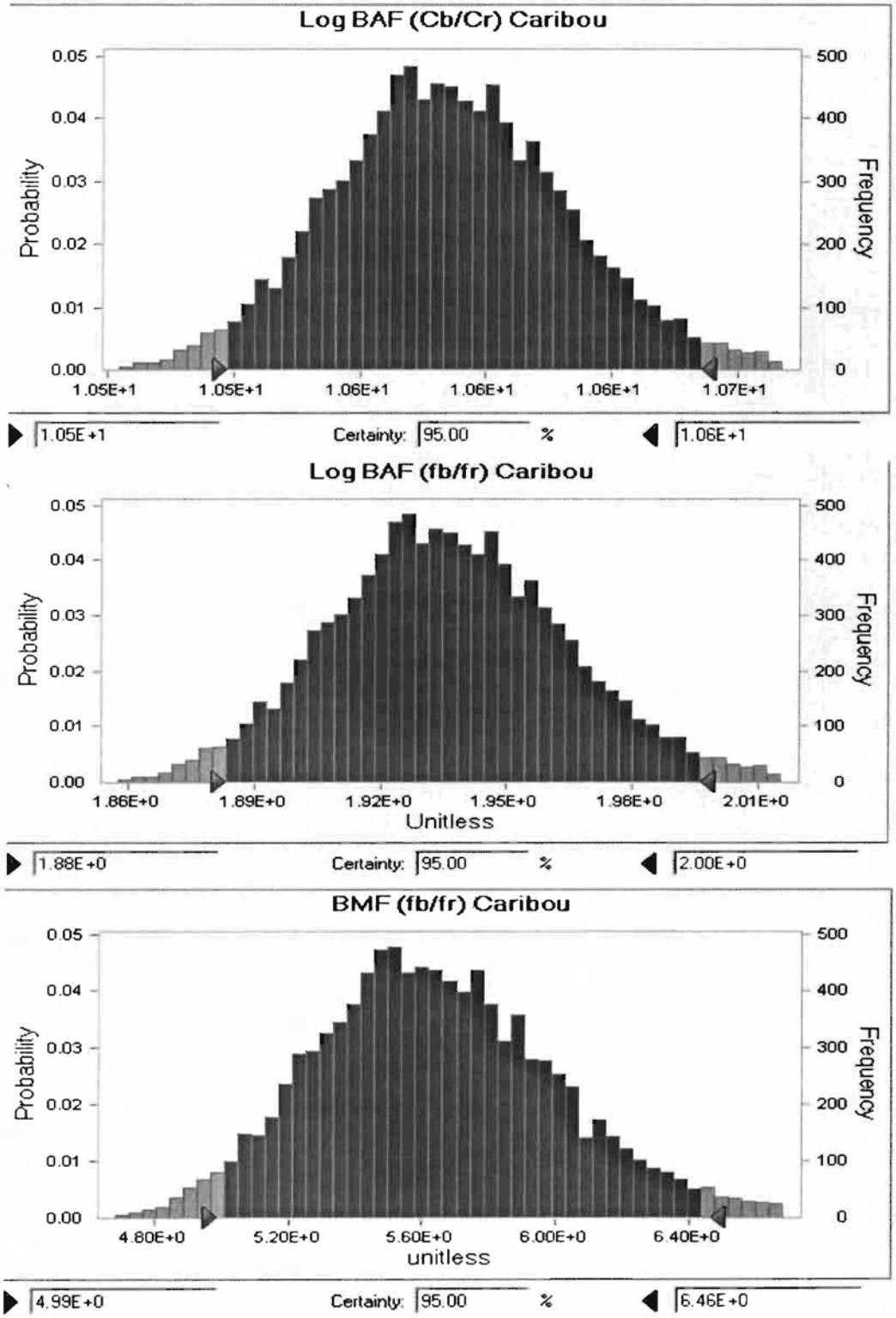

Figure 17: Monte Carlo simulation of model uncertainty test for wolf.

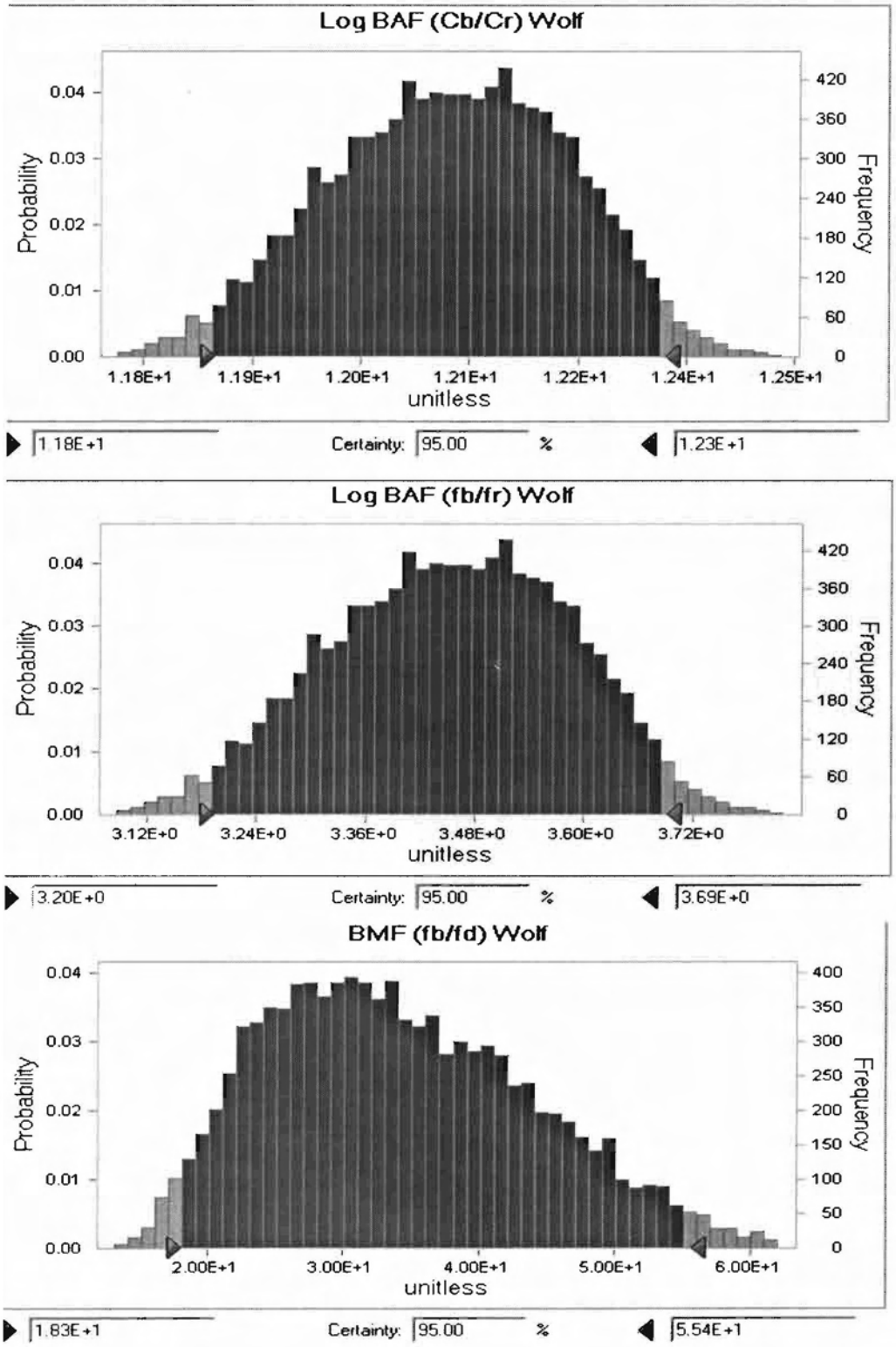

Model Performance Analysis

Table 18 shows the mean model bias (MB) and its 95% confidence interval for each organism included in the Canadian Arctic and Lake Ontario food webs. Model predicted and observed biota lipid normalized concentrations of non-metabolized POPs in caribou and wolf is displayed in Figure 18. This graph provides a visual demonstration of the model performance. The line of best prediction has a slope of 1, and represents model predicted BAFs being equal to those of observed in the field. Data points that fall below the line of best prediction indicates that the model predicted BAF values are greater than the observed values, i.e., the model is over-predicting the BAFs of these POPs in the organisms. Table 18 indicates the ratio of model predicted and field observed BAFs for non-metabolized POPs for caribou was 1.43 and for wolf was 5.31.

Figure 18 shows that the predicted Log BAFs are greater than observed ones for both caribou and wolf. This indicates that the model over predicted BAFs and concentrations of POPs in wolf and caribou. Only non-metabolizable POPs were included in model performance analysis, because of the assumption of zero-biotransformation of chemicals in parameterization. PCB 182 was not included in the plot of Figure 18 because the predicted lipid based concentrations were much higher than the observed ones for PCB 182, though it was in the Group I PCBs. This suggests that caribou and wolf might have metabolized PCB 182. It has been accepted that some POPs showed a lower bioaccumulation potential because they can be metabolized enzymatically during their passage through the food chain, especially in mammals, and there is evidence of metabolic transformation of PCBs after uptake by marine mammals (Boon, vanderMeer et al. 1997).

Furthermore, the previous field study of POP bioaccumulation in Canadian Arctic wolf and caribou showed that PCB 153 and 180 were bioaccumulative. In contrast, PCB 52 was not found to be biomagnified (Kelly and Gobas 2001). This suggests that PCB 52 was eliminated and/or metabolized efficiently in both caribou and wolves. There is also evidence of metabolism of certain organochlorines such as hexachlorobenzene (HCB) in both mammals and fish. Kasokat and colleagues (Kasokat, Nagel et al. 1989) found metabolism of HCB into pentachlorophenol (PCP) by zebra fish. It has been suggested that exposure to low levels of certain compounds (e.g. PCBs and HCB) may result in an induction of specific P 450-dependent monooxygenase activities. These enzyme systems might facilitate oxidative dechlorination reactions since the mechanism of reductive dechlorination was not involved in the conversion of HCB to pentachlorophenol PCP (Kasokat, Nagel et al. 1989). In addition, hexachlorobenzene and pentachlorobenzene were metabolized into pentachlorophenol, which was further transformed into tetrachlorohydroquinone by humans in both in *vitro* and in *vivo* studies (Mehmood, Williamson et al. 1996).

Table 18 also shows the mean MB for consumer organisms in Lake Ontario food web. The MB for species in the Lake Ontario food web ranged between 0.62 for alewife and 2.46 for oligochaete. The model over predicted oligochaete, diporeia, mysids, slimy sculpin, rainbow smelt, and herring gulls; and under predicted the rest of biota (i.e., zooplankton, alewife, and lake trout). Among these organisms, mean MB for alewife was 0.62 and for lake trout was 0.73. This indicates that the predicted BAFs for the biota were 38% and 27% less than the observed values for alewife and lake trout, correspondingly. Because alewife accounted for 70% of the diet of lake trout (Table 7), the model

prediction of POP concentrations in alewife directly affects the prediction of POP BAF and concentration in lake trout. On the other hand, because oligochaetes were not in the diet of any other consumer organisms in the food web, its over prediction did not affect the prediction of the other organisms.

Figure 19 to Figure 21 display the plots of predicted Log BAF and observed Log BAFs in Lake Ontario organisms. Error bars of the plots of slimy sculpin and alewife were not added because the standard deviations of the empirical data were not available. Figures 19 to 21 illustrate that the model predicted BAFs for all the consumer organisms were comparable with the observed ones.

Figure 22 a and b illustrate the model agreement of predicted TMF and TMF* with the observed TMF and TMF* correspondingly. Solid line represents perfect model agreement. These figures indicate that the model predicted TMF and TMF* for the Lake Ontario food web were comparable with the observed ones. However, there is not enough data to compare the TMF or TMF* with the observed ones for the Canadian Arctic food web.

The plots of Log MB versus K_{OW} and K_{OA} for caribou and wolf are shown in Figure 23. The plots of Log MB versus K_{OW} or K_{OA} for biota in Lake Ontario food web are shown in Figure 24 to Figure 26. These figures show no systematic variation in the model with the key chemical properties.

Table 18: The mean model bias for specific POPs (MB), with their 95% confidence intervals, sample size (n) and logarithmic equivalents (Log MB)

Species		MB	n	95%CI (MB) (min)	95%CI (MB) (max)	LOG MB	SD (LOG MB)
Zooplankton		0.81	60	0.18	3.62	-0.09	0.33
Oligochaete	*Oligochaete*	2.46	59	0.48	12.74	0.39	0.36
Mysids	*Mysidopsis bahia*	1.10	55	0.16	7.72	0.04	0.42
Diporeia	*Diporeia spp.*	1.32	59	0.15	11.35	0.12	0.47
Slimy sculpin	*Cottus cognatus*	1.00	53	0.08	12.11	0.00	0.54
Alewife	*Alosa pseudoharengus*	0.62	54	0.17	2.25	-0.21	0.28
Rainbow smelt	*Osmerus mordax*	1.28	45	0.19	8.87	0.11	0.42
Lake trout	*Salvelinus namaycush*	0.73	59	0.14	3.81	-0.14	0.36
Herring gull	*Larus argentatus*	1.31	24	0.05	32.82	0.12	0.68
Caribou	*Rangifer tarandus*	1.43	5	0.72	3.06	0.16	0.13
Wolf	*Canis lupus arctos*	5.31	5	0.91	55.21	0.73	0.36

n, number of chemicals

Figure 18: Observed versus predicted lipid-normalized POP concentrations (ng/g lipid) for the chemicals least likely to be metabolized in wolf and caribou. Solid line represents perfect model agreement.

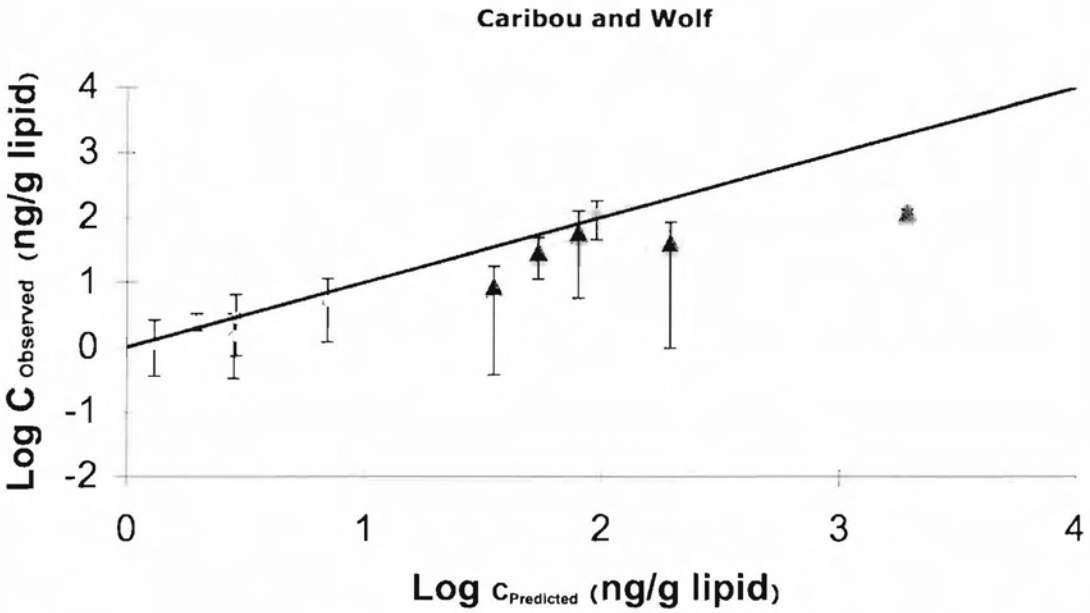

Note: Round symbols, Caribou data; triangular symbols, wolf data.

Figure 19: Observed versus model predicted BAF of selected hydrophobic organic substances in invertebrates of the Lake Ontario food web.

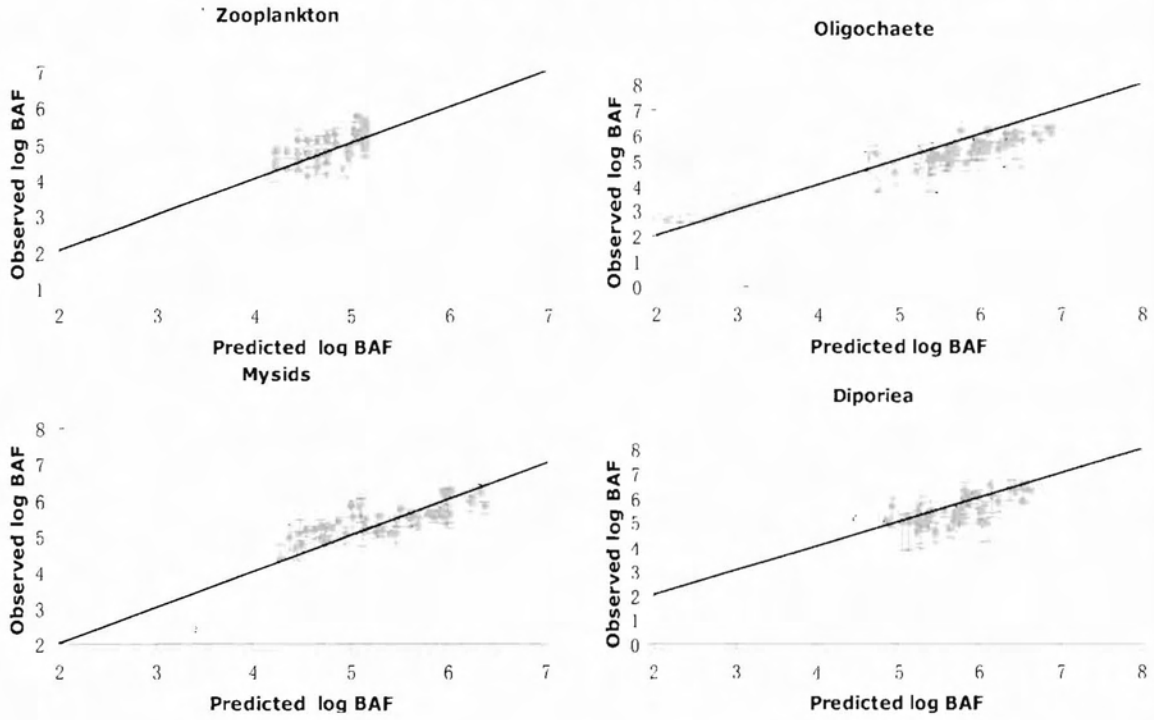

Figure 20: Observed versus model predicted BAF of selected hydrophobic organic substances in fish of the Lake Ontario food web.

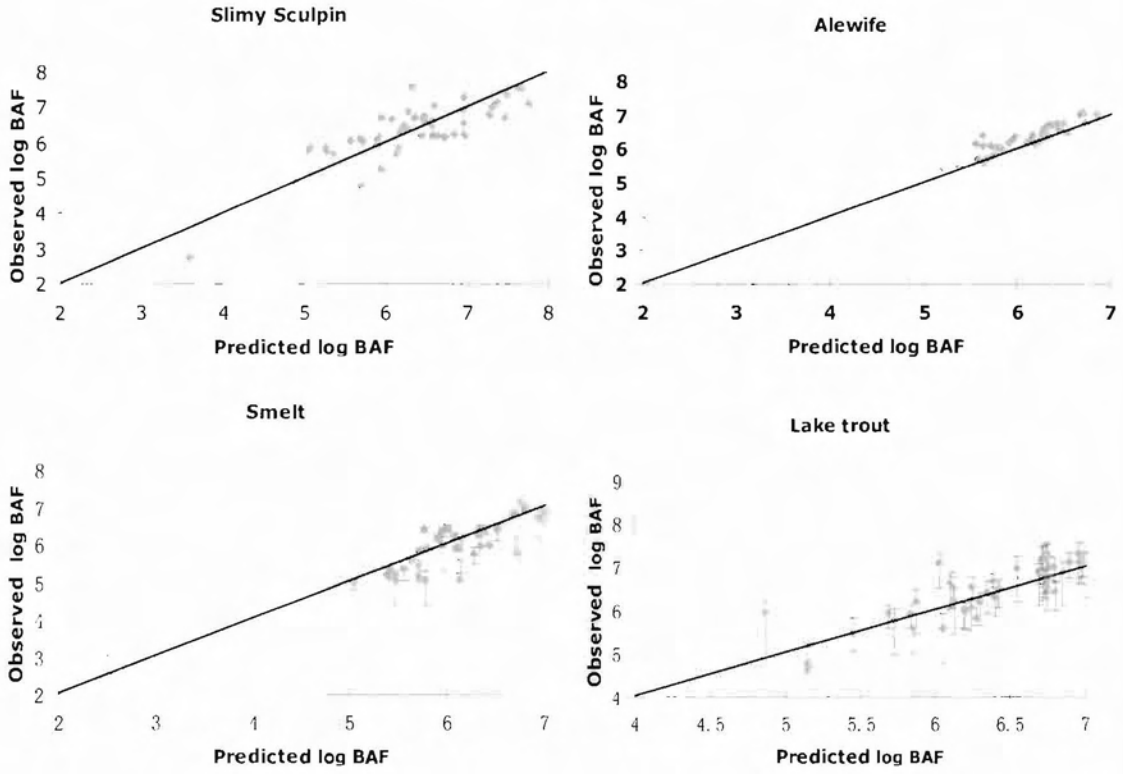

Figure 21: **Observed versus model predicted BAF of selected hydrophobic organic substances in herring gulls of the Lake Ontario food web.**

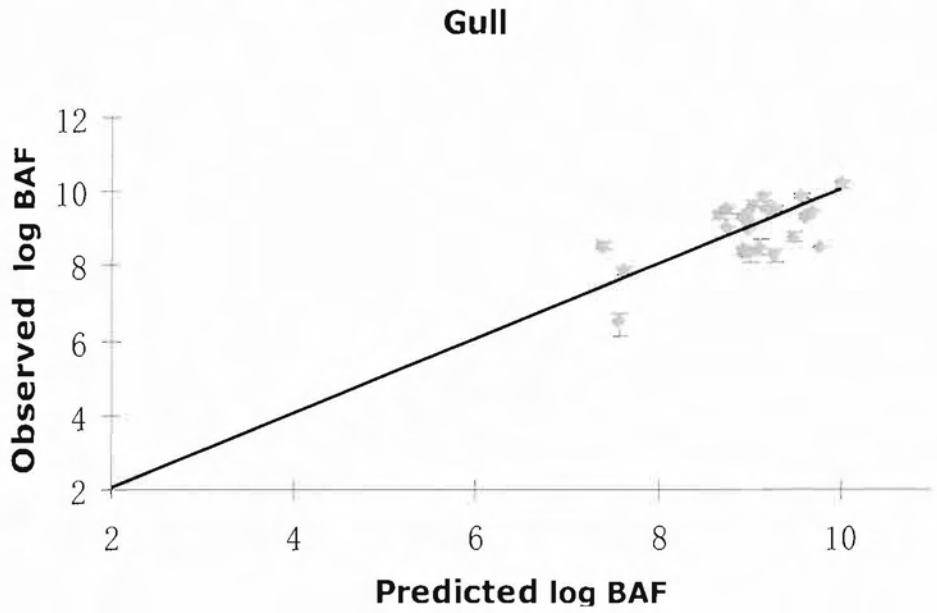

Figure 22: Observed versus model predicted TMF (a) and TMF*(b) of selected hydrophobic organic substances in the Lake Ontario food web.

a

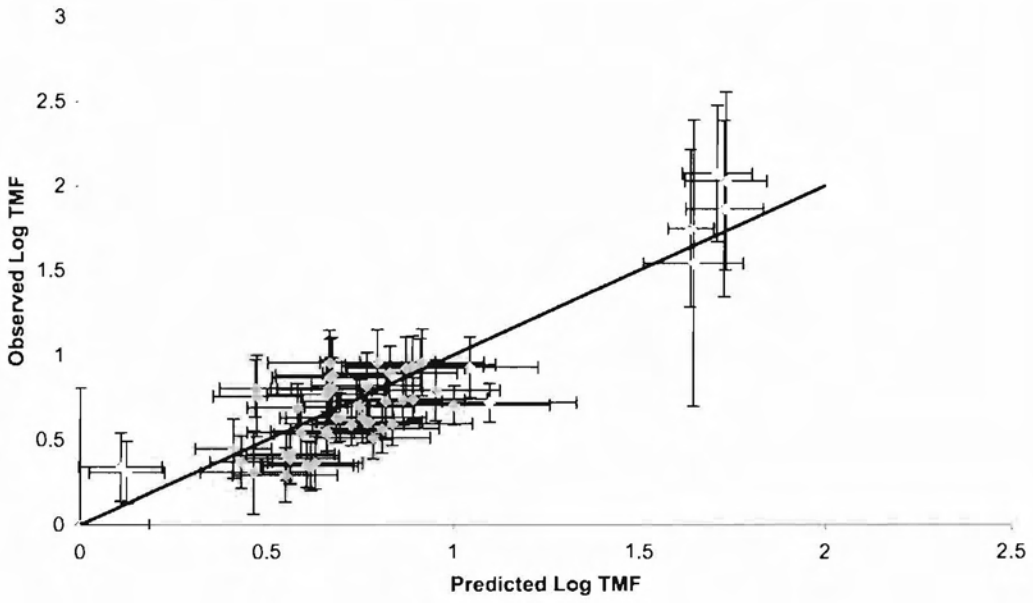

b

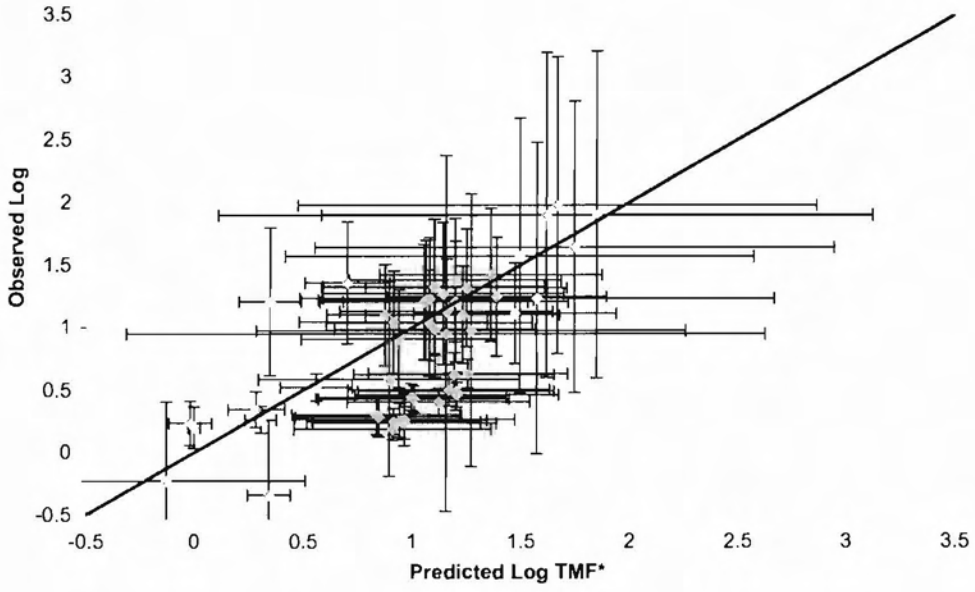

Figure 23: Model bias in the BAF for various chemical substances in mammals of the Canadian Arctic food web as a function of the K_{OA}.

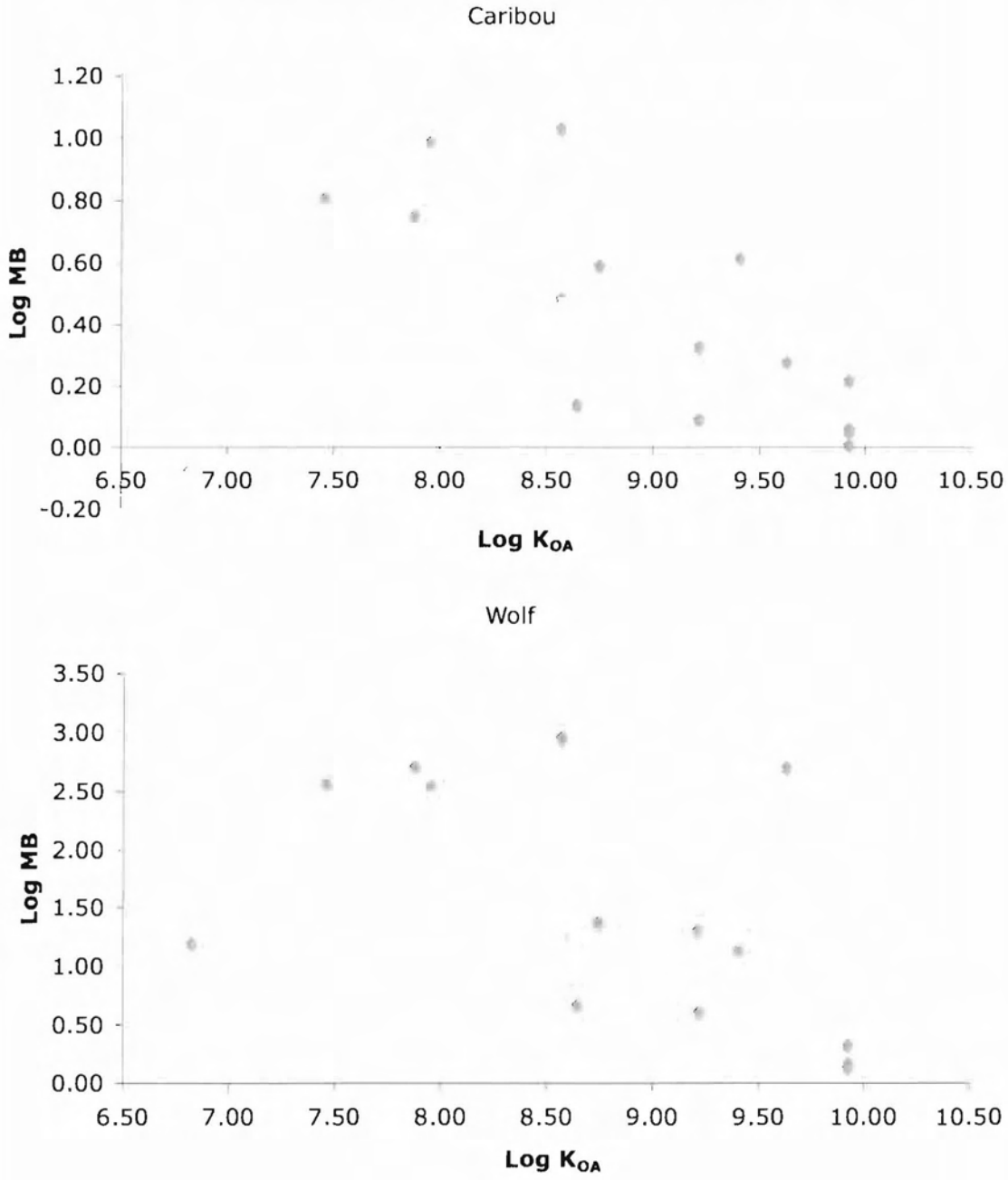

Figure 24: Model bias for various chemical substances in invertebrates of the Lake Ontario food web as a function of K_{OW}.

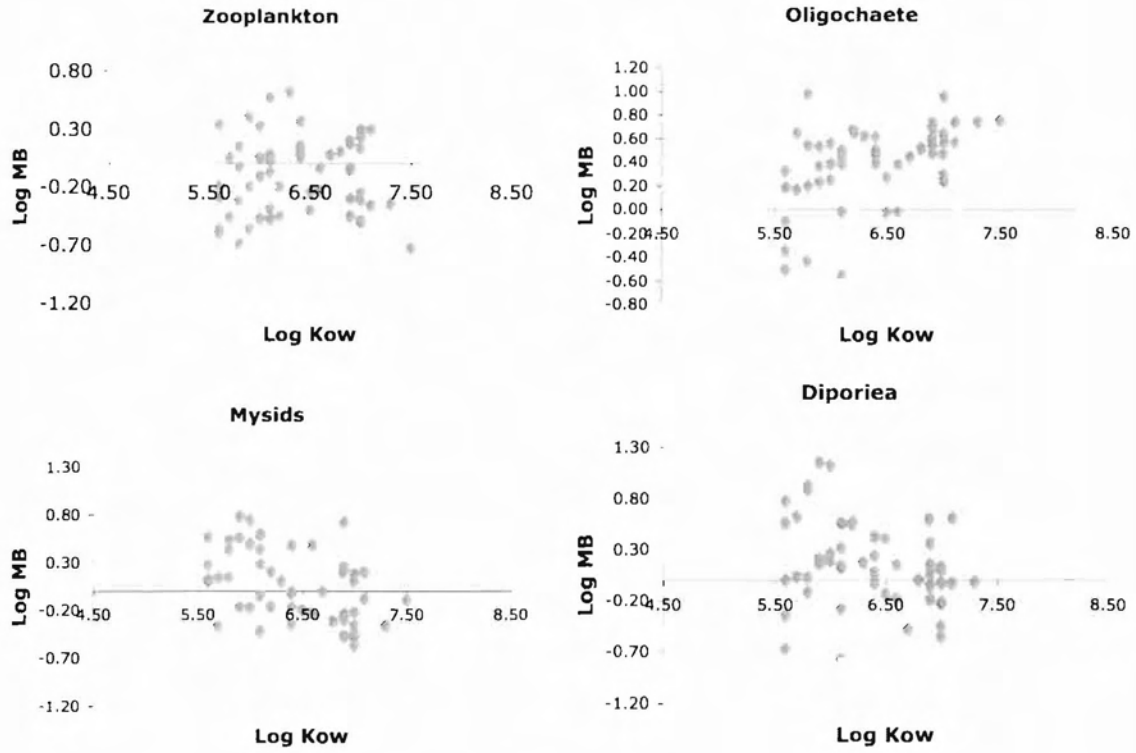

Figure 25: Model bias for various chemical substances in fish of the Lake Ontario food web as a function of K_{OW}.

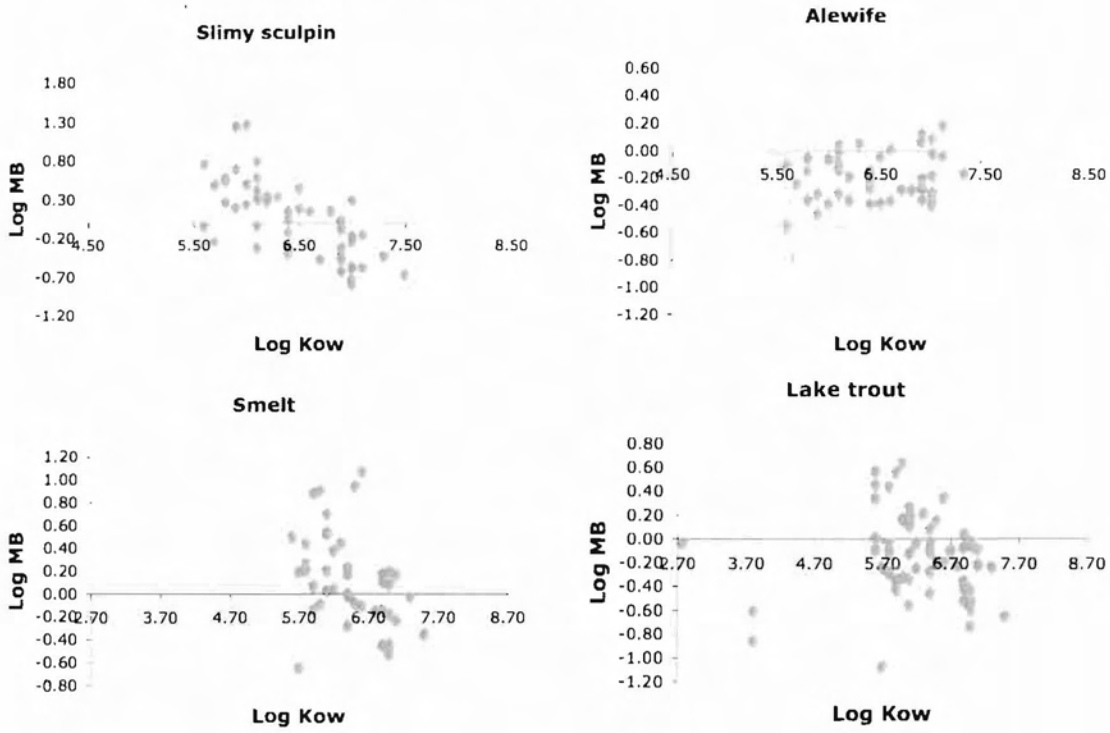

Figure 26: **Model bias for various chemical substances in herring gulls of the Lake Ontario food web as a function of K_{OA}.**

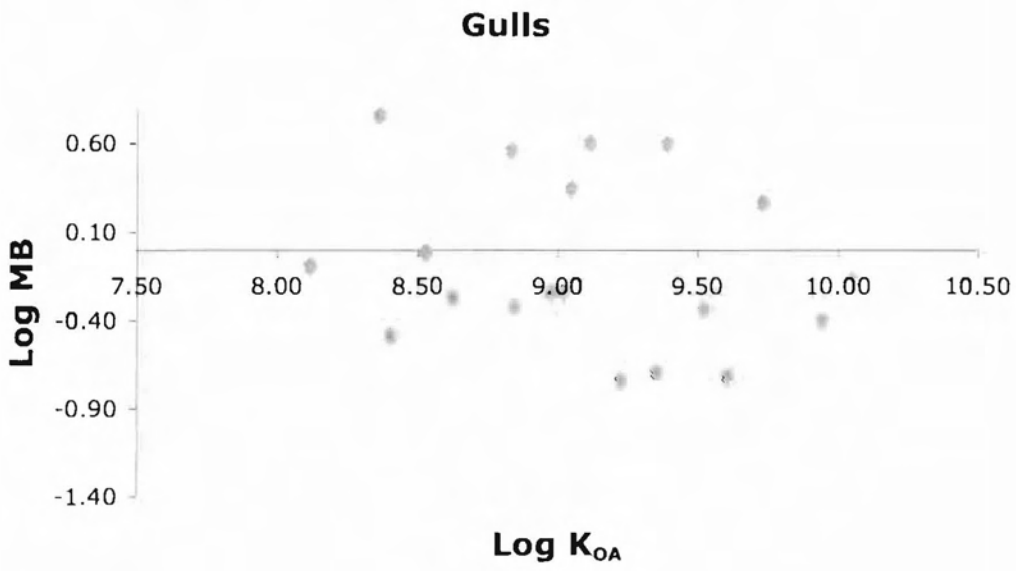

Model Comparisons

This section compares the present model performance of the bioenergetic bioaccumulation model with two previous BAF models. The present model performance, assumptions and parameterizations for the aquatic and terrestrial part were compared to the same previous aquatic BAF model in the same aquatic food web (Arnot and Gobas 2004), and the previous terrestrial model in the same terrestrial food chain (Kelly and Gobas 2003).

Aquatic model

The previous aquatic BAF model for the Lake Ontario food web was a toxicokinetic model (Arnot and Gobas 2004). Whereas the present model is a combined bioenergetic and toxicokinetic mass balance model.

The previous aquatic BAF model was based on several assumptions. First, it assumed that chemical homogeneously distributed within the organism as long as differences in tissue composition and phase partitioning are taken into account. This was the same for the present model. Both models were able to provide whole organism body burden or concentration prediction of organic substances. Second, both models also assumed that individual organisms could be described as a single compartment in terms of its exchange with its surrounding environment. Third, the previous model applied to scenarios where changes in chemical concentrations over time were relatively slow or of secondary concern. This was the same as the present model. Fourth, the previous model assumed that chemical elimination via egg deposition or sperm ejection was considered as growth dilution, which was the same as the present model. At last, the previous model assumed steady state, which is the same as the present model.

Model bias of biota involved in previous and present aquatic BAF models are displayed in Table 19. The present model overall MB (1.15) and MB for individual biota were not as close to 1 as the recent previous aquatic BAF model in 2004 (1.04). However, the model bias of the present model was within an acceptable range, especially for a model that is applicable to both aquatic and terrestrial food webs, and requires such a simplified model parameterization process. In addition, the present model is not limited to fish and aquatic invertebrates but applies to all consumer organisms, unlike the previous model (Arnot and Gobas 2004).

Table 19: Model bias of biota involved in previous and present aquatic BAF models.

MB	1993 (Gobas)	2004 (Arnot and Gobas)	This model
$MB_{Zooplankton}$	0.42	1.17	0.81
$MB_{Diperia}$	1.95	1.04	1.32
MB_{Mysids}	1.95	1.04	1.10
$MB_{Oligochaete}$	1.95	1.04	2.46
$MB_{Slimy\_sculpin}$	N/A	N/A	1.00
$MB_{Alewife}$	N/A	N/A	0.62
MB_{Smelt}	0.52	1.00	1.28
MB_{Trout}	0.52	1.00	0.73
$MB_{Herring\_gull}$	N/A	N/A	1.05
MB_{TOT}	0.86	1.04	1.15

Sources: 1993 model (Gobas 1993)and 2004 model (Arnot and Gobas 2004).

Terrestrial model

The BAF model developed by Kelly and Gobas (Kelly and Gobas 2003) in the lichen-caribou-wolf Arctic food chain was a toxicokinetic model, whereas the present model is a bioenergetic mass balance model. Both the previous and present models were two-compartment models.

The previous model was based on the assumption that the gastrointestinal magnification was the primary mechanism driving gastrointestinal uptake and biomagnification of POPs. This assumption was the same as the present model.

In terms of model parameterization, milk and urinary eliminations of POPs were taken into account in the previous terrestrial BAF model (Kelly and Gobas 2003). The present model considered milk secretion as a form of growth dilution, but did not take urinary loss into account. Loss of POPs through urinary secretion and excretion should of minimum importance. Because most of the chemicals included in the present model were hydrophobic and unlikely to be excreted through urine.

Model performance comparisons between the present and previous lichen-caribou-wolf model is not applicable. Because the present model assumed zero biotransformation in parameterization, and the model was only applied to non-metabolizable chemical, whereas the previous model included biotransformation of chemicals in the calculation (Kelly and Gobas 2003).

Conclusion

This bioenergetic/bioaccumulation model used limited empirical data and derived BAFs for both aquatic and terrestrial food webs with a single function by adjusting the input parameters. This bioenergetic/ bioaccumulation model did not only simplify the process in assessing the bioaccumulation of POPs in both aquatic and terrestrial animals, but also balanced the energy budget in the animals. Mass-balanced toxicokinetic models require a more extensive parameterization, as bioenergetic information to characterize uptake and elimination needs to be collected on an organisms specific basis, often from various sources (Kooijman 1995); and in most cases, the energy were not balanced in these toxicokinetic models. Moreover, this model incorporated the exchange of POPs through respiration and diet, which are more realistic than BCF or BMF.

The predicted BAF values for biota are applicable in human health and ecological risk assessment, as well as for deriving site-specific air, water and sediment for different environmental protection purposes. The model can also be used to calculate human BAF values of various POPs in different food webs involves human as the top predator.

The assumption of dietary preferences in the terrestrial and aquatic food webs is a source of uncertainty in predictions of POP concentrations in consumers. For instance, herring gull in Lake Ontario may consume other fish species that were not included in the model, or migrated from another region. In addition, dietary preference shifts overtime causes temporal variation (Gobas, Zgraggen et al. 1995).

The model assumes a constant rate of respiratory efficiency, digestive efficiency and growth efficiency. It also assumes the POP concentrations in the environment have reached equilibrium, thus the concentrations do not change over time. However,

growth/production efficiency and digestive efficiency can change over time. Firstly, the degree of chemical accumulation in consumer can be age-dependent. For example, POP concentrations in adult wolves were found to be greater than those in juvenile wolves in Canadian Arctic. This is mainly because the amount of accumulation of POPs cumulates over time. Another reason for age-dependent concentration is that adult animals often contain greater lipid content than in juveniles (deBruyn and Gobas 2006). This can result in a greater bioaccumulation degree for adults than for juveniles, given the same exposure duration, since the BMF increases with the lipid content of the consumer organisms (deBruyn and Gobas 2006). Secondly, environmental concentrations vary overtime and throughout seasons. These seasonal variations are not consistent with the steady state level of the model. In addition, the model cannot make accurate prediction of the BAF when uptake and elimination rates are time varying.

Further more, this bioaccumulation model assumes a zero metabolic transformation rate, which leads to an overestimation of bioaccumulation factors or concentration in consumers for chemicals that are metabolized or degraded at a significant rate.

Reference List

Arnot, J. A. (2003). Bioaccumulation modeling of organic chemicals in aquatic ecosystems. Biological Sciences. Burnaby, Canada, Simon Fraser University. **Master of Environmental Toxicology**.

Arnot, J. A. and F. Gobas (2006). "A review of bioconcentration factor (BCF) and bioaccumulation factor (BAF) assessments for organic chemicals in aquatic organisms." Environmental Reviews **14**(4): 257-297.

Arnot, J. A. and F. A. P. C. Gobas (2004). "A food web bioaccumulation model for organic chemicals in aquatic ecosystems." Environmental Toxicology and Chemistry **23**(10): 2343-2355.

Barber, M. C., L. A. Suarez, et al. (1991). "Modeling bioaccumulation of organic pollutants in fish with an application to PCBs in Lake-Ontario salmonids." Canadian Journal of Fisheries and Aquatic Sciences **48**(2): 318-337.

Best, R. C. (1985). "Digestibility of ringed seals by the polar bear." Canadian Journal of Zoology-Revue Canadienne De Zoologie **63**(5): 1033-1036.

Board, F. a. N. (2005). Dietary Reference Intakes for Energy, Carbohydrate, Fiber, Fat, Fatty Acids, Cholesterol, Protein, and Amino Acids. Washington, DC, National Academies Press.

Boon, J. P., J. vanderMeer, et al. (1997). "Concentration-dependent changes of PCB patterns in fish-eating mammals: Structural evidence for induction of cytochrome P450." Archives of Environmental Contamination and Toxicology **33**(3): 298-311.

Boyd, I. L. (2002). "Estimating food consumption of marine predators: Antarctic fur seals and macaroni penguins." Journal of Applied Ecology **39**(1): 103-119.

Braune, B. M. and R. J. Norstrom (1989). "Dynamics of organochlorine compounds in herring gulls: III. Tissue distribution and bioaccumulation in Lake Ontario gulls." Environmental Toxicology and Chemistry **8**(10): 957-968.

Brody, S. (1945). Bioenergetics and growth with special reference to the efficiency complex in domestic animals. New York, Hafner Publishing Company, INC.

Calow, P. and C. R. Fletcher (1972). "New radiotracer technique involving c-14 and cr-51, for estimating assimilation efficiencies of aquatic, primary consumers." Oecologia **9**(2): 155-&.

CEPA (1999). Canadian environmental protection act, Department of Justice, Canada.

Clark, K. E., F. Gobas, et al. (1990). "Model of organic-chemical uptake and clearance by fish from food and water." Environmental Science & Technology **24**(8): 1203-1213.

Clark, T. P., R. J. Norstrom, et al. (1987). "Dynamics of organochlorine compounds in Herring Gulls (Larus Argentatus): ii. A two-compartment model and data for ten compounds." Environmental Toxicology and Chemistry **6**(7): 547-559.

Connolly, J. P. and C. J. Pedersen (1988). "A Thermodynamic-Based Evaluation of Organic-Chemical Accumulation in Aquatic Organisms." Environmental Science & Technology **22**(1): 99-103.

deBruyn, A. M. H. and F. A. P. C. Gobas (2006). "A bioenergetic biomagnification model for the animal kingdom." Environ. Sci. Technol. **40**(5): 1581-1587.

Drouillard, K. G. and R. J. Norstrom (2000). "Dietary absorption efficiencies and toxicokinetics of polychlorinated biphenyls in ring doves following exposure to Aroclor (R) mixtures." Environmental Toxicology and Chemistry **19**(11): 2707-2714.

Elliott, J. M. and W. Davison (1975). "Energy equivalents of oxygen-consumption in animal energetics." Oecologia **19**(3): 195-201.

Erickson, R. J. and J. M. McKim (1990). "A simple flow-limited model for exchange of organic-chemicals at fish gills." Environmental Toxicology and Chemistry **9**(2): 159-165.

Fisk, A. T., R. J. Norstrom, et al. (1998). "Dietary accumulation and depuration of hydrophobic organochlorines: Bioaccumulation parameters and their relationship with the octanol/water partition coefficient." Environmental Toxicology and Chemistry **17**(5): 951-961.

Fraser, A. J., I. C. Burkow, et al. (2002). "Modeling biomagnification and metabolism of contaminants in harp seals of the Barents Sea." Environmental Toxicology and Chemistry **21**(1): 55-61.

Gobas, F. (1993). "A model for predicting the bioaccumulation of hydrophobic organic-chemicals in aquatic food-webs - application to Lake-Ontario." Ecological Modelling **69**(1-2): 1-17.

Gobas, F., J. R. McCorquodale, et al. (1993). "Intestinal-absorption and biomagnification of organochlorines." Environmental Toxicology and Chemistry **12**(3): 567-576.

Gobas, F., D. C. G. Muir, et al. (1988). "Dynamics of dietary bioaccumulation and fecal elimination of hydrophobic organic-chemicals in fish." Chemosphere **17**(5): 943-962.

Gobas, F., J. B. Wilcockson, et al. (1999). "Mechanism of biomagnification in fish under laboratory and field conditions." Environmental Science & Technology **33**(1): 133-141.

Gobas, F., M. N. Zgraggen, et al. (1995). "Time response of the Lake-Ontario ecosystem to virtual elimination of PCBs." Environmental Science & Technology **29**(8): 2038-2046.

Gobas, F., X. Zhang, et al. (1993). "Gastrointestinal Magnification - the Mechanism of Biomagnification and Food-Chain Accumulation of Organic-Chemicals." Environmental Science & Technology **27**(13): 2855-2863.

Gobas, F. A. P. C. and H. A. Morrison (2000). Bioconcentration and biomagnification in the aquatic environment. Handbook of Property Estimation Methods for Chemicals, Environmental and Health Sciences R. S. Boethling and D. Mackay. New York, Lewis Publishers. **9:** 189-231.

Golley, F. B. (1968). "Secondary productivity in terrestrial communities." American Zoologist **8**(1): 53-&.

Gorokhova, E. (1998). "Exploring and modeling the growth dynamics of Mysis mixta." Ecological Modelling **110**(1): 45-54.

Harner, T. (2008). PUF Disk Effective Air Volume Calculation for Target Chemicals. F. A. P. C. Gobas.

Hoff, R. M., D. C. G. Muir, et al. (1992). "Annual cycle of polychlorinated-biphenyls and organohalogen pesticides in air in southern Ontario .1. air concentration data." Environmental Science & Technology **26**(2): 266-275.

Hu, J. Y., H. J. Zhen, et al. (2006). "Trophic magnification of triphenyltin in a marine food web of Bohai Bay, north China: Comparison to tributyltin." Environmental Science & Technology **40**(10): 3142-3147.

Humphreys, W. F. (1978). "Ecological energetics of Geolycosa-Godeffroyi (Araneae Lycosidae) with an appraisal of production efficiency in ectothermic animals." Journal of Animal Ecology **47**(2): 627-652.

Jason Pelish , D. S., and Lyle Johnson (2003). Specturm Chemical Factsheet, Oxygen, Spectrum Laboratories Inc. GA, U.S.A.

Kasokat, T., R. Nagel, et al. (1989). "Metabolism of chlorobenzene and hexachlorobenzene by the zebra fish, brachydanio-rerio." Bulletin of Environmental Contamination and Toxicology **42**(2): 254-261.

Kelly, B. C. and F. A. P. C. Gobas (2001). "Bioaccumulation of persistent organic pollutants in lichen-caribou-wolf food chains of Canada's Central and Western Arctic." Environmental Science & Technology **35**(2): 325-334.

Kelly, B. C. and F. A. P. C. Gobas (2003). "An arctic terrestrial food-chain bioaccumulation model for persistent organic pollutants." Environmental Science & Technology **37**(13): 2966-2974.

Kelly, B. C., F. A. P. C. Gobas, et al. (2004). "Intestinal absorption and biomagnification of organic contaminants in fish, wildlife, and humans." Environmental Toxicology and Chemistry **23**(10): 2324-2336.

Kelly, B. C., M. G. Ikonomou, et al. (2007). "Food web-specific biomagnification of persistent organic pollutants." Science **317**(5835): 236-239.

Kooijman, S. (1995). "The stoichiometry of animal energetics." Journal of Theoretical Biology **177**(2): 139-149.

Kovecses, J., G. D. Sherwood, et al. (2005). "Impacts of altered benthic invertebrate communities on the feeding ecology of yellow perch (Perca flavescens) in metal-

contaminated lakes." Canadian Journal of Fisheries and Aquatic Sciences **62**(1): 153-162.

Lasker, R. (1960). "Utilization of organic carbon by a marine crustacean - analysis with carbon-14." Science **131**(3407): 1098-1100.

Li, N. Q., F. Wania, et al. (2003). "A comprehensive and critical compilation, evaluation, and selection of physical-chemical property data for selected polychlorinated biphenyls." Journal of Physical and Chemical Reference Data **32**(4): 1545-1590.

Mackay, D. (1979). "Finding fugacity feasible." Environmental Science & Technology **13**(10): 1218-1223.

Mackay, D. and A. Fraser (2000). "Bioaccumulation of persistent organic chemicals: mechanisms and models." Environmental Pollution **110**(3): 375-391.

Mackay, D. and S. Paterson (1982). "Fugacity revisited - the fugacity approach to environmental transport." Environmental Science & Technology **16**(12): A654-A660.

Mackintosh, C. E., J. Maldonado, et al. (2004). "Distribution of phthalate esters in a marine aquatic food web: Comparison to polychlorinated biphenyls." Environmental Science & Technology **38**(7): 2011-2020.

McKenzie, D. J., P. B. Pedersen, et al. (2007). "Aspects of respiratory physiology and energetics in rainbow trout (Oncorhynchus mykiss) families with different size-at-age and condition factor." Aquaculture **263**(1-4): 280-294.

McKim, J., P. Schmieder, et al. (1985). "Absorption dynamics of organic-chemical transport across trout Gills as related to octanol water partition-coefficient." Toxicology and Applied Pharmacology **77**(1): 1-10.

Mehmood, Z., M. P. Williamson, et al. (1996). "Metabolism of organochlorine pesticides: The role of human cytochrome P450 3A4." Chemosphere **33**(4): 759-769.

Moser, G. A. and M. S. McLachlan (2001). "The influence of dietary concentration on the absorption and excretion of persistent lipophilic pollutants in the human intestinal tract." Chemosphere **45**: 201-211.

Nagy, K. A. (1987). "Field Metabolic-rate and food requirement scaling in mammals and birds." Ecological Monographs **57**(2): 111-128.

Nagy, K. A. (2005). "Field metabolic rate and body size." Journal of Experimental Biology **208**(9): 1621-1625.

Norstrom, R. (2002). "Understanding bioaccumulation of POPs in food webs-Chemical, biological, ecological and environment considerations." J. Environ. Sci. Pollut. Res. **9**(300).

Norstrom, R. J. (2002). "Understanding bioaccumulation of POPs in food webs - Chemical, biological, ecological and environment considerations." Environmental Science and Pollution Research **9**(5): 300-303.

Oliver, B. G. and A. J. Niimi (1988). "Trophodynamic analysis of polychlorinated biphenyl congeners and other chlorinated hydrocarbons in the Lake-Ontario ecosystem." Environmental Science & Technology **22**(4): 388-397.

Penry, D. L. (1998). "Applications of efficiency measurements in bioaccumulation studies: Definitions, clarifications, and a critique of methods." Environmental Toxicology and Chemistry **17**(8): 1633-1639.

Piiper, J., P. Dejours, et al. (1971). "Concepts and basic quantities in gas-exchange physiology." Respiration Physiology **13**(3): 292-&.

Scheid, P. and J. Piiper (1970). "Analysis of gas exchange in avian lung - theory and experiments in domestic fowl." Respiration Physiology **9**(2): 246-&.

Schlummer, M., G. A. Moser, et al. (1998). "Digestive tract absorption of PCDD/Fs, PCBs, and HCB in humans: Mass balances and mechanistic considerations." Toxicology and Applied Pharmacology **152**(1): 128-137.

Sharpe, S. and D. Mackay (2000). "A framework for evaluating bioaccumulation in food webs." Environmental Science & Technology **34**(12): 2373-2379.

Shen, L. and F. Wania (2005). "Compilation, evaluation, and selection of physical-chemical property data for organochlorine pesticides." J. Chem. Eng. Data **50**(3): 742-768.

Sherwood, G. D., J. Kovecses, et al. (2002). "Simplified food webs lead to energetic bottlenecks in polluted lakes." Canadian Journal of Fisheries and Aquatic Sciences **59**(1): 1-5.

Straile, D. (1997). "Gross growth efficiencies of protozoan and metazoan zooplankton and their dependence on food concentration, predator-prey weight ratio, and taxonomic group." Limnology and Oceanography **42**(6): 1375-1385.

Thomann, R. V. (1989). "Bioaccumulation model of organic-chemical distribution in aquatic food-chains." Environ. Sci. Technol. **23**(6): 699-707.

Thomann, R. V. and J. P. Connolly (1984). "Model of PCB in the Lake-Michigan Lake Trout food-chain." Environ. Sci. Technol. **18**(2): 65-71.

Thomann, R. V. and J. P. Connolly (1992). "An equilibrium-model of organic chemical accumulation in aquatic food webs with sediment interaction." Environmental Toxicology and Chemistry **11**(5): 615-629.

USEPA. (2008). "MDL Definition -- What is a total maximum daily load (TMDL)?" Impaired Waters and Total Maximum Daily Loads, from http://www.epa.gov/owow/tmdl/intro.html.

Vander Zanden, M. J. and J. B. Rasmussen (1999). "Primary consumer delta C-13 and delta N-15 and the trophic position of aquatic consumers." Ecology **80**(4): 1395-1404.

Vucetich, J. A. and R. O. Peterson (2004). "The influence of prey consumption and demographic stochasticity on population growth rate of Isle Royale wolves Canis lupus." Oikos **107**(2): 309-320.

Wang, W. X. and N. S. Fisher (1999). "Assimilation efficiencies of chemical contaminants in aquatic invertebrates: A synthesis." Environmental Toxicology and Chemistry **18**(9): 2034-2045.

Webster, E., C. E. Cowan-Ellsberry, et al. (2004). "Putting science into persistence, bioaccumulation, and toxicity evaluations." Environmental Toxicology and Chemistry **23**(10): 2473-2482.

Welch, H. E. (1968). "Relationships between assimilation efficiencies and growth efficiencies for aquatic consumers." Ecology **49**(4): 755-&.

Appendices

Appendix A: Other Bioenergetic Parameters

Dietary chemical uptake efficiency

There are two points of views of dietary chemical uptake efficiency, assimilation efficiency and absorption efficiency. Assimilation efficiency is the fraction of ingested elements or compounds that is incorporated into biological tissue, whereas absorption efficiency is the fraction of ingested material that is taken up across the membranes of the cells of the gut wall (Penry 1998; Wang and Fisher 1999). Thus assimilation efficiency equals absorption minus metabolism. Comparisons of toxicant concentrations in ingested food and tissues of organisms at a reasonable measurement time scale that allow chemical metabolism to occur can represent assimilation efficiency (Penry 1998). However, the term of absorption/uptake efficiency and assimilation efficiency were interchangeable in many bioaccumulation models (Gobas, Muir et al. 1988). In the present study, E_D represents the chemical absorption efficiency, which is equivalent to $D_{GB}/(D_{GB}+D_F)$, the ratio of the rate of chemical absorption from the gut to the sum of chemical absorption and fecal elimination. Where D_{GB} is the gut to body uptake rate, described as the sum of simultaneous parallel processes including micellar transport, direct aqueous diffusion and diffusion across the cell membrane (Kelly, Gobas et al. 2004). When assuming the total chemical ingested is either absorbed by the body or eliminated from faeces, assimilation efficiency equals absorption efficiency. In bioaccumulation modelling, most of the studies assumed fecal elimination is the major

excretion route of POPs and metabolism of POPs was not considered (Kelly and Gobas 2003; Arnot and Gobas 2004), these assumptions allows using absorption efficiency instead of assimilation efficiency in the models.

Chemical absorption efficiencies were measured by the mass-balance method as the chemical input with food and contaminant output with faeces, normalized to the chemical intake (Calow and Fletcher 1972; Schlummer, Moser et al. 1998; Drouillard and Norstrom 2000; Moser and McLachlan 2001). The method of measuring the true assimilation efficiency of POPs is complicated and was rarely investigated. Fisk and colleagues obtained assimilation efficiencies of organochlorines in fish by fitting the body concentration data that were measured in the fish carcass (whole fish minus liver and GI tract) to the integrated form of the kinetic rate for constant dietary exposure using iterative nonlinear regression (Fisk, Norstrom et al. 1998). Thus the assimilation efficiency was a product of the fish carcass organochlorine concentration, feeding rate, concentrations in the food, depuration rate constants (determined by fitting the data to a first order decay curve) and time (day).

It was believed that chemical dietary absorption efficiency is a constant with K_{OW} for some chemicals, but it declines with Log K_{OW} above ~6.0 for other chemicals (Thomann 1989; Gobas, McCorquodale et al. 1993; Kelly, Gobas et al. 2004), this was explained by the low aqueous concentrations of highly hydrophobic compounds in the unstirred water layer, which controls the rate of intestinal uptake from the intestinal tract to across the luminal membrane (Kelly, Gobas et al. 2004).

Animal digestive efficiency

The total energy content of ingested food is either used for respiration/metabolism, production or lost as waste through fecal egestion and excretion. Digestion is a set of enzymatic and chemical reactions such as solubilization, adsorption/desorption from ingested particles, chemical hydrolysis, breaking down ingested material into components that can be absorbed across the gut wall (Penry 1998). Penry (1998) defined digestion efficiency (*DE*) as a function of the measurements of the amount of some component *F* in ingested food (F_0) (unit: mg) and the undegraded amount of component *F* remaining in egested faeces (F_E) (unit: mg) (Penry 1998):

$$DE = 1 - \left(\frac{F_E}{F_0} \right) \quad \textbf{(42)}$$

Animal digestive efficiency and assimilation efficiency of ingested food components are the same, while assuming elimination and excretion of food components are mainly through faeces, and all of the digestion is incorporated in tissue, in other words, assimilated. The present model used digestive efficiency for lipid, protein and carbohydrates, which vary among animals. Best (1985) measured digestibility of ringed seals by polar bear in terms of lipid, protein and carbohydrate (Best 1985). An indigestible marker, chromic sesquioxided (Cr_2O_3), was added to the diets of polar bear. Chrominum determinations of the food and faeces were made using an atomic absorption spectrophotometer. Digestibility was determined by comparing the Chrominum proportion in diet with that in the faeces (Best 1985).

Field metabolic rate

Total energy assimilated is used in respiration (R) and production (P). R refers to the processes of utilizing oxygen to break down carbohydrates, protein and lipid and other dietary constituents. The term respiration is also referred to as field metabolism and it is measured by the field metabolic rate (FMR), which is the total energy expenditure of a free-living consumer organisms under natural conditions (Nagy 1987).

The field metabolic rate is different from the basal metabolic rate. Basal metabolism is also called post-absorptive metabolism and standard metabolism, is the heat production during complete rest in a thermoneutral environment in post-absorptive condition; it is the resting energy metabolism in a thermoneutral environmental. The work of blood circulation under basal conditions is estimated to account for from 5 to 15 per cent of the total basal metabolism energy; the remaining basal metabolism energy represents the cost of maintaining purposeless enzyme activities, and maintaining temperature (Brody 1945). On the other hand, field metabolic rate is the total energy expenditure when a consumer is under natural conditions in the field, i.e. it is actively foraging and eating.

Doubly labeled water (DLW) method was used to measure FMR (in kJ metabolized per day) in a variety of vertebrate and invertebrate animals (Nagy 1987; Nagy 2005). In theory, when the water in an animal has been enriched with stable or radioactive isotopes of oxygen and hydrogen, the loss of hydrogen isotope over time is proportional to water flux through its body, but the loss of oxygen isotope is faster, because oxygen is lost not only as water, but also as CO_2 due to rapid isotopic equilibration in blood between H_2O and dissolved CO_2 (Nagy 2005). Thus, the rate of

CO_2 production can be estimated from the difference between the washout rates of the two isotopes, which represents CO_2 production only. However, this method only works reliably in air-breathing animals, where a substantial fraction (around 15%) of the isotopic oxygen leaves the animal as CO_2. In water-breathing and amphibious animals, such as fishes and frogs, water molecules move through the animal so fast that they take out the oxygen isotope rapidly as water, and the relatively small amount of oxygen isotope lost as CO_2 is difficult to detect and quantify accurately.

However, in the present model, after simplifying the BAF formula and eliminating D_M from the formula, FMR cancels out in the numerator and denominator. Thus FMR was not involved in parameterization process.

Net growth efficiency

There are two types of growth efficiencies, net growth efficiency (i.e. e=P/Assimilated energy) versus gross growth efficiency (i.e. e=P/I). Net growth efficiency is the ratio of energy used in production and energy assimilated, whereas, gross growth efficiency is the ratio of energy used in production and energy ingested (Straile 1997). On the other hand, growth efficiency is viewed as a function of both temperature and diet, and it is measured either as the change in length or the change in weight with age for fish and invertebrates (Thomann 1989; Thomann and Connolly 1992).

Experimental methods for measuring growth efficiencies include the isotopically labelled organic carbon. For example, the utilization of organic carbon by a marine crustacean was analyzed with carbon-14 (Lasker 1960). The carbon-14/total organic carbon ratio in the algal sample was the key to calculate the total carbon contributed by

the algae in the fecal pellets and in the eviscerated euphasii. In the experiment, the carbon egested in fecal pellets and in the eviscerated euphausii was calculated from the fractionation of carbon by radioactivity (unit: cpm) over the total organic carbon, as the ratio was set to be constant in the food, faeces and consumer's body after 24 hours (Lasker 1960). Knowing the ratio of the fractionation of radioactive carbon and total organic carbon in the food enabled the calculation of the total organic carbon utilized in growth. This method was further developed and applied to measuring growth efficiencies for protozoan and metazoan zooplankton (Straile 1997).

Welch found lowering the assimilation efficiency of an animal, increased its net growth efficiency; because the less energy an animal extracts from its food, the greater is the percentage used for growth, and the less is used for respiration (Welch 1968). Note that animals with high assimilation efficiencies tend to be carnivores, whereas those with lower assimilation efficiencies tend to be herbivore/detritivores (Welch 1968).

Metabolic transformation

Metabolic transformation may have a significant effect on the magnitude of chemical bioaccumulation in consumers. Metabolic transformation depends on the first order reaction rate of a chemical (K_M) and body size of a consumer (Thomann and Connolly 1984). The previous field study of POP bioaccumulation in Canadian Arctic wolf and caribou showed that fugacities of PCB 153 and 180 increased significantly ($p < 0.05$) with increasing trophic level. In contrast, fugacities of PCB 52 were not statistically different between trophic levels (Kelly and Gobas 2001). This suggested that relative to PCB 153 and 180, PCB 52 was eliminated and/or metabolized efficiently in both caribou and wolves. In addition, some animals like harbour seals will metabolize certain PCB

congeners at significant rates. In studies with harbour seals, PCB 153 was observed to be the dominant PCB congener and known to be the least metabolized PCB congener (Boon, vanderMeer et al. 1997). It is possible to estimate the metabolic transformation of each PCB congener relative to a reference congener by setting K_M equals to zero for PCB 153, and calibrate other PCBs to it, and compare model predicted value to empirical value.

There is also evidence of metabolisms of organochlorines and hexachlorobenzene (HCB) in both mammals and fish. Kasokat and colleagues (Kasokat, Nagel et al. 1989) found metabolism of HCB into pentachlorophenol (PCP) by zebra fish. Exposure to low levels of certain compounds (e.g. PCBs and HCB) may result in an induction of specific P 450-dependent monooxygenase activities. It was suggested that these enzyme systems might facilitate oxidative dechlorination reactions since the mechanism of reductive dechlorination was not involved in the conversion of HCB to pentachlorophenol (PCP) (Kasokat, Nagel et al. 1989). In addition, hexachlorobenzene and pentachlorobenzene were metabolized into pentachlorophenol which was further transformed into tetrachlorohydroquinone by human in both in *vitro* and in *vivo* studies (Mehmood, Williamson et al. 1996).

Oxycalorific coefficient

The rate of heat production is usually calculated from the oxygen consumption by utilising a known energy equivalent, the Oxycalorific coefficient (Qox) (Elliott and Davison 1975). The standard value of Qox for an animal is usually given as 3.38 cal for each mg of oxygen consumed. However, values of Qox in the literature varies (Elliott and Davison 1975). As the value of Qox depends on the proportions of carbohydrate, fat and protein in the diet, different value have been proposed for different animals; the energy

equivalent for converting rate of oxygen consumption into rate of heat production is 3.53 cal mg-1, for carbohydrate oxidation, 3.28 cal mg-1 for fat oxidation (Elliott and Davison 1975). Qox values for the respiration of standard protein are the same at 3.25 cal mg-1 for ureotelic and uricotelic animals, and about 2% less at 3.2 cal mg-1 for ammoniotelic animals (Elliott and Davison 1975).

Appendix B: CD-ROM Data

The CD-ROM attached forms a part of this work.

The bioenergetic bioaccumulation model can be opened in MSExcel or spreadsheet program.

File name: Bioenergetic bioaccumulation model

File size: 13.1 MB.